Universidade de Aveiro Departamento de Química
2020

João Dinis Oliveira Abranches

Desvendando o Mecanismo da Hidrotropia: Rumo a um Futuro Sustentável

Unveiling the Mechanism of Hydrotropy: Towards a Sustainable Future

Universidade de Aveiro Departamento de Química
2020

João Dinis Oliveira Abranches

Desvendando o Mecanismo da Hidrotropia: Rumo a um Futuro Sustentável

Unveiling the Mechanism of Hydrotropy: Towards a Sustainable Future

Dissertação apresentada à Universidade de Aveiro para cumprimento dos requisitos necessários à obtenção do grau de Mestre em Engenharia Química, realizada sob a orientação científica do Professor Doutor João A. P. Coutinho, professor catedrático do Departamento de Química da Universidade de Aveiro, e co-orientação do Professor Doutor Seishi Shimizu, professor do Departamento de Química da Universidade de York.

This work was developed within the scope of the project CICECO-Aveiro Institute of Materials, UIDB/50011/2020 & UIDP/50011/2020, financed by national funds through the FCT/MEC and when appropriate co-financed by FEDER under the PT2020 Partnership Agreement. FCT is also acknowledged for the financial support through the project SAICTPAC/0040/2015 and for the author's research grant.

The surest way to corrupt a youth is to instruct him to hold in higher esteem those who think alike than those who think differently.

Friedrich Nietzsche

o júri

presidente

Professora Doutora Maria Inês Purcell de Portugal Branco
Professor Auxiliar do Departamento de Química da Universidade de Aveiro

Professor Doutor Steven Abbott
Professor Visitante do Departamento de Engenharia Mecânica da Universidade de Leeds

Professor Doutor João Manuel Costa Araújo Pereira Coutinho
Professor Catedrático do Departamento de Química da Universidade de Aveiro

agradecimentos

Uma dissertação raramente resulta do trabalho de um indivíduo apenas. Portanto, quero agradecer a todo o grupo de investigação PATh por me terem acolhido. Um agradecimento especial à Liliana, à Mónia, à Jordana, à Bruna, e ao Nicolas, por estarem sempre disponíveis para abraçarem novos desafios e aventuras. Uma palavra de agradecimento também a todos os coautores que ajudaram a dar vida aos trabalhos nos quais se baseia esta dissertação.

Este trabalho não é uma instância isolada do meu percurso académico; é, sim, a reta final de uma longa etapa, cujos obstáculos ultrapassei apenas porque tive a felicidade de conhecer pessoas extraordinárias com as quais aprendi e cresci. Quero deixar-lhes uma palavra de agradecimento.

Ao Professor Marcos Larriba, por me ter ensinado o valor da amizade na ciência.

Ao Professor Simão Pinho, incansável no seu esforço em ajudar, discutir e tornar os nossos trabalhos melhores e mais profundos.

Ao Professor Seishi Shimizu, por todas as longas horas de discussão enriquecedora, sempre na presença de uma agradável chávena de chá.

E ao Professor João Coutinho, meu mentor, por ter acreditado em mim, por todas as oportunidades que me concedeu, e por me ter dado a liberdade que necessito para fazer aquilo que faço melhor.

Finalmente, um agradecimento especial à minha família, aos meus amigos, e em particular à Fabiana, por serem a minha maior fonte de coragem e inspiração.

palavras-chave

Hydrotropia · Química Sustentável · Efeito Hidrofóbico · Éteres de Glicerol · Cyrene · Ácidos Fenólicos

resumo

Os hidrótropos, pela sua capacidade de aumentar a solubilidade de substâncias hidrofóbicas em água, podem expandir a aplicabilidade do mais verde e mais abundante de todos os solventes. No entanto, e embora a ampliação do repertório de solventes mais seguros esteja alinhada com os princípios da química verde e seja essencial para um futuro sustentável, a hidrotropia é frequentemente negligenciada como uma ferramenta promissora para a química verde. Isto deve-se à falta de conhecimento fundamental relativo ao seu mecanismo, o que dificulta o desenho de novos sistemas hidrotrópicos e limita a sua aplicação a alguns exemplos bem conhecidos.

Este trabalho começa por usar éteres de glicerol como um caso de estudo de hidrotropia, investigando a sua capacidade de aumentar a solubilidade de ácido gálico e siríngico em água. Os resultados obtidos sugerem que a capacidade hidrotrópica depende da concentração do hidrótropo na água. Além disso, usando o conceito da constante de Setschenow, mostra-se que as hidrofobicidades do soluto e do hidrótropo desempenham um papel importante no aumento da solubilidade por hidrotropia.

Com base nos resultados preliminares obtidos para os éteres de glicerol, obteve-se aqui, pela primeira vez, usando ^{1}H-RMN, evidência experimental para a teoria cooperativa da hidrotropia, que sustenta que a hidrotropia ocorre devido à agregação de hidrótropos em torno do soluto mediada pela água. Além disso, uma nova abordagem computacional para quantificar a apolaridade é introduzida e usada para esclarecer o papel da apolaridade do soluto e do hidrótropo no mecanismo de hidrotropia. De facto, mostra-se que o número de moléculas de hidrótropo agregadas à volta do soluto é máximo quando há uma correspondência entre a apolaridade de ambas as espécies.

Usando os novos conceitos de hidrotropia desenvolvidos ao longo do trabalho, a solubilidade de solutos hidrofóbicos em Cyrene, um solvente verde produzido a partir de fontes renováveis, e suas misturas com água são aqui exploradas. Mostra-se que a hidrotropia é o mecanismo de solubilização de solutos hidrofóbicos no sistema água-Cyrene, na maior parte da sua gama de concentração. Além disso, demonstra-se que a forma cetona do Cyrene é o principal hidrótropo do sistema. Os parâmetros do modelo cooperativo correlacionam-se com a hidrofobicidade dos solutos, o que é explorado para prever com sucesso as curvas de solubilidade do ácido ftálico, aspirina, ácido gálico e vanilina nas misturas água-Cyrene. Finalmente, mostra-se que a água, quando adicionada ao Cyrene em pequena quantidade, atua como um co-solvente, estabelecendo uma forte ponte de hidrogénio com o soluto. Isto mostra que um sistema pode solubilizar solutos hidrofóbicos através de mecanismos muito diferentes, dependendo da concentração de cada espécie.

keywords

Hydrotropy · Sustainable Chemistry · Hydrophobic Effect · Glycerol Ethers · Cyrene · Phenolic Acids

abstract

Hydrotropes, with their ability to increase the solubility of hydrophobic substances in water, can expand the applicability of the greenest and most abundant of all solvents. However, and even though broadening the repertoire of safer solvents is in line with the principles of green chemistry and is essential for a sustainable future, hydrotropy is often overlooked as a promising tool for green chemistry. This is due to a lack of fundamental understanding on its mechanism, which hampers the design of novel hydrotropic systems and limits its applications to a few well-known examples.

This work starts by using glycerol ethers as a case-study of hydrotropy by investigating their ability to enhance the solubility of gallic and syringic acids in water. The results obtained suggest that the solubility enhancement ability of a hydrotrope, and by extension its hydrotropic capability, depends on its concentration in water. Furthermore, using the concept of the Setschenow constant, it is shown that the hydrophobicities of both solute and hydrotrope play an important role in the solubility enhancement by hydrotropy.

Building on the preliminary results obtained with glycerol ethers, experimental evidence for the cooperative theory of hydrotropy, which holds that hydrotropy occurs due to water-mediated aggregation of hydrotropes around the solute, is obtained here for the first time, using ^{1}H-NMR. Moreover, a new computational approach to quantify apolarity is introduced, and is used to clarify the role of the apolarity of both solute and hydrotrope. In fact, it is shown that the number of hydrotrope molecules aggregated around the solute is maximum when there is a match between the apolarity of the two species.

Using these newly-found fundamental concepts of hydrotropy, the solubility of hydrophobic solutes in Cyrene, an emerging bio-based green solvent, and its mixtures with water is herein explored. It is shown that hydrotropy is the solubilization mechanism of hydrophobic solutes in the water-Cyrene system, in most of its concentration range. Furthermore, the ketone form of Cyrene is shown to be the principal hydrotrope of the system, with the diol form acting as a hydrotrope only at low Cyrene concentration. The parameters of the cooperative model are shown to be correlated with the hydrophobicity of the solutes, which is explored to successfully predict the solubility curves of phthalic acid, aspirin, gallic acid and vanillin in water-Cyrene mixtures. Finally, it is shown that water, when added to Cyrene in a small amount, acts as a cosolvent by establishing strong hydrogen bonding with the solute. This shows that a system may solubilize hydrophobic solutes through very different mechanisms, depending on the concentration of each species.

Table of Contents

List of Figures

List of Tables

Acronyms

[0.0.0] – Glycerol

[1.0.0] – 3-Methoxypropane-1,2-diol

[2.0.0] – 3-Ethoxypropane-1,2-diol

[3.0.0] – 3-Propoxypropane-1,2-diol

[4.0.0] – 3-Butoxypropane-1,2-diol

[5.0.0] – 3-Pentoxypropane-1,2-diol

[6.0.0] – 3-Hexoxypropane-1,2-diol

[1.0.1] – 1,3-Dimethoxypropan-2-ol

[2.0.2] – 1,3-Diethoxypropan-2-ol

^{1}**H-NMR** – Proton Nuclear Magnetic Resonance

$\boldsymbol{A}$ – Slope of Collander Equation

$\boldsymbol{B}$ – Intercept of Collander Equation

$\boldsymbol{C_H}$ – Hydrotrope Molar Concentration ($mol \cdot L^{-1}$)

COSMO-RS – Conductor-like Screening Model for Real Solvents

DFT – Density Functional Theory

$\boldsymbol{E_{HB}}$ – Total Hydrogen Bonding Interaction Energy

$\boldsymbol{G_{S,H}}$ – Solute-Hydrotrope KBI

$\boldsymbol{G_{S,H}}$ – Solute-Water KBI

$\boldsymbol{K_1}$ – Partition Coefficient Between Generic Solvent 1 and Water

$\boldsymbol{K_2}$ – Partition Coefficient Between Generic Solvent 2 and Water

KBI – Kirkwood-Buff Integral

$\boldsymbol{K_H}$ – Setschenow Constant

$\boldsymbol{K_{O,W}}$ – Octanol/Water Partition Coefficient

$\boldsymbol{max}$ – Maximum Attainable Relative Solubility (Mole Fraction Based)

NMP – N-methyl-2-pyrrolidone

NMR – Nuclear Magnetic Resonance

$\boldsymbol{P}$ – COSMO-RS Contact Probability

$\boldsymbol{P^*_{C,W}}$ – Partition Coefficient Between Cyrene and Water at Solute Saturation

$\boldsymbol{p(\sigma)}$ - σ-Profile

$\boldsymbol{R}$ – Ideal Gas Constant

$\boldsymbol{S}$ – Solute Molar Solubility ($mol \cdot L^{-1}$)

$\boldsymbol{S_0}$ – Solute Molar Solubility in Water ($mol \cdot L^{-1}$)

SBS – Sodium Benzene Sulfonate

$\boldsymbol{S_{Cyrene}}$ – Solute Solubility in Cyrene ($mol \cdot L^{-1}$)

STS – Sodium Toluene Sulfonate

$\boldsymbol{S_{Water}}$ – Solute Solubility in Water ($mol \cdot L^{-1}$)

SXS – Sodium Xylene Sulfonate

$\boldsymbol{T}$ – System Absolute Temperature (K)

$\boldsymbol{T_m}$ – Solute Melting Temperature (K)

VOC – Volatile Organic Compounds

$\boldsymbol{V_{Water}}$ – Volume Ratio Between Added Water and Initial System

$\boldsymbol{wt_{Solute}}$ – Fraction of Recovered Solute

$\boldsymbol{x_H}$ – Hydrotrope Mole Fraction

$\boldsymbol{x_S}$ – Solute Saturation Mole Fraction (Solubility)

$\boldsymbol{x_{S,0}}$ – Solute Saturation Mole Fraction (Solubility) in Water

$\boldsymbol{x_{Total\ Cyrene}}$ – Cyrene Mole Fraction After Chemical Equilibrium

$\boldsymbol{x_{Water}}$ – Water Mole Fraction

$\boldsymbol{\gamma_S}$ – Activity Coefficient of the Solute

$\boldsymbol{\delta_{max}}$ – Maximum Attainable Relative Solubility (Molarity Based)

$\Delta_m \boldsymbol{C_P}$ – Solute Heat Capacity Change upon Melting ($J \cdot K^{-1} \cdot mol^{-1}$)

$\Delta_m \boldsymbol{h}$ – Solute Enthalpy of Fusion ($J \cdot mol^{-1}$)

$\boldsymbol{\Delta\delta_H}$ – Change in Proton Chemical Shift

$\boldsymbol{\sigma}$ – Polarization Charge-Density

Chapter 1
Introduction

1.1 Hydrotropy

Solvents play a crucial role in most chemical processes, both at an industrial and laboratorial scale. Volatile organic compounds (VOC) were traditionally used as solvents without considering their health and environmental impact. This took a turn in the last century, where long-term exposure to organic solvents started to be connected with health problems, such as neuropsychiatric conditions and cancer,[1–6] and environmental issues started to be addressed.[7–10] Thus, the design of safer solvents, one of Anastas' twelve principles of green chemistry,[11] is of utmost importance for a sustainable future.[12,13] Ionic liquids, deep eutectic solvents and supercritical fluids are among the solvents that are being thoroughly studied due to their sustainable character.

Hydrotropes are a class of water-soluble compounds with an amphiphilic structure that are able to increase the solubility of hydrophobic substances in water.[14] Hydrotropy has been applied in several fields, such as drug formulation and biomass fractionation, with a great success.[15–20] Hydrotropes, in their ability to increase the solubility of hydrophobic substances in water, can expand the applicability of the greenest and most abundant of all solvents. Broadening the repertoire of safer solvents is in line with the principles of green chemistry[11] and is essential for a sustainable future.[12,13,21] However, since proposed by Neuberg[22] in 1916, most compounds studied as hydrotropes are petrochemical-based, such as sodium benzene sulfonate (SBS), sodium toluene sulfonate (STS) or sodium xylene sulfonate (SXS). Non-ionic alkyl-hydrotropes such as ethylene glycol ethers and propylene glycol ethers have also been proposed.[14,23,24]

In extraction and separation processes, a key advantage of hydrotropy is the fact that solutes can be recovered by a simple addition of water. That is, the solubility enhancement of a solute due to the presence of the hydrotrope depends on the concentration of the latter. When its concentration decreases due to the addition of water, so does its hydrotropy efficiency which, in some cases, leads to the precipitation of the solute. This is especially relevant since water has a prohibitively high heat capacity and enthalpy of vaporization, rendering separation processes based on evaporation or distillation energetically and economically expensive. A simple process for the extraction of a hydrophobic solute and solvent recovery is illustrated below in Figure 1.1.

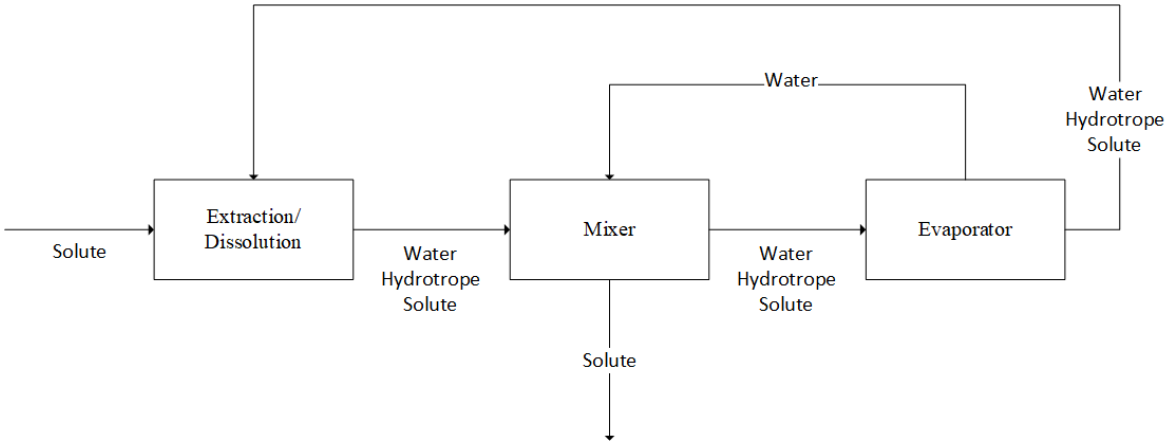

Figure 1.1. *Schematic illustration of an extraction process using hydrotropy, emphasizing the solvent recovery by the addition of water.*

The mechanism of hydrotropy is still not fully understood, despite a century of research[22] and an ongoing debate in the literature.[23,25–33] Traditional speculations regarding the mechanism of hydrotropy revolved around (i) bulk-phase self-aggregation (or pre-clustering) of hydrotropes analogous to micellar solubilization,[23,25,33] (ii) "water structure" disruption by the hydrotrope that would behave like chaotropic agents weakening the hydrophobic effect[26,27] and (iii) specific stoichiometric association between solute and hydrotrope.[28,29] However, none of these hypotheses are supported by statistical thermodynamics descriptions of hydrotropy[30,31] which suggest that hydrotrope accumulation around the solute is driven by a strong water-mediated (or hydrophobic) interaction between hydrotrope and solute. Because the interaction of the apolar (or hydrophobic) moiety of a molecule with water is much weaker than a water-water hydrogen bond, it is driven out to associate with another hydrophobic moiety, resulting in strong agglomeration of hydrotrope around the solute.

1.2 Work Outline

Due to the poor understanding of the mechanism of hydrotropy, its development is hampered, and its application potential not sufficiently recognized. This work seeks to address this shortcoming by presenting an in depth study of hydrotropy, expanding on the work of Shimizu and co-authors,[34] where the mechanism of hydrotropy is rationalized, to design novel hydrotropic systems based on compounds with high sustainability character.

This work starts, in Chapter 3, by studying the use of glycerol ethers (with alkyl side chain ranging from to one six methyl groups) as hydrotropes to enhance the solubility of gallic and syringic acids in water. These compounds were selected due to their biological and industrial applications and for serving as model molecules for lignin solubilization. From this data, and using the concepts of

Setschenow constant, hydrophobicity, and the cooperative hydrotropy model, it becomes clear that apolarity is an important aspect of hydrotropy.

Building on the discussion of Chapter 3, Chapter 4 provides, for the first time, experimental evidence for the mechanism of hydrotropy. Then, a new computational technique is developed to quantify apolarity and is used to show that it is the driving force of hydrotropy, clarifying the role of both solute and hydrotrope in the aggregation process.

The newly found concepts of Chapter 4 are applied to Cyrene, an emerging bio-based green solvent that has been shown to have the ability to increase the solubility of hydrophobic substances in water,[35,36] in Chapter 5. Using the cooperative model of hydrotropy,[34] it is shown that hydrotropy is the solubilization mechanism of hydrophobic solutes in the water-Cyrene system, in most of its concentration range. The parameters of the cooperative model, namely the number of hydrotrope molecules aggregated around the solute and the maximum solubility increase, are shown to be correlated with the hydrophobicity of the solutes quantified by their octanol-water partition coefficient. This result not only supports the mechanism of hydrotropy presented in Chapter 4, but also adds a predictive ability to the cooperative model, which is then explored to successfully predict the solubility curves of phthalic acid, aspirin, gallic acid and vanillin in water-Cyrene mixtures.

Finally, the use of COSMO-RS (a quantum chemistry-based excess Gibbs energy model)[37–39] as a predictable tool for hydrotropy is explored in Chapter 6, using the Cyrene-based systems studied in Chapter 5. Furthermore, the contact probability framework of COSMO-RS is used to understand the ability of water to act as a co-solvent of Cyrene, effectively showing that hydrophobic solutes dissolve in water/Cyrene mixtures by two different mechanisms, depending on the concentration of Cyrene in the system.

Chapter 2
Computational Methods

2.1 Solid-Liquid Equilibrium

The solubility of a substance in a liquid solvent is described by the following solid-liquid equilibrium expression:[40,41]

$$\ln(x_S \cdot \gamma_S) = \frac{\Delta_m h}{R} \cdot \left(\frac{1}{T_m} - \frac{1}{T}\right) + \frac{\Delta_m C_P}{R} \cdot \left(\frac{T_m}{T} - \ln\frac{T_m}{T} - 1\right) \quad (2.1)$$

where x_S is the saturation mole fraction (solubility) of the solute in the system, γ_S is its activity coefficient, T_m is its melting temperature, $\Delta_m h$ is its enthalpy of fusion (at temperature T_m), $\Delta_m C_P$ is its heat capacity change upon melting, R is the ideal gas constant and T is the absolute temperature of the system. Since the influence of the $\Delta_m C_P$ term in Equation 2.1 is relatively small, and considering that its value is not easily obtained experimentally and is seldom available in the literature, Equation 2.1 is often simplified, leading to: [40–42]

$$\ln(x_S \cdot \gamma_S) = \frac{\Delta_m h}{R} \cdot \left(\frac{1}{T_m} - \frac{1}{T}\right) \quad (2.2)$$

In the case where the melting properties of the solute are known (T_m and $\Delta_m h$), Equation 2.2 can be used to predict solubility data if coupled with a Gibbs excess free energy model able to predict the activity coefficient of the solute in the liquid mixture. This is explored in Chapter 6 of this work, where COSMO-RS is used to predict γ_S, which is coupled with Equation 2.2 to predict the solubility of hydrophobic solutes in water, Cyrene and Cyrene-water mixtures. Note that γ_S depends on the composition of the final system and its absolute temperature. Temperature is a known variable; however, the final composition of the system depends on the solubility of the solute (x_S) which, in turn, depends on its activity coefficient. Thus, x_S is iteratively calculated using Equation 2.2, where in each iteration COSMO-RS is used to calculate γ_S.

2.2 COSMO-RS

COSMO-RS (Conductor like Screening Model for Real Solvents) is a quantum chemistry-based thermodynamics model able to predict the chemical potential of compounds in liquid mixtures.[37–39] Within the framework of COSMO-RS, the geometry and charge density surface of each molecule needs to be previously optimized using DFT and the COSMO solvation model. From this, the model constructs a histogram, the so-called σ-profile, which describes the amount of area segment of polarity σ that a molecule possesses. Finally, the model relies on pair-wise interactions between all area segments of all molecules present in the system in order to calculate their chemical potentials and, thus, their activity coefficients.

The concepts and framework of COSMO-RS are used in Chapters 4 and 6. In both instances, each molecule (either solute or hydrotrope) was optimized using TURBOMOLE, through its interface

TmoleX,[43] by adopting the COSMO-BP-TZVP template available in the software package. This template uses a def-TZVP basis set for all atoms, a DFT with the B-P86 functional and the COSMO solvation model (continuum with infinite permittivity). The molecule file obtained was used as input for the software COSMOtherm,[44,45] which implements the model COSMO-RS using the BP_TZVP_19.ctd parametrization.

In Chapter 6, the studied solutes were also optimized through the COSMO-BP-TZVPD-FINE template of TmoleX,[43] which uses a def2-TZVPD basis set for all atoms, a DFT with the B-P86 functional and the COSMO solvation model (continuum with infinite permittivity and a cavity fine grid size). This was carried out to perform a comparation between the BP_TZVP_19.ctd and BP_TZVPD_FINE_19.ctd parametrizations of COSMOtherm.

2.3 Cooperative Hydrotropy Model

Shimizu and Matubayasi[34] developed a statistical thermodynamics-based model (henceforth named cooperative hydrotropy model) to describe hydrotropy. The foundations of this model, which was developed not only to describe the usual sigmoidal solubility curves found in hydrotropy but also to give insight into the interactions between solute and hydrotrope molecules, are presented in Chapter 1, namely that hydrotropy occurs due to water-mediated aggregation of hydrotropes around the solute. The model can be expressed in the following manner:

$$ln\left[\frac{1-\frac{x_S}{x_{S,0}}}{\frac{x_S}{x_{S,0}}-\left(\frac{x_S}{x_{S,0}}\right)_{max}}\right] = m \cdot ln(x_H) + b \tag{2.3}$$

where x_S is the solute saturation mole fraction (solubility) in the hydrotropic system, $x_{S,0}$ is the solute saturation mole fraction in water and x_H is the mole fraction of the hydrotrope. Note that x_H is not the mole fraction of the hydrotrope in a solute-free basis but its mole fraction in the ternary water-hydrotrope-solute system. From the definition of x_S and $x_{S,0}$ it becomes clear that the term $x_S/x_{S,0}$ represents the relative solubility in mole fraction basis. As such, $\left(x_S/x_{S,0}\right)_{max}$ (henceforth *max*) is the maximum of the relative solubility caused by a given hydrotrope, i.e. the value of the plateau in the sigmoidal solubility curve. Finally, m and b are parameters that provide insight into the molecular interactions between solute and hydrotrope. More specifically, m represents the number of hydrotrope molecules in the vicinity of the solute.[34]

Although the model can be applied by extracting max from the experimental solubility data, this is not always trivial, especially when the solubility curve is not perfectly sigmoidal. A way to avoid this problem, which is used throughout this work, is to leave max as the adjustable parameter of the model. The modelling algorithm used goes as follow. A value is arbitrarily chosen for variable *max*.

Then, the m and b parameters are extracted from the experimental data as the slope and intercept of the linearized curve defined as:

$$Y = ln\left[\frac{1-\frac{x_S}{x_{S,0}}}{\frac{x_S}{x_{S,0}}-\left(\frac{x_S}{x_{S,0}}\right)_{max}}\right]; x = ln(x_H) \tag{2.4}$$

Using the calculated m and b parameters, the experimental data is reproduced using the model and the quadratic error between predicted and experimental data is calculated. Variable *max* is then varied until the sum of the quadratic errors is minimized.

The modelling described above is used in Chapter 3 of this work since most of the experimental data available pertains to a dilute concentration of the hydrotrope. However, when the concentration of the hydrotrope is high, such as the cases explored in Chapter 5, a more rigorous approach is to use the following expression for the Shimizu and Matubayasi[34] model:

$$\ln\left[\frac{1-\frac{S}{S_0}}{\frac{S}{S_0}-\left(\frac{S}{S_0}\right)_{max}}\right] = m \cdot \ln(x_H) + b \tag{2.5}$$

where S is the molar solubility (mol/L) of the solute in the hydrotropic system, S_0 is its molar solubility in water (mol/L) and $(S/S_0)_{max}$ is the maximum attainable relative solubility (the value at the plateau which a typical hydrotropy solubility curve reaches, henceforth noted as δ_{max}). Finally, m retains its physical meaning from Equation 2.3 (number of hydrotrope molecules involved in the solvation of the solute) and b is related to the facility of inserting that number of hydrotrope molecules in the volume corresponding to the vicinity of the solute.

Chapter 3
Glycerol Ethers as Hydrotropes

This chapter is based on the following article:

Glycerol Ethers as Hydrotropes and Their Use to Enhance the Solubility of Phenolic Acids in Water
B. P. Soares, D. O. Abranches, T. E. Sintra, A. Leal-Duaso, J. I. García, E. Pires, S. Shimizu, S. P. Pinho and J. A. P. Coutinho
ACS Sustainable Chemistry & Engineering **(2020)**
DOI: 10.1021/acssuschemeng.0c01032

Dinis O. Abranches contributed with formal data analysis and writing of the original draft.

3.1 Glycerol Ethers

Recently, glycerol ethers have been shown to behave as hydrotropes, making them a promising bio-based alternative for the commonly petrochemical-based hydrotropes,[46] while possessing lower vapor pressures and higher boiling points than their glycol ethers counterparts.[47] Glycerol ethers are amphiphilic compounds that possess a central hydrophilic glycerol back-bone, conferring them a certain degree of polarity, and apolar alkyl side-chains.[46–48] Besides glycerol being abundantly available (as a by-product of biodiesel production, for example[49]), glycerol ethers are synthetized from it via a green pathway.[50] Moreover, glycerol ethers may be viewed as *designer molecules*, since it is possible to tune their physicochemical properties by changing the number and size of their alkyl groups.[46,48,51–53] The name of these compounds is usually abbreviated as [x.y.z], where x, y and z, as shown in Figure 3.1, represent the number of carbon atoms of the alkyl chains linked to the oxygens in the three different positions of the glycerol backbone. A value of zero in any of these variables means that there is a proton linked to the oxygen instead of an alkyl chain, i.e. there is a hydroxyl group in that position.

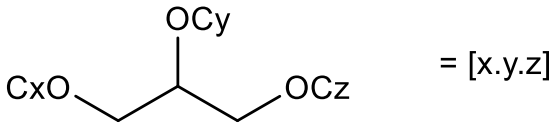

Figure 3.1. *Nomenclature for the alkyl glycerol ethers studied in this work.*

So far only a few works have been reported regarding the use of monoglycerol ethers as hydrotropes. Moity *et al*.[54] prepared three pentyl and three aryl 1-O-monoglyceryl ethers via esterification from glycerol, all presenting low volatility (vapor pressure below 0.01 kPa), and investigated their potential as hydrotropes. The results obtained show great solubility enhancement of a hydrophobic dye (Disperse Red 13), especially when using aryl monoglycerol ethers. Lebeuf et al.[55] have also studied the hydrotropic potential of mono, di and tri-alkyl glycerol ethers for a hydrophobic dye (Disperse Red 13). Some of the compounds studied, such as [2.1.1], [3.1.1], [4.1.1] and [2.2.2], have a solubility limit, not being fully miscible with water, and are also the most volatile. Among the hydrotropes studied, [5.0.0] presents the greater solubilization power at low concentrations (up to 30 wt.%) and possesses the highest boiling point (262 ºC), making it one of the best candidates to be used as an hydrotrope in that case.

In this chapter, the effect of the alkyl side chain of glycerol ethers on the solubility enhancement of two phenolic acids, the poorly water-soluble gallic and syringic acids (Figure 3.2), is studied (see section A1 of the Appendix for the list of glycerol ethers used). These solutes were selected as model compounds for this study due to their relevant bioactivities such as strong antioxidant properties,[56,57]

their presence in a wide variety of natural organic matrices and industrial applications,[57,58] and their different levels of polarity, with syringic acid being more hydrophobic than gallic acid (suggested by their different octanol/water partition coefficients[59]). Moreover, gallic and syringic acids are monomers of lignin and excellent model molecules for its solubility in hydrotropic systems, an active area of research.[16–18,60] The experimental data obtained was used to better understand the mechanism of hydrotropy, through the calculation of Setschenow constants.[61] Additionally, the recently proposed thermodynamics model of cooperative hydrotropy, developed by Shimizu and Matubayasi[34] and detailed in Chapter 2, was used to fit the solubility data, enabling an analysis for the estimation of the recovery ease of the solutes from the hydrotropic systems by using water as anti-solvent.

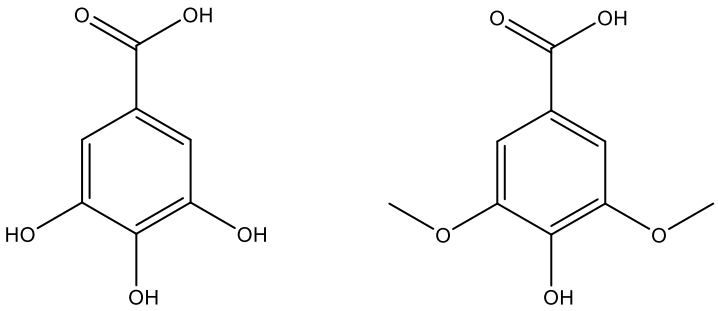

Figure 3.2. *Chemical structure of gallic acid (left) and syringic acid (right).*

3.2 Solubility Curves

The solubility of gallic acid and syringic acid in aqueous solutions of glycerol ethers was measured in the entire concentration range, at 303.2 K. Since [6.0.0] forms a two-phase system with water[46] at concentrations below 38 wt% its hydrotropic capability was studied only for gallic acid in the single-phase region. The solubility data for gallic acid is shown in Figure 3.3, where S and S_0 represent the solubility (mol/L) of gallic acid in the aqueous solutions of the hydrotrope and in pure water, respectively. Choosing attainable maximum solubility as the metric of interest, the ability of the linear glycerol ethers to enhance the solubility of gallic acid increases in the following order: [6.0.0] < [5.0.0] < [4.0.0] < [3.0.0] < [2.0.0] < [1.0.0]. Moreover, [1.0.1] is better than [2.0.2] while glycerol shows the least solubility enhancement. This initial analysis suggests that the shorter the alkyl chain of the hydrotrope, the better the solubility enhancement. Note that the maximum solubility of gallic acid in aqueous [1.0.0] or [1.0.1] is about the same, with the plateau being reached at a lower concentration for the [1.0.1] curve.

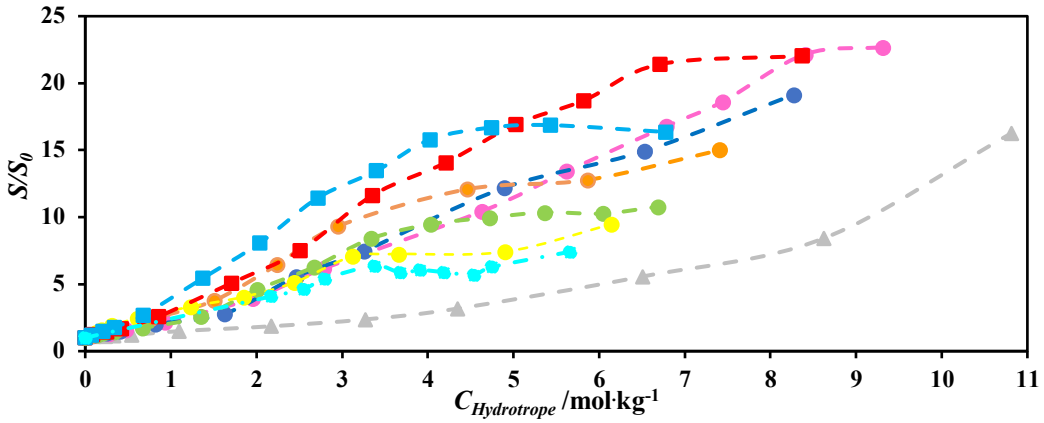

Figure 3.3. *Effect of glycerol ether (hydrotrope) concentration on the solubility of gallic acid in aqueous solutions of [1.0.0]●, [2.0.0] ●, [3.0.0] ●, [4.0.0] ●, [5.0.0] ●, [6.0.0] ●, [1.0.1] ■, [2.0.2] ■ and glycerol ▲, at 303.2 K. S/S_0 is the relative solubility (expressed in mol/L) of the solute and $C_{Hydrotrope}$ is the concentration of the hydrotrope in the solvent (solute-free basis). Dashed lines are visual guides.*

The solubility data for syringic acid is depicted in Figure 3.4. Contrary to what is seen in Figure 3.3, most of the solubility curves depicted in Figure 3.4 pass through a maximum, with glycerol and [1.0.0] as the exceptions, suggesting an optimal concentration of hydrotrope. Again considering attainable maximum solubility as the metric of interest, the conclusions drawn from Figure 3.3 for gallic acid hold true for syringic acid as well. Hence, it appears that the smaller the hydrotrope the better the solubility enhancement. Interestingly, the increase in solubility of syringic acid is proportionally much more pronounced than that for gallic acid. For instance, it is possible to reach a 77-fold increase in the solubility of syringic acid using [1.0.1] while a 22-fold increase in solubility was achieved for gallic acid with the same hydrotrope.

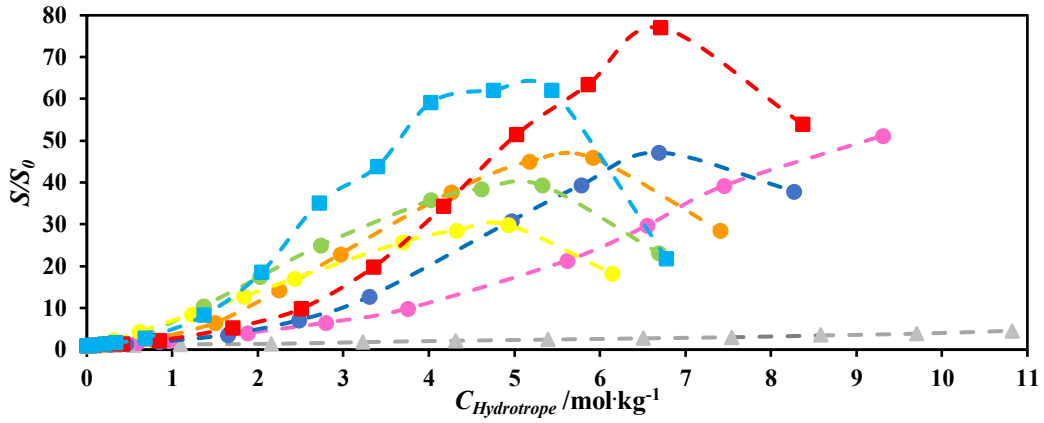

Figure 3.4. *Effect of glycerol ether (hydrotrope) concentration on the solubility of syringic acid in aqueous solutions of [1.0.0]●, [2.0.0] ●, [3.0.0] ●, [4.0.0] ●, [5.0.0] ●, [1.0.1] ■, [2.0.2] ■ and glycerol ▲, at 303.2 K. S/S_0 is the relative solubility (expressed in mol/L) of the solute and $C_{Hydrotrope}$ is the concentration of the hydrotrope in the solvent (solute-free basis). Dashed lines are visual guides.*

The solubility enhancement of gallic and syringic acids obtained using glycerol ethers as hydrotropes was compared against results using co-solvency with traditional solvents (Figure 3.5). As Figure 3.5 clearly demonstrates, glycerol ethers are much better solubilizing agents for gallic acid than traditional co-solvents such as methanol, acetonitrile and propan-2-ol. Even glycerol, the worst hydrotrope studied in this work, is better than traditional co-solvents. While methanol provides higher solubility values than glycerol in the solubilization of syringic acid, it is much inferior to [1.0.1] in most of the concentration range. Methanol is, indeed, commonly added to enhance the solubility of hydrophobic substances, but possesses high volatility and toxicity,[62] contrary to the glycerol ethers studied in this work.[51,52,63,64] It is interesting to note that the methanol solubility curve for gallic acid presents a linear shape, in contrast with its sigmoidal shape for syringic acid, similar to what is expected in hydrotropy.

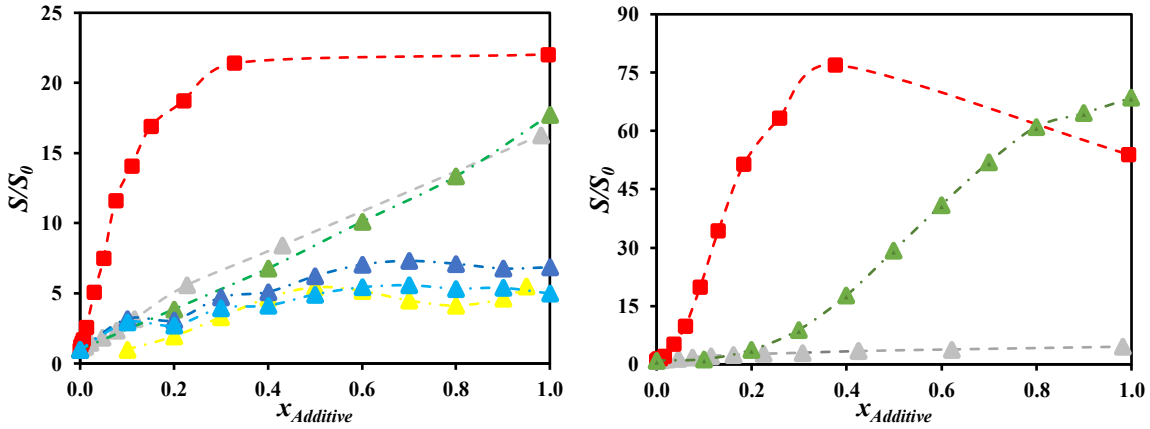

Figure 3.5. *Solubility enhancement of gallic acid (left panel) and syringic acid (right panel) using the hydrotropes [1.0.1]■, and [0.0.0]▲ (this work) and the co-solvents methanol▲*[65,66]*, ethanol▲*[67] *acetonitrile▲*[68] *and propan-2-ol▲*[68]*. S/S_0 is the relative solubility (expressed in mol/L) of the solute and the x-axis represents the mole fraction of the additive (hydrotrope or co-solvent) in the solvent (solute-free basis). Dashed lines are visual guides.*

3.3 Dilute Region

The pronounced effect of glycerol ethers as hydrotrope agents, when compared to traditional organic solvents, is of great interest for extraction processes, especially in the replacement of traditional volatile organic compounds. However, apart from studying the entire concentration range of hydrotrope, the careful analysis of the dilute hydrotrope region is also important for the following reasons. Firstly, from an application-wise perspective, using smaller quantities of additives (hydrotropes) is economically preferable. Secondly, from a fundamental perspective the identification of the molecular mechanism of hydrotropy is easier in the dilute region where effects can be isolated (contribution from the hydrotrope self-association in the bulk phase can, for instance, be neglected). To study the dilute region the Setschenow constant was used.[61] Originally this was

proposed as an empirical approach to describe the effect of a salt, or co-solvent on the solubility of a compound in aqueous solution, and has since been applied to describe the effect of hydrotropes on the aqueous solubility of solutes.[69,70] It has been shown, using statistical thermodynamics, that this approach has a sound physical basis in the dilute region.[71]

The Setschenow constant[61] quantifies the change in the solubility of a solute due to the presence of a hydrotrope, in the dilute region. It is herein defined as:

$$\ln(S) = K_H \cdot C_H \tag{3.1}$$

where S is the molar solubility of the solute, K_H is the Setschenow constant and C_H is the molarity of the hydrotrope. Equation 3.1 is valid from a hydrotrope molarity of zero up to a value where the variation of the natural logarithm of the solubility of the solute remains linear with the increase in the molarity of the hydrotrope (about 5 wt% for the hydrotropes studied in this work).

Besides being useful to quantify the hydrotropic power of a substance (albeit in the dilute region), Setschenow constants can also be linked to statistical thermodynamics. The Setschenow constants calculated as per Equation 3.1 are related to Kirkwood–Buff Integrals (KBI) through the following expression[71]:

$$K_H = G_{S,H} - G_{S,W} \tag{3.2}$$

where $G_{S,H}$ is the KBI between solute and hydrotrope and $G_{S,W}$ is the KBI between solute and water. Equation 3.2 shows that the higher the Setschenow constant is, the higher the preference of the solute to interact with the hydrotrope instead of with water and, consequently, the higher the solubility enhancement of the solute.

The Setschenow constants were calculated for all solute-hydrotrope pairs reported in this chapter (assuming density of the systems in the dilute region equal to that of water), except for [6.0.0] since solubility data in the dilute region is not available for this compound. These results are reported in Table 3.1. Interestingly, the values obtained are in contradiction with the initial qualitative analysis from Figures 3.3 and 3.4. That is, the hydrotropic power of glycerol ethers in the dilute region increases with the increase in size of the alkyl side chain, in line with previous studies[55]: [0.0.0] < [1.0.0] < [2.0.0] < [3.0.0] < [4.0.0] < [5.0.0].

Table 3.1. *Setschenow constants for gallic and syringic acids in the glycerol ether hydrotrope systems studied in this work, along with the hydrotrope molarity range considered in their calculation.*

	Hydrotrope	Setschenow Constant	Molarity Range /M
Gallic acid	[0.0.0]	0.149	0-0.3
	[1.0.0]	0.802	0-0.5
	[2.0.0]	0.976	0-0.3
	[3.0.0]	1.273	0-0.2
	[4.0.0]	1.528	0-0.2
	[5.0.0]	2.054	0-0.2
	[1.0.1]	1.171	0-0.3
	[2.0.2]	1.560	0-0.2
Syringic acid	[0.0.0]	0.129	0-0.6
	[1.0.0]	0.988	0-0.3
	[2.0.0]	0.759	0-0.3
	[3.0.0]	1.148	0-0.2
	[4.0.0]	1.604	0-0.2
	[5.0.0]	2.443	0-0.2
	[1.0.1]	1.401	0-0.3
	[2.0.2]	1.667	0-0.2

The results reported in Table 3.1 are in agreement with a previous study by Bauduin and co-workers[23] that suggested the apolar volume of an hydrotrope to be directly connected with its capability to enhance the solubility of a solute. In fact, the progressive increase, through the addition of methyl groups, in apolar volume of the glycerol ethers seems to positively correlate with the Setschenow constants obtained, shedding light into the molecular mechanisms of hydrotropy.

Considering Equation 3.2, which has shown that Setschenow constants increase if the KBI of the solute-hydrotrope pair increases or the KBI of the solute-water pair decreases, it makes sense that apolarity or hydrophobicity plays a role in hydrotropy. An increase in the hydrophobicity of the solute should lead to a decrease of its interaction with water, leading to a decrease of the solute-water KBI and a consequent increase in the Setschenow constant. This is exactly what is seen in this work: for the same hydrotrope, the Setschenow constant obtained for systems containing syringic acid are higher than that of gallic acid (syringic acid has a higher octanol/water partition coefficient than gallic acid, suggesting it is more hydrophobic than gallic acid[59]). On the other hand, increasing the hydrophobicity of the hydrotrope weakens its interaction with water, promoting interaction with the hydrophobic solute, leading to an increase in the solute-hydrotrope KBI, increasing the Setschenow constant, in accordance to what is reported in Table 3.1.

It is not yet clear why there is an inversion on the behavior of the hydrotropic power of glycerol ethers above a certain concentration range, with more hydrophobic hydrotropes being better at low concentrations and more hydrophilic hydrotropes being better at higher concentrations. The

Setschenow analysis above reveals that the size of the alkyl chain length appears to be the dominating factor at low concentrations. However, it is expectable that increasing hydrotrope concentration will also increase the activity coefficient of water, as supported by the immiscibility observed for [6.0.0]. That is, increasing the alkyl chain length of the hydrotrope increases its hydrophobicity, leading to a less favorable interaction to water for high hydrotrope concentration. Thus, above a certain concentration of these hydrotropes, the nefarious effect of being too hydrophobic prevails over favorable solute-hydrotrope interactions, leading to a drastic negative impact in the hydrotropic behavior.

3.3 Cooperative Hydrotropy Model

The solubility data obtained in this work was fitted using the statistical thermodynamics-based model developed by Shimizu and Matubayasi[34] and introduced in Chapter 2. The procedure for the application of the model is illustrated in Figure 3.6a) with Equation 2.4, and Figure 3.6b) with the actual fitting, both for the syringic acid-[3.0.0] solute-hydrotrope pair. Fitted curves and optimization details for all systems herein studied are provided in section A2 of the Appendix.

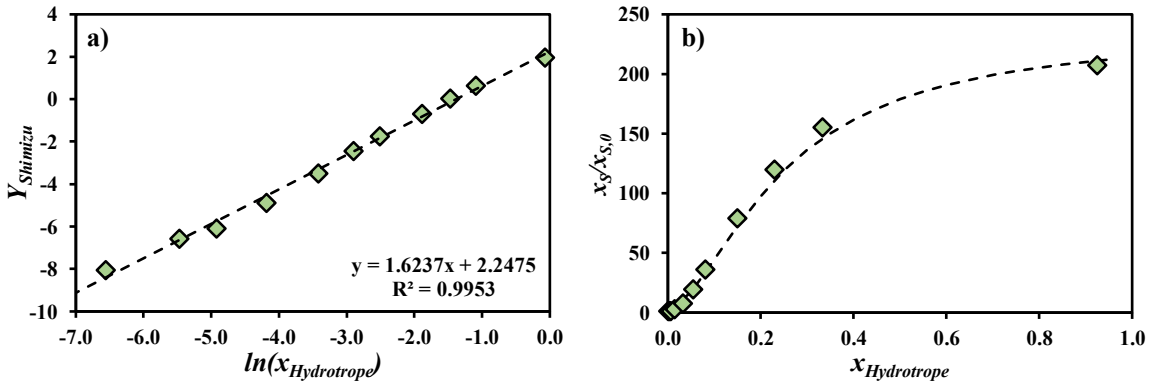

Figure 3.6. *Linearized plot of the cooperative hydrotropy model based on Equation 2.4 (left panel, ◆ experimental data, - - - least squares fit) and fitted experimental data (right panel, ◆ experimental data, - - - cooperative hydrotropy model) for the water-[3.0.0]-syringic acid system. The x-axis represents the mole fraction of the hydrotrope in the ternary system (as opposed to its mole fraction in the solvent free of solute).*

As Figures A2.1 and A2.2 show (see section A2 of the Appendix), the model reproduces the experimental data quite well. It is curious to note that the characteristic sigmoidal shape of hydrotropic solubility curves is much more patent in the systems with syringic acid than in the systems with gallic acid. Moreover, it is important to note that expressing the composition of hydrotrope in the actual ternary system instead of its composition in the solvent (solute-free basis) removes the maxima seen in the solubility curves depicted in Figures 2 and 3. No clear pattern can be identified on the model parameters, which are reported in Table A2.1 (section A2 of the Appendix).

The cooperative model employed in this work (Equation 2.3) can be applicable not only to cooperative (sigmoidal) solubility increases but also linear (non-cooperative cases), such as those seen for gallic acid. In the latter case, *m* becomes close to 1, leading to a very large *max* variable. Thus, the general applicability of the model is supported by its success in describing both linear and sigmoidal solubility curves.

3.4 Solute Recovery

Besides quantifying their dissolution ability, it is fundamental to address the recovery of solute from hydrotropic solutions. For most organic solvents, a simple evaporation suffices. However, evaporating water from a hydrotropic solution would increase hydrotrope concentration which, generally, would increase the solubility of the solute. Moreover, the hydrotropes are often non, or poorly volatile. There is, however, a clever turnaround that allows for the easy recovery of solute from an hydrotrope solution with similar energy cost when compared to traditional solvents: the use of water as anti-solvent. As proposed in previous works,[24,72–74] addition of water to an hydrotropic solution may induce the precipitation of the solute due to the dilution of the hydrotrope, providing an easy and straightforward approach to recover the solute in high purity.

Whether this approach to solute recovery is feasible was here evaluated by calculating the recoverable fraction of dissolved solute, using the solubility curves modelling reported in the previous section. The calculation algorithm and detailed results are reported in section A3 of the Appendix. Figure 3.7 illustrates the recovery curves (recovered solute fraction versus water volume fraction added) obtained using the hydrotrope [1.0.1] for gallic acid and syringic acid. Note that a negative solute fraction is possible, meaning that there is no precipitation and the system is no longer saturated, thus, being able to dissolve more solute.

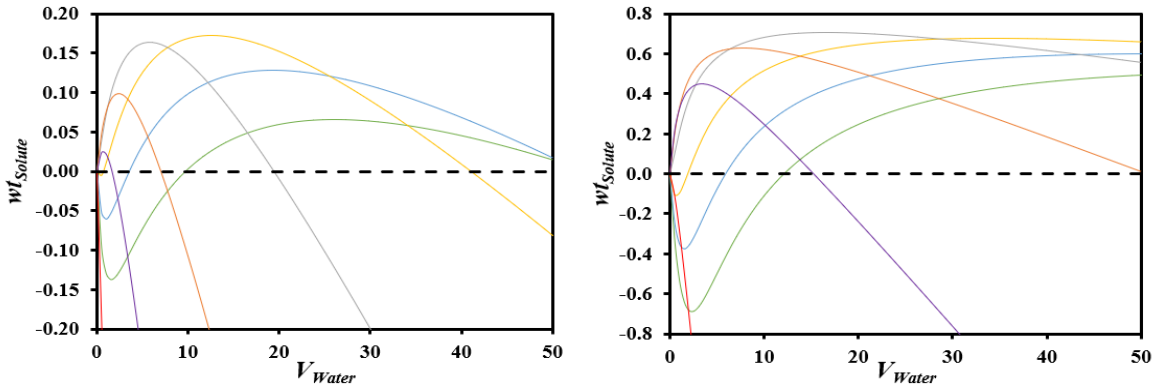

Figure 3.7. *Estimated fraction of gallic acid (left panel) and syringic acid (right panel) recovered from hydrotrope solution (wt_{Solute}) by the addition of water (V_{Water} is the volumetric ratio between added water and initial system), with an initial hydrotrope mole fraction of 0.01 —, 0.05 —, 0.1 —, 0.2 —, 0.4 —, 0.6 — and 0.8 —. A negative value indicates that no precipitation happens, with the system being able to dissolve further solute.*

Surprisingly, addition of water does not always lead to solute precipitation. Considering the examples depicted in Figure 3.7, both hydrotrope and its composition clearly play a role in determining the feasibility of recovering the solute by using water as anti-solvent. For instance, in this case (gallic acid-[1.0.1] system), the solute can only be recovered if the hydrotrope mole fraction is in the 0.05-0.4 range, with a maximum recovery of 17% achieved in the 0.2-0.4 hydrotrope mole fraction range. If the hydrotrope mole fraction is higher than 0.4, the solute may still be recoverable but only after the addition of a large quantity of water. Below a mole fraction of 0.05, solute recovery is unfeasible. These conclusions are similar for the syringic acid-[1.0.1] system. In this case, the solute can be recovered in a narrower mole fraction window, but up to 70% can be recovered.

Despite the increased volume of water when water is added to a hydrotropic system, the hydrotrope becomes less concentrated, which makes hydrotropy less effective. Whether any amount of solute precipitates from a hydrotrope solution after adding water is determined by the trade-off between these two factors. Thus, the recovery of solute is more favorable as the slope of the solute solubility curve increases, which corresponds to a bigger change in solubility due to a smaller change in hydrotrope concentration. It is also important to note that, since syringic acid is much less soluble in water than gallic acid, it is easier to recover it since the first factor (solute dissolution in the new water volume) loses importance. Moreover, the slope of the solubility curves tends to be higher in mid composition ranges of hydrotrope (sigmoidal shape), explaining the recovery windows positioned in mid hydrotrope mole fractions.

Figure A3.1 reveals that, in terms of gallic acid recovery, it is better to use a hydrotrope mole fraction of 0.2-0.8 for the most hydrophilic hydrotropes ([1.0.0] and [2.0.0]), whilst a 0.05-0.2 window is better for the least hydrophilic ones. Interestingly, it is impossible (using the addition of water) to recover gallic acid dissolved in aqueous [5.0.0] solutions. The same conclusions hold true for syringic acid, as Figure A3.2 shows, albeit in narrower mole fraction windows, similarly to what was concluded through the analysis of Figure 3.7. The biggest difference is the fraction of solute recovered, which is much higher for syringic acid than for gallic acid, due to the almost 10-fold difference between their solubility in pure water.

Chapter 4
The Mechanism of Hydrotropy

This chapter is based on the following article:

Unveiling the Mechanism of Hydrotropy: Evidence for Water-Mediated Aggregation of Hydrotropes Around the Solute
D. O. Abranches, J. Benfica, B. P. Soares, A. Leal-Duaso. T. E. Sintra, E. Pires, S. P. Pinho, S. Shimizu and J. A. P. Coutinho
Chemical Communications **(2020)**
DOI: 10.1039/D0CC03217D

Dinis O. Abranches contributed with conceptualization, methodology, formal data analysis and writing of the original draft. This article was highlighted in Nature Reviews Chemistry (https://doi.org/10.1038/s41570-020-0202-3).

Despite stemming from the principles of statistical thermodynamics and its consequent superiority, in terms of theoretical grounds, to the previous hypothesis for the mechanism of hydrotropy, no direct experimental evidence has been to this day reported for the water-mediated accumulation mechanism proposed. In this chapter it will be shown that (1) the hydrophobic interaction between a hydrotrope and a solute is the driving force for the accumulation and that (2) such interaction can be quantified via a measure for apolarity derived using COSMO-RS. Both results are crucial to understand the mechanism of hydrotropy and support the hypothesis of strong water-mediated solute-hydrotrope apolar interactions.

4.1 ^{1}H-NMR

Proton nuclear magnetic resonance (^{1}H-NMR) is herein employed to provide experimental evidence for hydrotrope-solute aggregation. The strategy is based on the well-known principle that the chemical shifts of the protons of a molecule dissolved in water may change due to the presence of another substance.[69,75] More precisely, a chemical shift that diminishes in the presence of another substance infers a higher shielding of that proton or a less probable contact between it and water. Thus, the chemical shifts of the protons associated to apolar moieties (namely methyl groups) of a hydrotrope dissolved in water can be measured in the presence and absence of a solute. If the solute induces the aggregation of hydrotropes around itself through water-mediated apolar interactions, as is predicted by statistical thermodynamics, the chemical shift of the protons associated to the apolar moieties of the hydrotrope should decrease.

Gallic acid and syringic acid were chosen as solutes and monoalkylglycerol ethers, listed in Table 4.1, as hydrotropes. Note that the apolarity of monoalkylglycerol ethers can be made to vary smoothly through the progressive increase in the length of their alkyl chain. Likewise, gallic acid and syringic acid are structurally similar but present different hydrophobicities. Furthermore, Kunz and co-authors pointed out the necessity to study this class of hydrotropes.[32] The solubilities of both acids in monoalkylglycerol ether aqueous solutions were studied in Chapter 3. For each hydrotrope-solute pair, ^{1}H-NMR spectra were acquired thrice. In each case, the concentration of hydrotrope was maintained (0.4 mol/kg) but solute concentration was changed, from zero solute, which serves as reference for the chemical shifts of the hydrotrope, to concentrations below and above solute solubility in pure water. The NMR peaks considered, clearly marked in section A4 of the Appendix, were those of the protons of the alkyl side chain of the monoalkylglycerol ether along with the sole proton of the second carbon of the glycerol head. The protons of the first and third carbon of the glycerol head were not analysed due to the difficulty of distinguishing their peaks in the NMR spectra.

Table 4.1. *Solute concentration in the hydrotropic systems (0.4 mol·kg^{-1} of hydrotrope) whose ^{1}H-NMR spectra was measured in this work.*

Hydrotrope	Gallic Acid Concentration /mol·kg^{-1}	Syringic Acid Concentration /mol·kg^{-1}
	0	0
[1.0.0]	0.06	0.005
	0.12	0.010
	0	0
[2.0.0]	0.06	0.005
	0.12	0.010
	0	0
[3.0.0]	0.06	0.005
	0.12	0.010
	0	0
[4.0.0]	0.06	0.008
	0.12	0.013
	0	0
[5.0.0]	0.06	0.010
	0.12	0.018

The results obtained using gallic acid as a solute (Figure 4.1a as an illustrative example and Figure A5.1 of section A5 of the Appendix) show that the chemical shift of the protons diminishes as the concentration of solute increases. This means that the apolar moieties of the hydrotropes are statistically less prone to interact with water, providing evidence for the idea of association between these moieties and the apolar moieties of the solute. Moreover, the decrease in chemical shift seen in Figures 4.1a and A5.1 is proportional to the concentration of solute. This is expected since if more solute is present in the system, more hydrotrope is needed to interact with it. Because syringic acid is much less soluble in water, its concentration was one order of magnitude lower than that of gallic acid in the NMR experiments, leading to smaller changes in the chemical shifts of the hydrotrope. In some cases, the changes produced are comparable to the experimental uncertainty of the technique (*ca.* 0.002 ppm). Nevertheless, the conclusions taken from the NMR results of gallic acid hold true for syringic acid as well, as depicted in Figures 4.1b and A5.2 (section A5 of the Appendix)

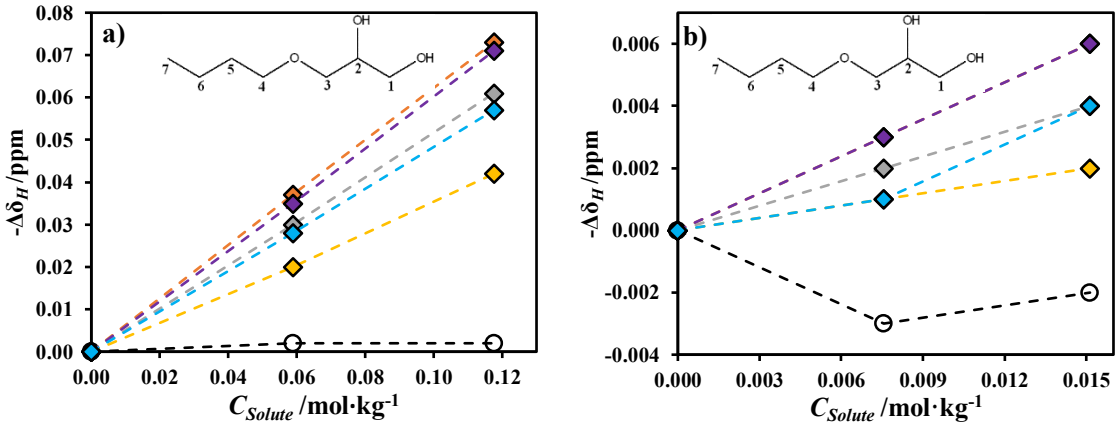

Figure 4.1. *Change in chemical shift of the protons ($-\Delta\delta_H$) associated to water and several methyl groups of [4.0.0] (structure as inset) dissolved in water (0.4 mol/kg) as a function of a) gallic acid or b) syringic acid concentration. Legend: -○- water; -◇- 2nd carbon; -◇- 4th carbon; -◇- 5th carbon; -◇- 6th carbon; -◇- 7th carbon.*

The NMR results question the idea that pre-clustering of the hydrotrope is fundamental in hydrotropy. Hydrotropes unquestionably do possess a degree of aggregation (clustering) with themselves. However, the hydrotrope aggregation (whether it is present depends on the system) clearly changes with the addition of the solute, providing clear evidence that the solute is not merely entering a "micelle"-like bulk-phase pre-clustering of the hydrotrope. If this were the case, there should be no change in the chemical shifts of the hydrotrope protons, since alternating from a previously hydrotrope-hydrotrope contact to a hydrotrope-solute contact would not make the hydrotrope less prone to interact with water, hence would not lead to a decrease in the chemical shifts.

Insight is given by Figures 4.1, A5.1 and A5.2 not only into its existence but also into the geometry of aggregation. In fact, the peak assigned to the protons of the second carbon of the hydrotrope always shifts less than the remaining peaks. This means that the second carbon is less prone to aggregation, which is explained by its higher degree of polarity, brought about by the presence of hydroxyl groups in its vicinity. Moreover, for all systems, the peak assigned to the protons in the last methyl group of the side alkyl chain is consistently the second less-shifting peak. That is, the second less-shifting peak for [2.0.0] is that of carbon 5, for [3.0.0] is that of carbon 6, for [4.0.0] is that of carbon 7 and for [5.0.0] is that of carbon 8 (see insets of Figure A4.1 for clarification). This can be interpreted in terms of interaction geometry; a parallel contact between hydrotrope and solute covers more apolar area, thus being more energetically favourable to water, than a hydrotrope tail-solute contact.

It has been argued that, for certain types of apolar yet slightly hydrophilic solutes, hydrotropy could occur due to hydrotrope-solute interactions through their polar functional groups.[33] This is clearly not the case for the solutes and hydrotropes studied in this work, since NMR spectroscopy revealed

that the aggregation of hydrotrope around the solute happens through apolar contacts, even giving information about the geometry of these contacts.

4.2 Apolar Factors

Having provided direct, experimental evidence for the hydrotrope-solute aggregation, its driving force is now addressed. As a quantitative measure for the apolarity of a molecule, the unnormalized σ-profile framework of COSMO-RS has been adopted.[37] This is a histogram representing the amount of molecular surface with a given polarization charge-density, σ. The unnormalized σ-profile framework should prove advantageous for the study of hydrotropy since it can quantify the apolarity of both hydrotrope and solute. Moreover, the geometry and polarity of molecules optimized within the COSMO solvation model should more closely resemble that which is found in a real aqueous solution than molecules optimized in the gas phase. Details for the optimization of the solute and hydrotrope molecules herein studied are given in Chapter 2.

To study the relationship between apolarity and hydrotropy using the σ-profile framework, an apolar factor was defined:

$$\int_{-0.0082}^{+0.0082} p(\sigma) \cdot (0.0082 - |\sigma|) \cdot d\sigma \tag{4.1}$$

This factor is a measure of the area under the curve of the apolar region, with the apolar/polar limit being defined as σ = -0.0082 e/Å^2 and σ = +0.0082 e/Å^2, in line with previous studies.[37,76] The amount of apolar surface area, $p(\sigma)$, is weighted by the actual polarity of the surface, with regions near the apolar/polar limit being progressively penalized by the term $(0.0082 - |\sigma|)$. The Setschenow constant (the ratio between solubility enhancement and hydrotrope concentration in the dilute region) of several hydrotropic systems previously reported in the literature was correlated against this apolar factor. Section A6 of the Appendix contains the apolar factors of these hydrotropes and the correlations obtained for systems taken from the literature where the Setschenow constants were reported for different hydrotropes but the same solute. Figure 4.2 below depicts the correlations obtained for the glycerol ether systems studied in this chapter. The results obtained show that, for the same family of hydrotropes, the solubility enhancement of the solute positively correlates with the apolar factor of the hydrotrope. This supports the view of water-mediated aggregation of hydrotrope around the solute and supports the idea of hydrotrope apolarity as the driving force of hydrotropy.

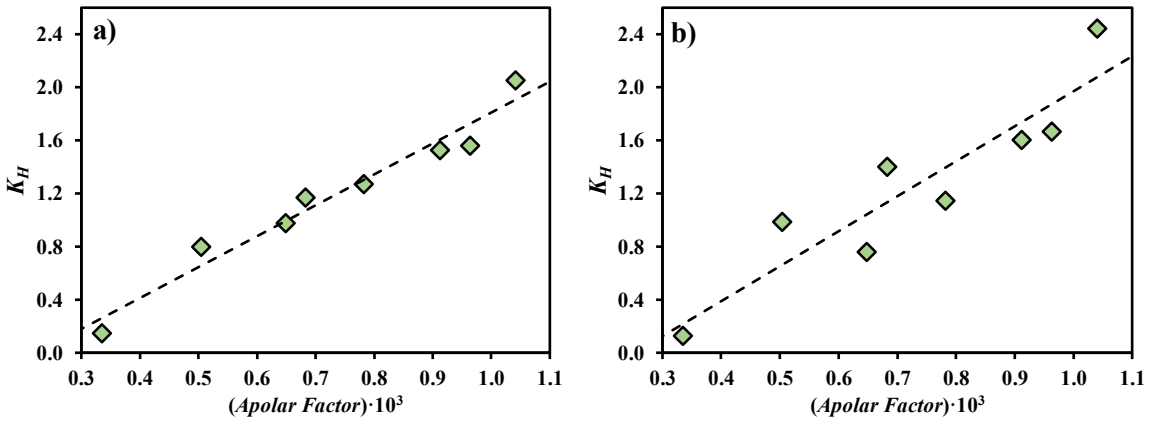

Figure 4.2. *Setschenow constants (Chapter 3) for a) gallic acid or b) syringic acid in glycerol ether-based hydrotropic solutions as a function of the apolar factor of the hydrotrope. The dashed line is the straight line fitted to the data using the least squares method.*

Shimizu and Matubayasi[34] derived a hydrotropy model based on cooperative water-mediated hydrotrope-solute aggregation using statistical thermodynamics. When regressed against experimental solubility curves, this model returns the average number of hydrotrope molecules in the vicinity of the solute (parameter *m*). Since this model was previously applied to the systems herein studied (Chapter 3), Figure 4.3 depicts this parameter plotted against the apolar factor of the corresponding hydrotrope. The resulting plot shows that *m* reaches a maximum for both gallic acid and syringic acid. Surprisingly, this maximum is located at the apolar factor of the solute. As described above, solute-hydrotrope interactions are established between their apolar moieties, resulting in strong and favourable interactions only due to the presence of water. However, there is no distinction between apolar moieties of solute and hydrotrope. Consequently, a hydrotrope that is more apolar than the solute will tend to agglomerate with itself more promptly than with the solute. Put differently, in terms of apolar contacts, it is as if there are three different forms of hydrotrope present in the system: free hydrotrope, hydrotrope associated with solute and hydrotrope associated with itself. This, again, disputes the pre-clustering hypothesis, since more self-aggregation of the hydrotrope leads to less aggregation around the solute.

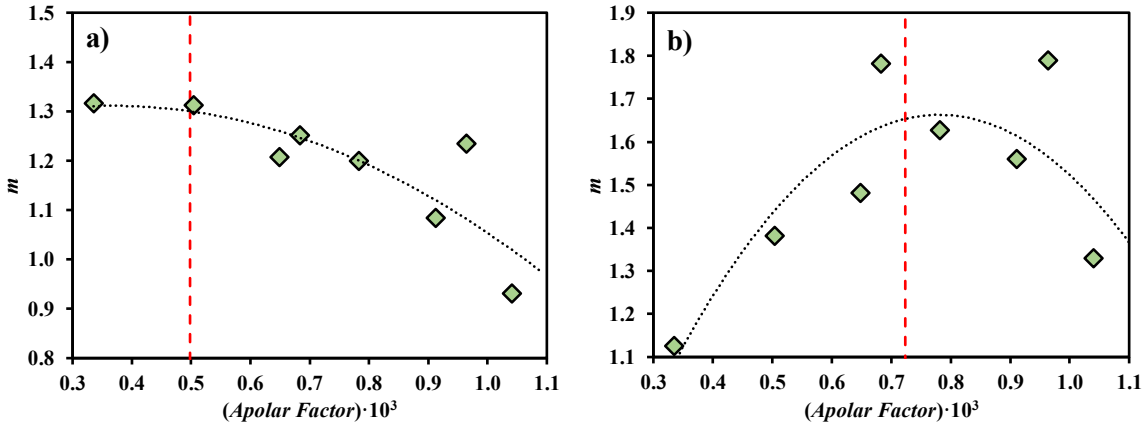

Figure 4.3. *Dependency of the number of hydrotrope molecules in the vicinity of the solute (m) on the apolar factor of the hydrotrope, estimated using the cooperative hydrotropy model for a) gallic acid and b) syringic acid in aqueous solutions of glycerol ethers. The black dashed line is a visual guide whilst the red dashed line represents the apolar factor of the solute.*

Note that links between hydrophobicity of the hydrotrope and the extent of hydrotropy have been proposed before.[23,32,33] However, this is the first time that these parameters (hydrotropy extent and apolarity of the hydrotrope) are quantified and shown to correlate remarkably well with each other. Furthermore, it is shown that the apolarity of the hydrotrope is not the only factor influencing hydrotropy. In fact, the driving force for aggregation is the balance between apolarity of both solute and hydrotrope, as demonstrated by Figure 4.3.

Figure 4.3 shows that hydrotropes that are more apolar than the solute will tend to aggregate less around it. This does not translate, however, into a maximum on the solubility enhancement (Figure 4.2) for the case of glycerol ethers. This is rationalized by taking into account that even though the most apolar hydrotropes may statistically possess less molecules around the solute, they are able to cover more of its apolar area due to their larger size and chain linearity, and, thus, increase its solubility.

In conclusion, experimental evidence based on ^{1}H-NMR chemical shifts is here reported for the first time showing that hydrotrope molecules aggregate around the solute, which supports the cooperativity theory of hydrotropy. Moreover, it was shown that apolarity of both hydrotrope and solute is the driving force of hydrotropy, with strong solute-hydrotrope interactions arising in the presence of water. These interactions are statistical and are established between apolar moieties of both solute and hydrotrope, instead of interactions between their polar functional groups. These water-mediated interactions are, however, not exclusive to solute-hydrotrope pairs and the number of hydrotropes aggregated around the solute is maximum when the apolarity of hydrotrope and solute is the same. The results reported in this work are, thus, of the utmost importance in the understanding of the water-mediated hydrotrope-solute interactions hypothesis and provide the necessary

background to design new hydrotrope molecules for specific applications. A schematic illustration of the mechanism of hydrotropy, in light of these findings, is provided in Figure 4.4.

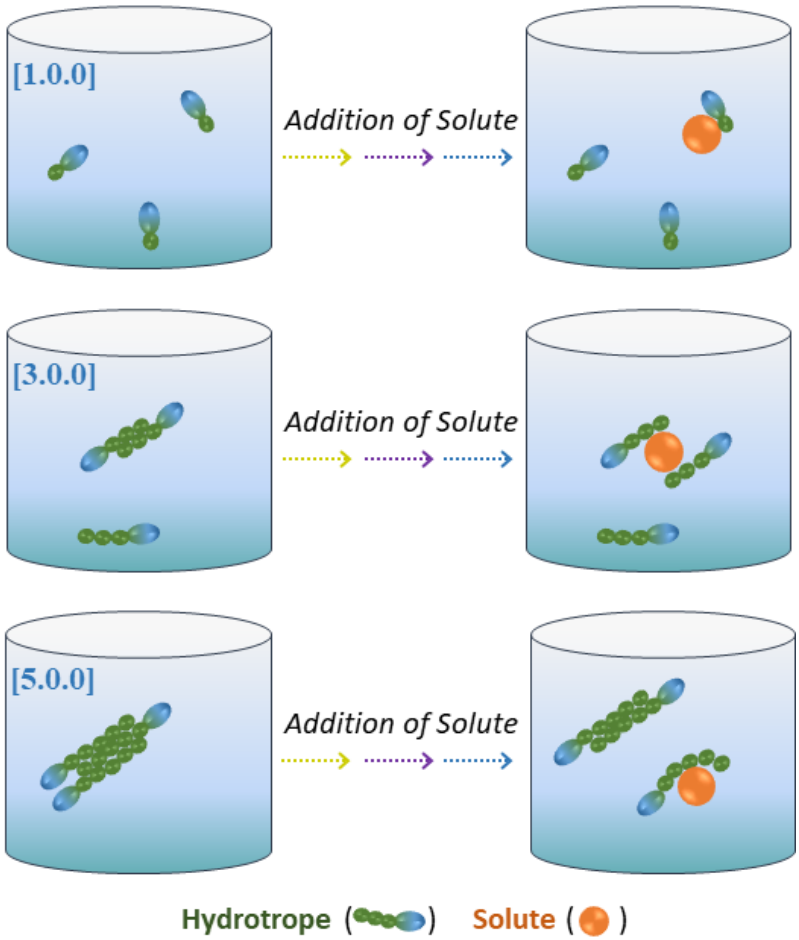

Figure 4.4. *Schematic illustration of the hydrotropy mechanism, evidencing the main findings in this work. In the first case, apolarity of the hydrotrope is small and the driving force for aggregation is low; in the second case, apolarity of the hydrotrope is equal to that of the solute and the driving force for aggregation is maximized, resulting in more hydrotrope molecules aggregated around the solute; in the third case, apolarity of the hydrotrope is greater than that of the solute and, thus, driving force for hydrotrope-hydrotrope aggregation is larger than that of hydrotrope-solute aggregation.*

Chapter 5
Hydrotropy in Cyrene

This chapter is based on the following submitted article:

The Perspective of Cooperative Hydrotropy on the Solubility in Aqueous Solutions of Cyrene
D. O. Abranches, J. Benfica, S. Shimizu and J. A. P. Coutinho
Industrial & Engineering Chemistry Research

Dinis O. Abranches contributed with conceptualization, methodology, formal data analysis and writing of the original draft.

5.1 Cyrene

Dihydrolevoglucosenone, more commonly known as Cyrene, is a novel green solvent produced from cellulose in a two-step process.[35,77–79] A good hydrogen bond accepting capacity, owing to its one carbonyl and two ether groups, makes Cyrene a polar yet aprotic solvent, with properties similar to other aprotic solvents such as NMP (N-methyl-2-pyrrolidone). Due to its biodegradability and the abundance of its precursor, Cyrene has attracted considerable interest, with studies showing it to be an excellent medium for a wide variety of chemical reactions,[80–87] including graphene processing.[88]

Recently, Cyrene was reported to be a hydrotrope that could enhance the solubility of various hydrophobic substances.[36] This is particularly interesting since the resulting solvent (water-Cyrene system) is classified as a bio-based and biodegradable solvent, whose properties, namely polarity, can be tuned by changing the concentration of its components. Despite its appeal, the behaviour of solutes in water-Cyrene mixtures is complex due to the reactivity of Cyrene with water. In fact, Cyrene reacts partially and reversibly with water to form the corresponding geminal diol. This geminal diol, in turn, is acidic, partially dissociating in water.[89] In this way, water-Cyrene mixtures are complex systems containing water, the ketone, and protonated and deprotonated diol forms of Cyrene. Considering that each of these individual species can have a different role (favourable or unfavourable) in the dissolution of a solute, an understanding of this chemical equilibrium is needed in order to develop the potential of water-Cyrene mixtures for novel applications. De bruyn et al.[36] pioneered the study of the hydrotropic capacity of water-Cyrene mixtures and concluded that the form of Cyrene responsible for the solubility increase of hydrophobic solutes was the geminal diol form.

The understanding the mechanism of hydrotropy built in the previous chapter can provide a useful insight as to which component of the water-Cyrene system is responsible for the solubility increase of hydrophobic substances. Since the ketone and diol forms of Cyrene possess approximately the same apolar surface area, both forms are expected to function as hydrotropes, which is at odds with the original proposal of De bruyn et al.[36] in which the germinal diol was the main component responsible for the hydrotropic behaviour on these systems. Such a question is underscored further by a structural point of view: the diol form interacts more extensively with water through hydrogen bonding than the ketone form, meaning that the latter is freer to interact with the solute than the former.

The objective of this chapter is to provide a theoretical framework on which the solvent capability of the delicate water-Cyrene system can be rationally explored. The data reported by De bruyn et al.[36] for the solubility of salicylic acid, ferulic acid, ibuprofen and caffeine in the water-Cyrene system, along with novel data for benzoic acid and syringic acid measured in this work, was studied

from the perspective of the cooperative hydrotropy model. The correlations obtained between the parameters of this model with the hydrophobicity of the solutes are then explored in order to predict the solubility curves of phthalic acid and aspirin (data from De bruyn et al.[36]) and of gallic acid and vanillin in water-Cyrene mixtures.

5.2 Cyrene-Water Chemical Equilibria

Carbonyl functional groups are known to react with water, forming geminal diols. Among other factors, the extent of this chemical equilibrium depends on the stability of the carbonyl group, which in turn depends on the electron donating ability of its vicinity groups.[90] Ketones are less prone to form geminal diols than aldehydes due to their additional alkyl group, which acts as an electron donating agent, stabilizing the carbonyl group. The equilibrium constant of acetone and its geminal diol, for example, is three orders of magnitude lower than that of acetaldehyde and its geminal diol. Ketones can, nevertheless, form geminal diols. A typical example is that of hexafluoroacetone, which, due to the electron withdrawing effect of the fluorine atoms, reveals an equilibrium constant with its diol nine orders of magnitude higher than that shown by acetone and its diol.[90]

When dissolved in water, Cyrene establishes an equilibrium to form its corresponding geminal diol,[36] as depicted in Figure 5.1. The extent of this equilibrium is large for a ketone, explained by considering the electron withdrawing effect of the ether groups in Cyrene, which destabilize the carbonyl group, in line with the previous paragraph. Moreover, the geminal diol formed partially dissociates, as suggested by the low pH of Cyrene-water mixtures.[89]

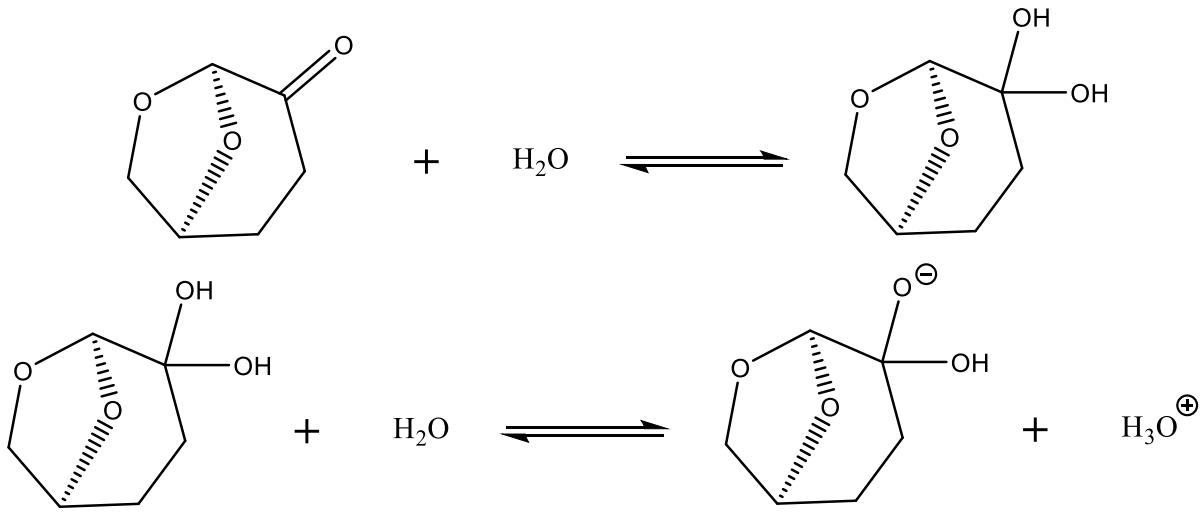

Figure 5.1. *Chemical equilibrium of Cyrene and its geminal diol in water (top panel) and dissociation of the geminal diol (bottom panel).*

De bruyn et al.[36] quantified the concentration of water and the ketone and diol forms of Cyrene present in the water-Cyrene system, over the full concentration range, from pure water to pure

Cyrene. They neglected the presence of the dissociated form of the diol (second reaction in Figure 1). As explained in section A7 of the Appendix, this is here justified as a good approximation since the concentration of the dissociated form of the diol is very small, as suggested by the pH of the system. In the absence of a *constant* equilibrium constant for this system, De bruyn et al.[36] speculated that this parameter changes with the concentration of water, most likely due to strong intermolecular hydrogen bonding between water and the diol form of Cyrene, resulting in large deviations to thermodynamic ideality. The experimental quantification of the various Cyrene forms presented by De bruyn et al.[36] allowed for the calculation of the mole fraction of the ketone and diol forms of Cyrene (both the non-dissociated and dissociated geminal diol are considered as the diol form of Cyrene), as explained in section A8 of the append and depicted in Figure 5.2.

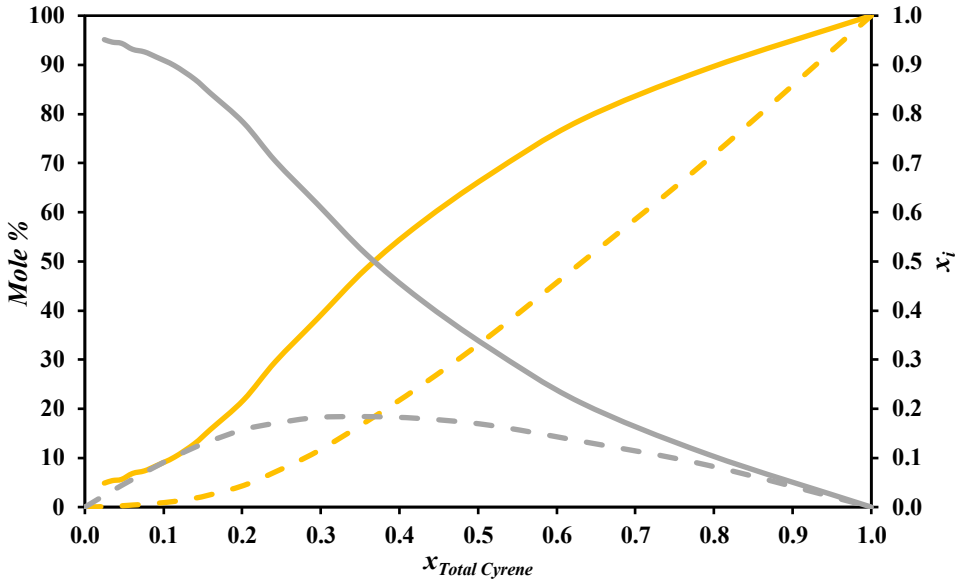

Figure 5.2. *Composition of water-Cyrene mixtures: mole percentage (left axis, full lines) and mole fraction (right axis, dashed lines) of ketone form (──, - - -) and diol form (──, - - -) of Cyrene as a function of its total mole fraction (sum of the mole fractions of ketone form and diol form), calculated, as described in section A8 of the Appendix, from the data reported by De bruyn et al.*[36].

Figure 5.2 reveals that Cyrene exists in water mostly as its diol form until a mole fraction of about 0.35, where the trend is reversed, and its ketone form becomes predominant. The amount of the geminal diol in the system water-Cyrene is maximum at a mole fraction of total Cyrene of about 0.3. This is important, since the maximum in the concentration of the geminal diol should correspond to the maximum in solubility of a hydrophobic solute, should the geminal diol be the principal responsible for the hydrotropic ability of Cyrene.

From Figure 5.1, it may be argued that changing the pH of the system could change the equilibrium of Cyrene in water. This would be problematic when studying acidic solutes, such as those used in

this work. However, it is shown in section A7 of the Appendix that setting the pH value of the system to 1 does not significantly impact the water-Cyrene equilibrium.

5.3 Hydrotropy in Aqueous Solutions of Cyrene

When measuring the solubility of a substance in a multicomponent system, it is a common practice to prepare first the solvent with the desired composition and then add the solute. As such, hydrotropy data is typically reported as solubility of the solute against the hydrotrope fraction in the solvent (solute-free basis). Even though it is practical, thermodynamic analysis requires these data to be converted to mole fractions in the resulting multicomponent system. This is especially important in the case of Cyrene, since its reaction with water significantly alters the composition of the solvent and that of the final mixture. This conversion is detailed in section A9 of the Appendix. Henceforth, all data is analysed in terms of the total mole fraction of Cyrene in the final system after equilibrium is achieved ($x_{Total\ Cyrene}$), defined as the sum of mole fractions of the ketone and diol forms of Cyrene.

To establish the role of each Cyrene species in the solubilization of hydrophobic solutes, solubility data for benzoic and syringic acids, herein experimentally measured, are first discussed. Unlike for other hydrotrope systems, such as those based on glycerol ethers (Chapter 3), fitting the cooperative hydrotropy model to the full concentration range of Cyrene is not possible. Instead, the model needs to be fitted separately to the region of $x_{Total\ Cyrene}$ between 0 and about 0.2 and to the region of $x_{Total\ Cyrene}$ between about 0.2 and the mole fraction corresponding to the solubility maximum. These results are reported in Figure 5.3 (left) along with the left-hand-side of Equation 2.5 as a function of $\ln(x_{Total\ Cyrene})$ (Figure 5.3, right), which is an intuitive way of understanding the change in dissolution regime. As will be explained below, this is not a limitation of the model; instead, the necessity for two different fittings stems from the transition between the diol form as the main hydrotrope to the ketone form as the main hydrotrope.

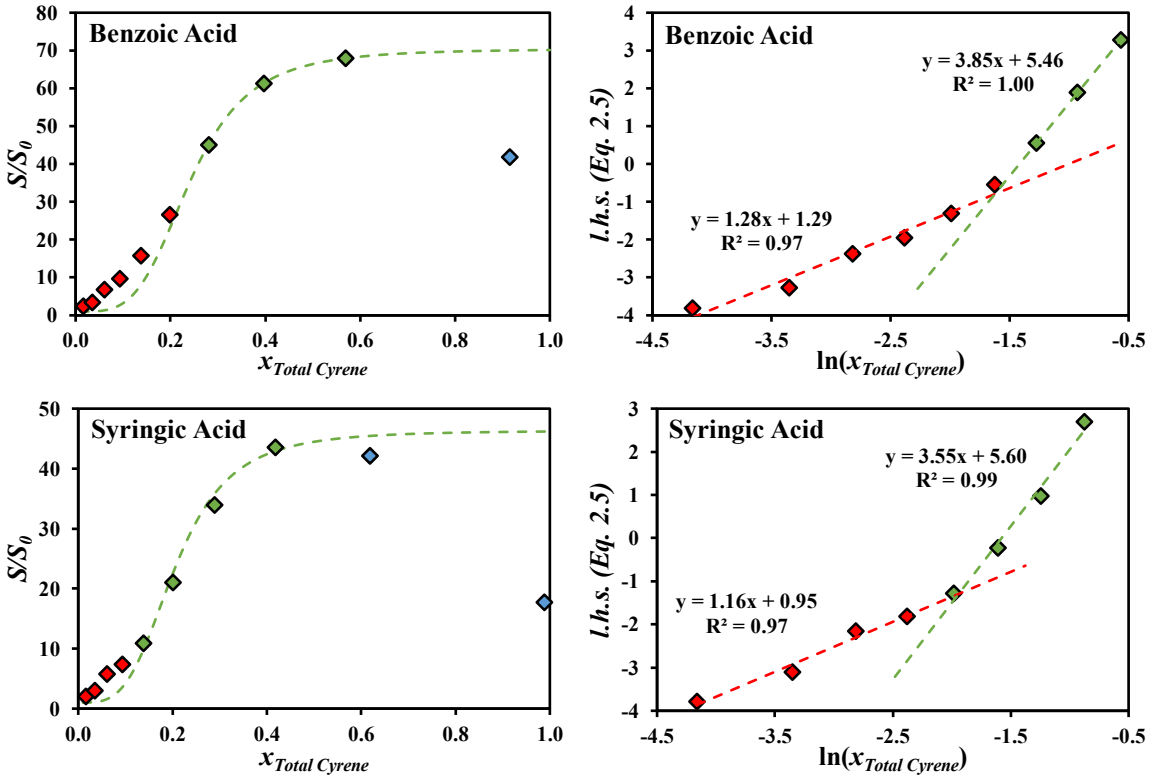

Figure 5.3. *Left: solubility increase (S/S_0) of the hydrophobic solute (◆,◆,◆), along with the fitted curves of the cooperative hydrotropy model using the red data points (red dashed line) and the green data points (green dashed line). Right: linearized form of Equation 2.5, where the y-axis is the left-hand-side of Equation 2.5.*

From the application of the cooperative hydrotropy model reported in Figure 5.3, it is evident that the solubility curves of hydrophobic solutes in water-Cyrene mixtures can be divided into three regions, depending on the concentration of Cyrene. At low concentration of Cyrene ($x_{Total\ Cyrene}$ from 0 to about 0.2) the m parameter of the model takes a value of around 1. Then, there is a sharp transition (Figure 3, right) and at medium concentration of Cyrene ($x_{Total\ Cyrene}$ from about 0.2 until solubility maximum is attained) the m parameter takes a value of around 4. Finally, the occurrence of the maximum and consequent solubility decrease indicates that, above a certain concentration of Cyrene, water is no longer the *principal* solvent of the system and hydrotropy is replaced by another mechanism of solvation. Note that, due to its underlying assumptions, the cooperative hydrotropy model can only describe increases in solubility but cannot describe maxima or solubility decrease.

The results of Figure 5.3 are remarkable, especially considering that the cooperative hydrotropy model is being applied using only one adjustable parameter (δ_{max}), and are a strong indicator that the mechanism of solvation in the water-Cyrene system, in most of its concentration range, is, in fact, hydrotropy (herein defined as water-mediated aggregation of hydrotrope molecules around the solute, in line with Chapter 4). Bearing in mind that i) hydrotropy is driven by the apolarity of both

solute and hydrotrope and ii) the ketone form of Cyrene is much more hydrophobic than its diol form, the parameter transition reported in Figure 3, occurring at around $x_{Total\ Cyrene} = 0.2$, can be interpreted as hydrotropy occurring due to mainly aggregation of the diol form around the solute for low concentrations of Cyrene and due to mainly aggregation of the ketone form around the solute at high concentrations of Cyrene. Since the ketone form is more hydrophobic than the diol form, the driving force of hydrotropy is larger with the former than the latter, leading to a much greater m value or, in other words, leading to more hydrotrope molecules aggregating around the solute and, thus, a better solubility enhancement.

Figure 5.2 of the previous section revealed that a total Cyrene mole fraction of around 0.3 maximizes the amount of geminal diol form present in the water-Cyrene system. Interestingly, Figure 3 reveals that the maximum in solubility of the hydrophobic solutes studied occurs at a total Cyrene mole fraction much greater than 0.3, when the concentration of the diol is less than 20%. If the geminal diol was in fact the component responsible for the hydrotropic ability of the system, as suggested by De bruyn et al.,[36] the maximum in solubility should appear at much lower concentrations of Cyrene. This, coupled with the results of Figure 3 and the discussion of the last paragraph, strongly suggests that the principal component driving solubilization is the ketone form of Cyrene, with the geminal diol playing a secondary role, in line with the foundations of the cooperative theory of hydrotropy. It is not being claimed, though, that the diol form of Cyrene does not act as a hydrotrope. As Figure 3 revealed, for low concentrations of Cyrene where its ketone form is virtually absent, the diol form is indeed acting as a hydrotrope, but with a much lower efficiency than the ketone form. Furthermore, it is also not being claimed that only the diol form of Cyrene acts as a hydrotrope at low concentration and that only the ketone form of Cyrene acts as a hydrotrope at large concentration. The aggregation of hydrotropes around the solute is statistical; these are short-lived clusters without a definite structure, unlike, for instance, micelles. As such, it is plausible that the ketone and diol forms of Cyrene both aggregate at the same time around the solute. However, what the cooperative hydrotropy model shows is that the driving force for aggregation (quantified by m) between the diol form and the solute is much lower than that between the ketone form and the solute. Thus, aggregation of the ketone form around the solute becomes predominant as the concentration of Cyrene increases. That is why $x_{Total\ Cyrene}$ is used in the fitting of the cooperative hydrotropy model, instead of the mole fractions of the individual Cyrene forms.

Having established that the ketone form of Cyrene is the principal hydrotrope in the water-Cyrene system, the solubility curves of salicylic acid, ferulic acid, ibuprofen and caffeine in the water-Cyrene system are now studied. These are depicted in Figure 5.4, along with the cooperative hydrotropy model fitted to the green data points, as explained above. Note that data on the solubility of mandelic

acid is also available,[36] but, unlike the other solutes mentioned, mandelic acid significantly disrupts the ketone-diol equilibrium of Cyrene,[91] hampering its analysis, most likely due to its much higher solubility in pure water. It is, thus, left out of this analysis.

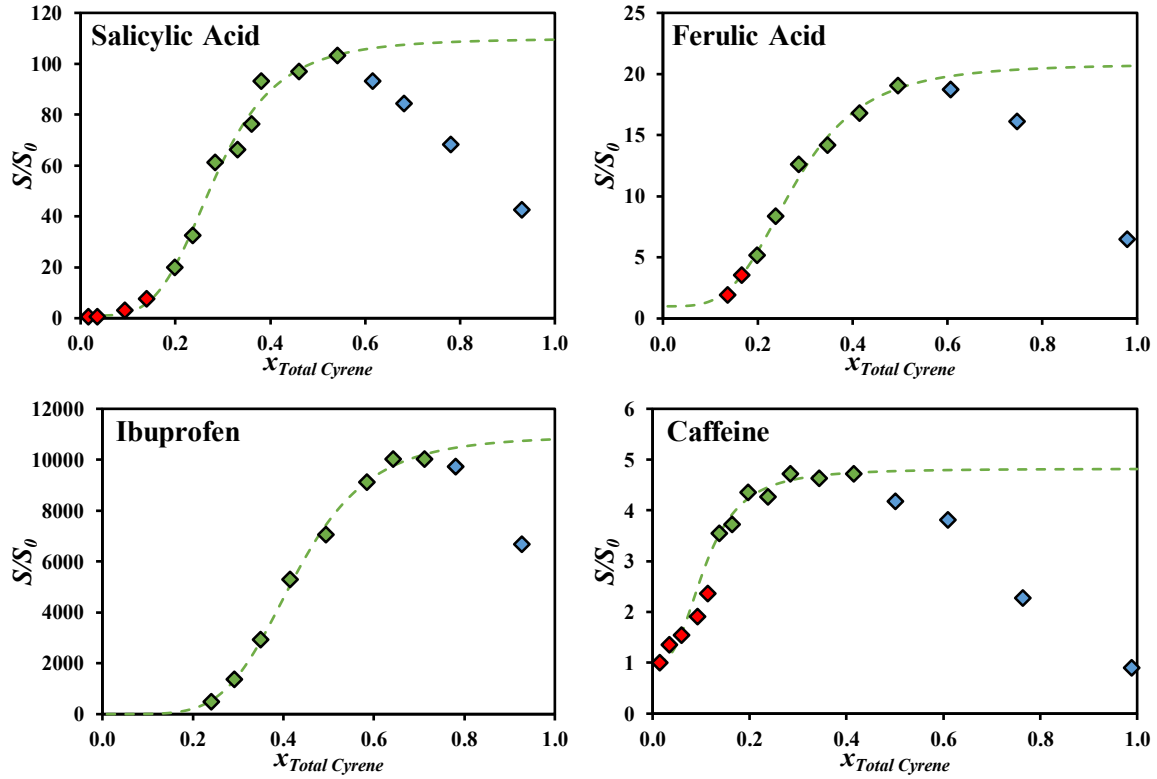

Figure 5.4. *Solubility increase (S/S_0) of the hydrophobic solute as a function of total Cyrene mole fraction (◆,◆,◆), along with the fitting curves of the cooperative model using only the green data points (green dashed line). Data by De bruyn et al.*[36]

In a similar way to Figure 5.3, Figure 5.4 shows that the cooperative hydrotropy model is able to describe the solubility enhancement of hydrophobic solutes due to the presence of Cyrene, reinforcing that hydrotropy is indeed the mechanism of solvation in most of its concentration range. The parameters of the cooperative hydrotropy model (m, b and δ_{max}) for the solubility curves depicted in Figures 5.3 and 5.4 are reported in Table 5.1.

Table 5.1. *Parameters of the cooperative model fitted to the Cyrene-based hydrotropic systems studied in this work along with logarithm of the partition coefficient between octanol and water of the solutes.*

Substance	δ_{max}	m	b	$\log(K_{O,W})$[92]
Benzoic Acid	70	3.85	5.46	1.87
Syringic Acid	46	3.55	5.60	1.04
Salicylic Acid	110	4.28	5.39	2.26
Ferulic Acid	21	3.75	4.80	1.51
Ibuprofen	10935	5.17	4.40	3.97
Caffeine	5	2.87	6.37	0.07

The parameter m of the cooperative hydrotropy model is interpreted as the effective number of hydrotrope molecules aggregated around the solute. In Chapter 4 it was shown that, for a given solute and a series of homologous hydrotropes, m increases with the apolar volume of the hydrotrope until the apolar volumes of solute and hydrotrope match, decreasing thereafter. That is, the larger the apolar volume of the hydrotrope, the weaker the interaction with water and the greater the driving force for aggregation with the solute, as first proposed by Kunz and co-authors.[23] However, when the hydrotrope has a larger apolar volume than the solute, the driving force for hydrotrope-hydrotrope aggregation is greater than that of solute-hydrotrope aggregation, leading to a decrease in m.

In contrast with the example above, several solutes are studied for the same hydrotrope in this work. It is, thus, expected that m increases with the apolarity of the solute. To test this hypothesis, the hydrophobicity of the solutes studied above (benzoic acid, syringic acid, salicylic acid, ferulic acid, ibuprofen and caffeine) was quantified using the logarithm of their octanol/water partition coefficients ($K_{O,W}$). This parameter, listed in Table 5.1 for each solute, is a measure of the preference of the solute to be solvated by an apolar medium instead of water, or, more correctly, is a measure of the preference of water to not solvate the solute. Within the framework of cooperative hydrotropy, it makes sense that the number of hydrotropes aggregated around the solute through their apolar moieties (quantified by m) is proportional to the preference of the solute to be surrounded by an apolar medium (quantified by $K_{O,W}$). Figure 5.5 depicts the correlation obtained between m and $\log(K_{O,W})$.

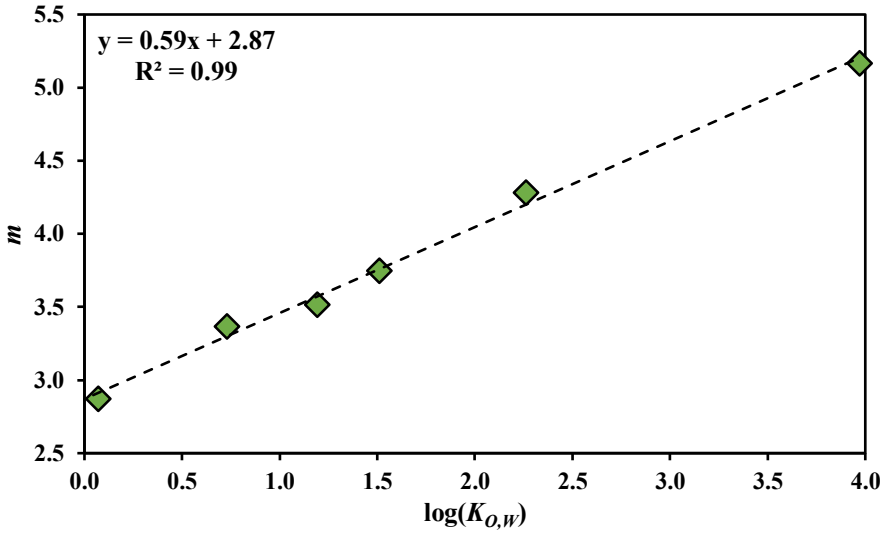

Figure 5.5. *Parameter m of the cooperative hydrotropy model for the hydrophobic solutes studied in this work as a function of the logarithm of the partition coefficient between octanol and water of the solute. The dashed line is the fitted line using the least squares method (coefficients of determination is 0.99).*

Figure 5.5 reveals an excellent correlation between m and $\log(K_{O,W})$. Again, this is interpreted as the number of hydrotrope molecules around the solute being dependent on the preference of the solute to be surrounded by apolar moieties instead of water molecules. These results support the idea of apolarity as the driving force of hydrotropy and complement those previously reported in Chapter 4. Note that a dependence of m on the apolar volume of the solute is anticipated. In other words, the larger the solute the more hydrotrope molecules are needed to cover its apolar area. However, the apolar size of the solute is encoded in $\log(K_{O,W})$ since the apolar size plays a role on partition from water to an apolar medium.

The success of $\log(K_{O,W})$ in describing m suggests that there may be similar correlations for δ_{max} and b. Finding such correlations not only help understanding the mechanism of hydrotropy but would add an important predictive component to the cooperative hydrotropy model, allowing the prediction of the solubility of hydrophobic substances in water-Cyrene mixtures. In fact, $\log(\delta_{max})$, as depicted in Figure 5.6, also correlates remarkably well with $\log(K_{O,W})$.

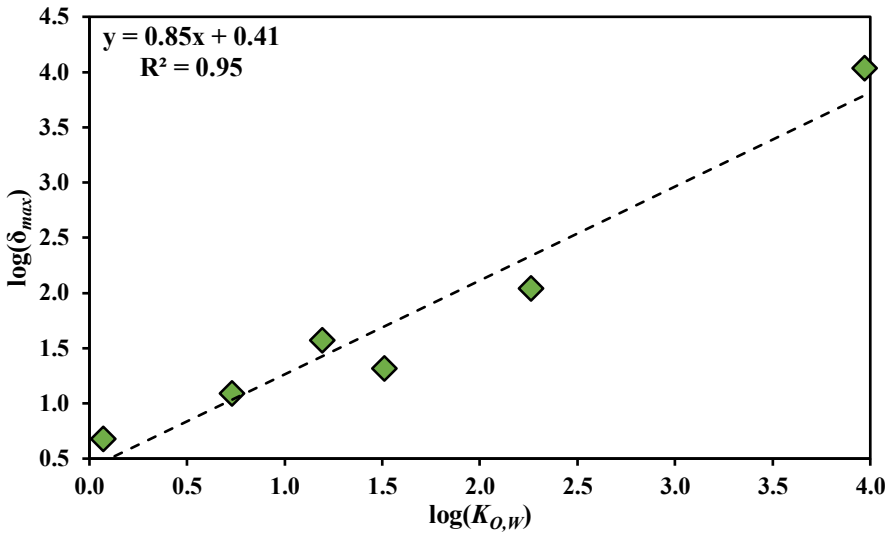

Figure 5.6. *Logarithm of parameter δ_{max} of the cooperative hydrotropy model for the hydrophobic solutes studied in this work as a function of the logarithm of the partition coefficient between octanol and water of the solute. The dashed line is the fitted line using the least squares method (coefficients of determination is 0.95).*

By definition, δ_{max} can be interpreted as the partition coefficient of the solute between water and the hydrotropic system, measured at solute saturation instead of solute dilution. As such, the correlation depicted in Figure 5.6 bears a resemblance to the work of Collander,[93] where it was shown that the partition coefficient of a solute between a solvent and water (K_1) could be correlated to the partition coefficient of the same solute but between a different solvent and water (K_2) according to the following expression:

$$\log(K_1) = A \cdot \log(K_2) + B \tag{5.1}$$

where A and B are the slope and intercept of the line obtained by plotting $\log(K_1)$ against $\log(K_2)$. Even though the physical meaning of these parameters is not clear,[94] Equation 5.1 is known to yield a better correlation when the organic solvents are similar. In this sense, the correlation depicted in Figure 5.7 could be improved by defining a partition coefficient between Cyrene and water:

$$P^*_{C,W} = \frac{S_{Cyrene}}{S_{Water}} \tag{5.2}$$

where S_{Cyrene} and S_{water} are the molar solubility of the solute in Cyrene and water, respectively, and $*$ emphasises that this partition coefficient is calculated from the solute solubility as opposed to solute dilution. Figure 5.7 depicts the correlation obtained between $\log(\delta_{max})$ and $\log(P^*_{C,W})$. Even though it is clear that this correlation is better than that reported in Figure 5.6, it loses some of its predictive character since the solubility of the solute in pure water and pure Cyrene must be experimentally available, what is seldom the case, even when the hydrotrope is liquid. It nevertheless reinforces and supports the correlation with $\log(K_{O,W})$ presented above.

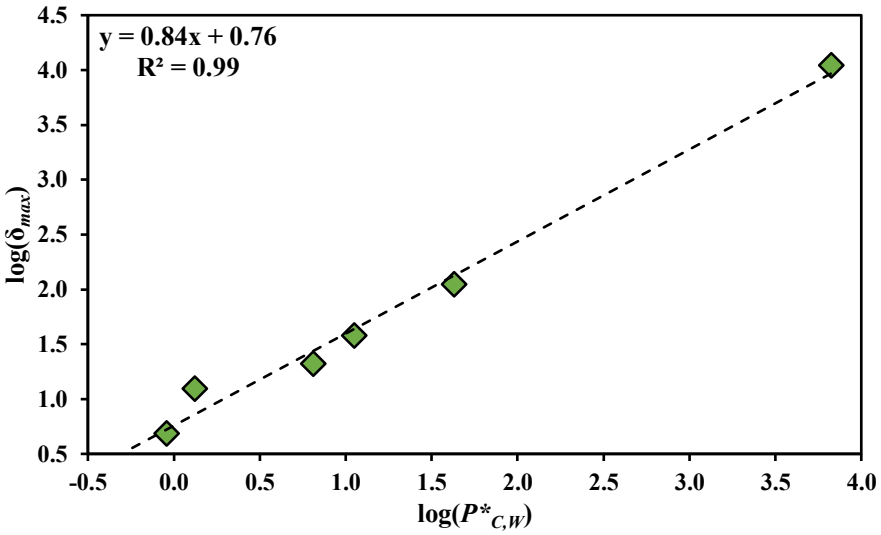

Figure 5.7. *Logarithm of parameter δ_{max} of the cooperative hydrotropy model for the hydrophobic solutes studied in this work as a function of the logarithm of the solubility ratio of the solute between pure Cyrene and pure water. The dashed line is the fitted line using the least squares method (coefficients of determination is 0.99).*

So far, both m and δ_{max} have been successfully correlated with the apolarity of the solute (quantified by $\log(K_{O,W})$). Contrary to these parameters, although the parameter b of the cooperative hydrotropy model may seem to pertain to a property of the hydrotrope (fugacity of inserting m hydrotrope molecules in the volume corresponding to the vicinity of the solute) and not of the solute, it depends on the quantity of hydrotropes to be inserted (m) around the solute, which, in turn, depends on the

hydrophobicity of the solute, as shown in Figure 5.5. As such, a decent correlation can be obtained between b and $\log(K_{O,W})$, as depicted in Figure 5.8.

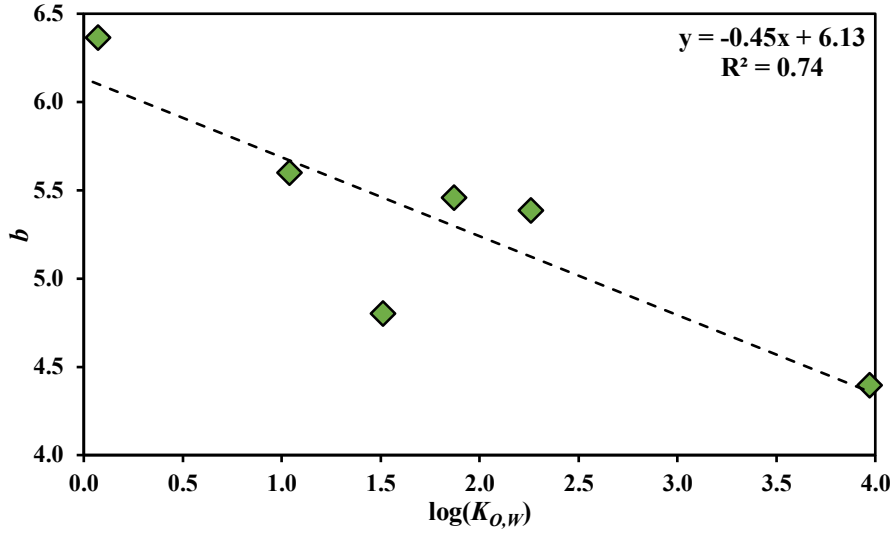

Figure 5.8. *Parameter b of the cooperative hydrotropy model for the hydrophobic solutes studied in this work as a function of the logarithm of the partition coefficient between octanol and water of the solute. The dashed line is the fitted line using the least squares method (coefficients of determination is 0.74).*

The correlations here reported for the parameters of the cooperative hydrotropy model (m, b and δ_{max}) support the notion that hydrotropy depends on the apolarity of both solute and hydrotrope. This is in line with Chapter 3 and 4 and contradicts the notion that only the hydrophobic volume of the hydrotrope is the major factor influencing hydrotropy.[23]

5.4 Solubility Prediction

So far, the usefulness of the cooperative hydrotropy model to describe the solubility of hydrophobic solutes in water-Cyrene mixtures has been explored. It must be highlighted that the correlations herein obtained are not purely empirical, since they possess physical meaning and can be interpreted in terms of the cooperative mechanism of hydrotropy and the foundations of its statistical thermodynamics-based model.

The correlations proposed for parameters m, b and δ_{max} add a predictive character to the cooperative hydrotropy model. This is explored in this section by predicting the solubility curves of phthalic acid, aspirin, gallic acid and vanillin in water-Cyrene mixtures. The choice of gallic acid and vanillin is based on their bioactivity, such as their antioxidant properties, and the fact that they are present in a wide variety of natural sources.[57,58,95–97] Moreover, they can be regarded as model molecules of lignin, making their study an important step in understanding the solubilization of this important natural polymer.[17,18,98]

The values obtained for the parameters of the cooperative hydrotropy model, using the correlations depicted in Figures 5.5, 5.6 and 5.8 are reported in Table 5.2 for the new solutes. The predicted solubility curves of phthalic acid, aspirin, gallic acid and vanillin are depicted in Figure 5.9.

Table 5.2. *Logarithm of the partition coefficient between octanol and water, along with the precited m and δ_{max} parameters of the cooperative hydrotropy model for the solutes whose solubility is predicted in this work.*

Solute	Log($K_{O,W}$)[92]	m	δ_{max}	b
Phthalic Acid	0.73	3.30	11	5.80
Aspirin	1.19	3.57	26	5.59
Gallic Acid	0.7	3.28	10	5.82
Vanillin	1.37	3.68	38	5.51

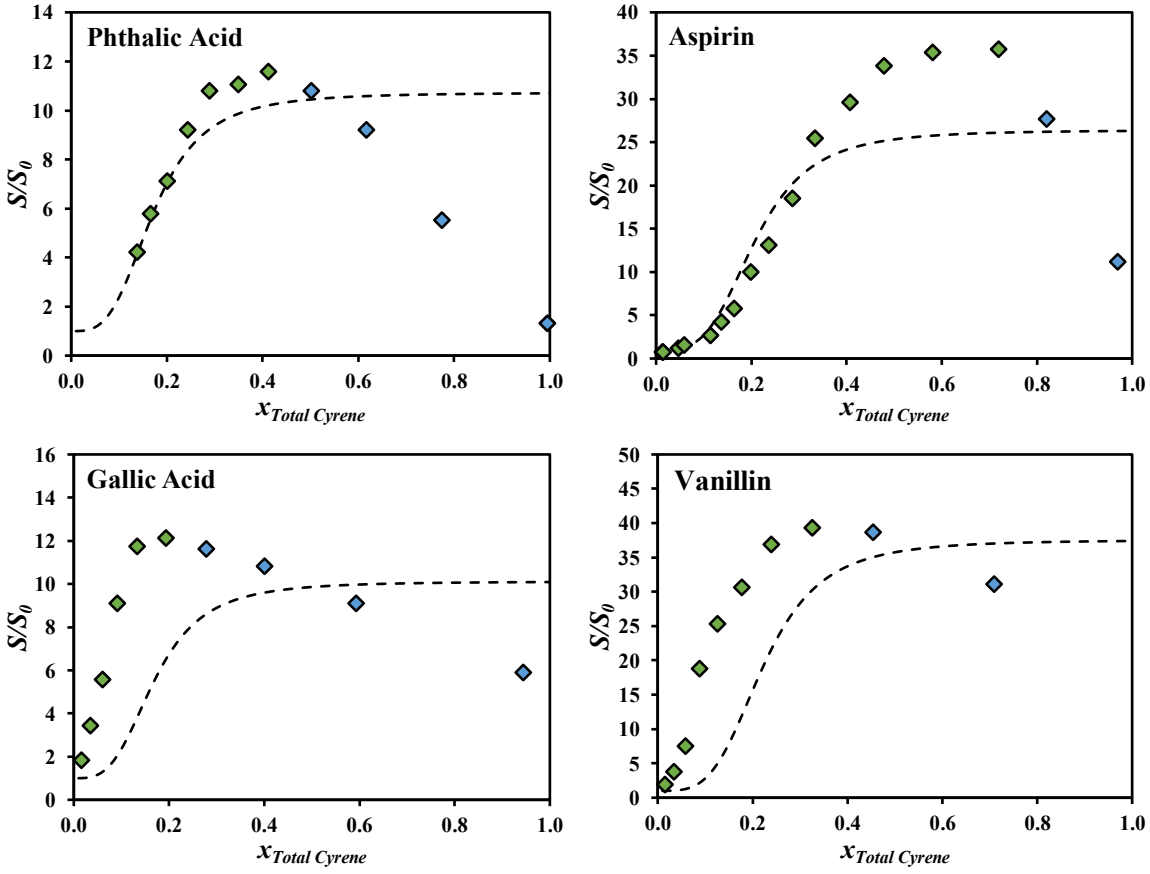

Figure 5.9. *Experimental solubility increase (S/S_0) of hydrophobic solutes as a function of total Cyrene mole fraction (◆,◆) along with the predicted solubility increase using the cooperative hydrotropy model and the correlations constructed throughout this work (dashed lines). Data from De bruyn et al.*[36] *(phthalic acid and aspirin, measured at 20 ºC) and this work (gallic acid and vanillin, measured at 30 ºC).*

Figure 5.9 reveals that the framework developed in this work can be used to successfully predict the solubility of hydrophobic solutes in water-Cyrene mixtures. Note that the predictions for gallic acid

and vanillin are not as accurate as those for phthalic acid and aspirin. This is probably due to the difference in temperature: the solubility data explored throughout this work was measured at 20 ºC, while the data reported for gallic acid and vanillin was measured at 30 ºC. The data for these two solutes was here experimentally measured at 30 ºC for two different reasons: first, to check the influence of temperature in the accuracy of the predictive methodology herein developed and, thus, the extent of its applicability, and second, to report data for gallic acid and vanillin at 30 ºC, facilitating future comparisons of the efficiency of Cyrene as a hydrotrope against previously reported hydrotropes in the literature, whose solubility enhancement for gallic acid and vanillin was reported at 30 ºC.

With respect to the influence of temperature on the prediction of solubility, Figure 5.9 shows that the maximum solubility enhancement prediction is accurate and not strongly influenced by temperature. This is reasonable, since the maximum solubility enhancement is a ratio between solute solubility in the mixture and in water, which may be quantitatively affected by temperature in the same way. However, the onset of hydrotropy (represented by parameters m and b) seems to occur at lower concentrations of Cyrene when temperature is increased (see Figure A9.1 of the Appendix for a comparison between solubility of syringic acid in water-Cyrene mixtures at 20 ºC and at 30 ºC), which may be explored to improve the efficiency of Cyrene as a hydrotrope.

Chapter 6
Water as a Cosolvent in Cyrene

This chapter is based on the following submitted article:

Solubility Enhancement of Hydrophobic Substances in Water/Cyrene Mixtures: A Computational Study
D. O. Abranches, J. Benfica, S. Shimizu and J. A. P. Coutinho
Industrial & Engineering Chemistry Research

Dinis O. Abranches contributed with conceptualization, methodology, formal data analysis and writing of the original draft.

6.1 COSMO-RS

In this Chapter, a computational study is carried out to explain the molecular mechanisms involved in the solubility increase of hydrophobic solutes when water is added to Cyrene. The objective is thus to complement the conclusions of the previous Chapter and build a complete understanding of the behaviour of the water-Cyrene system and its ability to dissolve hydrophobic substances in its entire composition range. Note that the use of COSMO-RS (as opposed to other predictive excess Gibbs energy models) is particularly useful in this work, since the two forms of Cyrene (ketone and diol) can be separately optimized and the solubility of the solutes can be predicted in the binary systems water-ketone or water-diol, something experimentally inaccessible.

The DFT optimization of the structure of the ketone form of Cyrene is straightforward, in the sense that there are no energetically relevant different conformers. This is not the case, however, for the diol form of Cyrene. In this work, three conformers of the diol were optimized, differing in the number of intramolecular hydrogen bonds established between the hydroxyl and ether groups (two, one, or no intramolecular hydrogen bonds). The σ-surface of these conformers are depicted in Figure 6.1. The σ-surface of the ketone form of Cyrene and of the solutes here studied are depicted in section A10 of the Appendix.

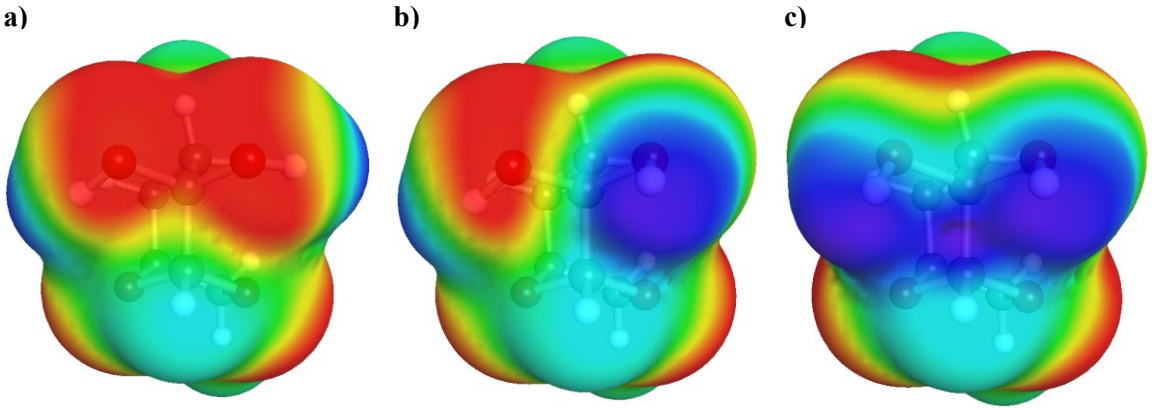

Figure 6.1. *Optimized geometry (σ-surface) of the three relevant conformers of the diol form of Cyrene. Their main difference lies on the amount of intramolecular hydrogen bonding: a) two intramolecular hydrogen bonds, b) one intramolecular hydrogen bond, and c) no intramolecular hydrogen bonds.*

As explained in Chapter 2 (section 2.1), the melting properties of the solutes are needed in order to predict their solubility by coupling COSMO-RS with the Solid-Liquid Equilibrium Equation. The melting properties used in this Chapter are listed in Table 6.1.

Table 6.1. *Melting temperature and corresponding enthalpy of fusion for the solutes studied in this Chapter.*

Substance	CAS Number	T_m /K	$\Delta_m h$ /kJ·mol^{-1}	Ref.
Acetylsalicylic Acid	50-78-2	412.7	31.01	[99]
Salicylic Acid	69-72-7	434.1	27.1	[100]
Ferulic Acid	1135-24-6	444.6	33.338	[101]
Phthalic Acid	88-99-3	463.5	36.5	[102]
Ibuprofen (Racemic)	15687-27-1	350.4	39.5	[103]
Caffeine	58-08-2	507.7	24.8	[104]
Syringic Acid	530-57-4	480.3	33.7	[105]
Vanillin	121-33-5	355.4	22.4	[106]

6.2 Solubility Prediction

The solubility of the compounds studied here (Table 1) are initially predicted in pure water and in pure Cyrene (ketone form). This was carried out using two different parametrizations of COSMO-RS, BP_TZVP_19.ctd and BP_TZVPD_FINE_19.ctd. The objective is to i) show that the model accurately predicts the solubility of the solutes in pure water and pure Cyrene, and ii) that the more computationally expensive BP_TZVPD_FINE_19.ctd parametrization offers no advantage for these systems over the more commonly used BP_TZVP_19.ctd. These results are reported in Figure 6.2.

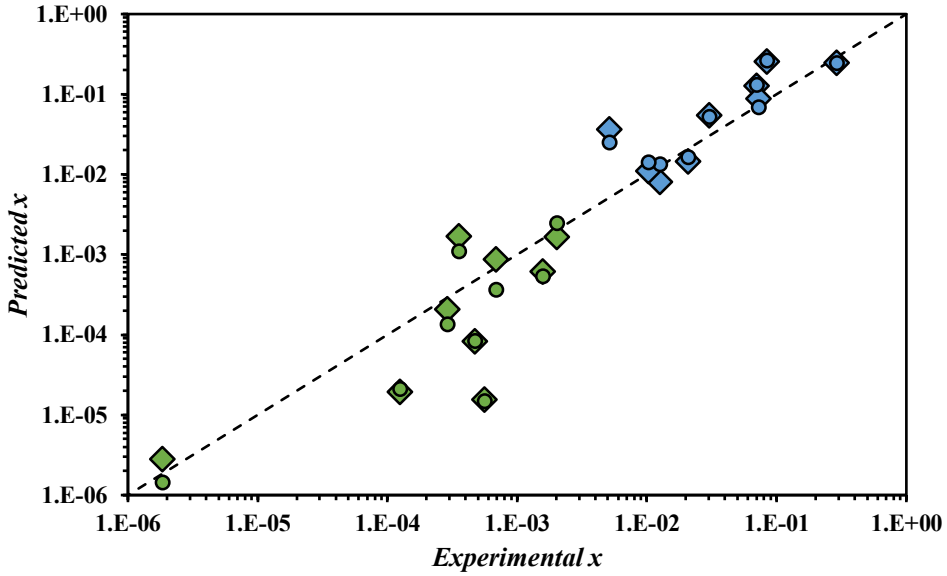

Figure 6.2. *Predicted VS experimental mole fraction solubility of the studied solutes in pure water (green) or pure Cyrene (blue), predicted using either the BP_TZVP_19.ctd. (diamond) or the BP_TZVPD_FINE_19.ctd (circle) parametrization of COSMO-RS. Experimental data taken from De bruyn et al.*[36] *and from Chapter 5.*

Since COSMO-RS was able to predict the solubility of the hydrophobic solutes in pure water and pure Cyrene, the model is now used to predict their solubility curves in the water/Cyrene system. The solubility of each solute was predicted considering only the presence of the ketone form of Cyrene, only the presence of its diol form, and the presence of both in the composition reported in Chapter 5. As such, Figure 6.3 depicts the solubility curves of aspirin, ibuprofen, salicylic acid, and vanillin in the systems water-ketone (black dashed line), water-diol (red dashed line) and water-ketone-diol (full line). These were the solutes whose solubility was accurately predicted by COSMO-RS in a quantitative manner. The curves of the remaining solutes are depicted in section A11 of the Appendix. Note that the curves depicted in Figure 6.1 were calculated considering the diol as possessing just one intramolecular hydrogen bond. These calculations were repeated for the other two conformers of the diol, and the resulting solubility curves are reported in section A12 of the Appendix. Note that there is no significant difference between considering one or two intramolecular hydrogen bonds, but the predictions are much worse when no intramolecular hydrogen bonding is considered.

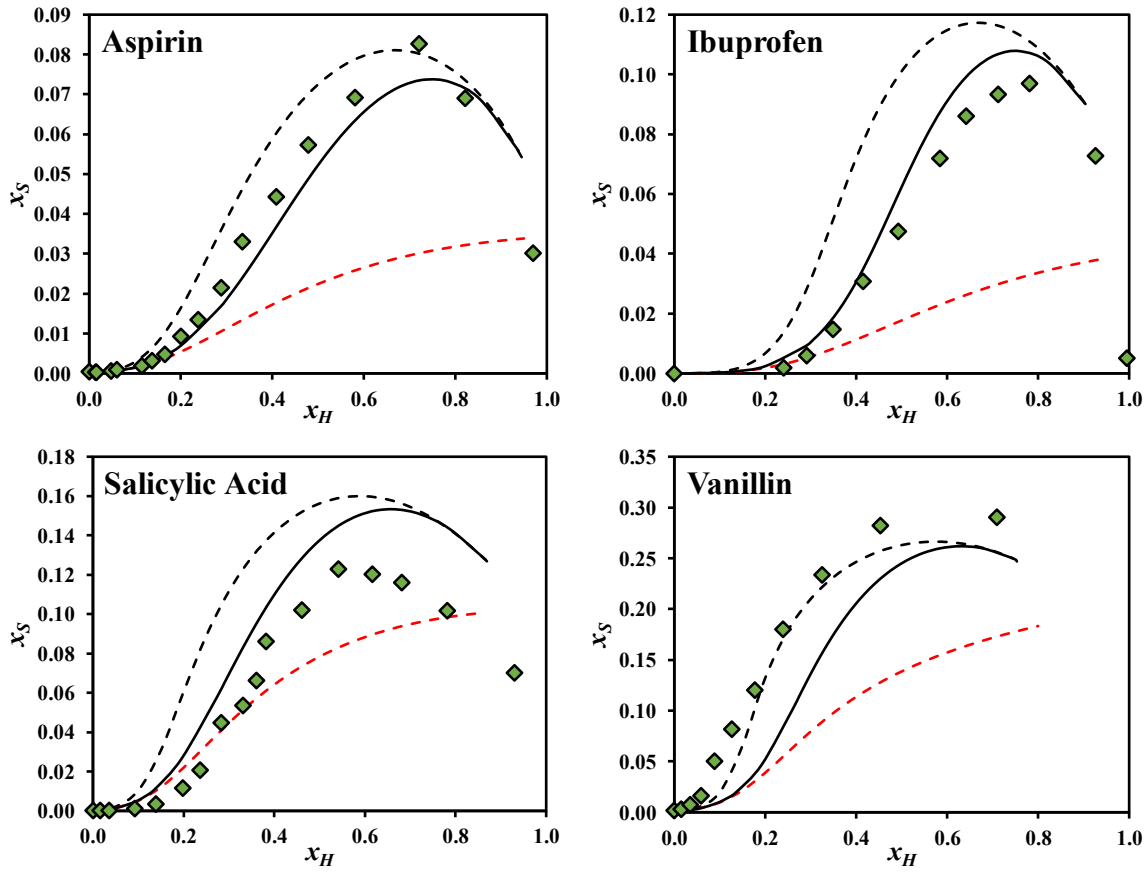

Figure 6.3. *Predicted solubility of aspirin, ibuprofen, salicylic acid, and vanillin on water-ketone mixtures (black dashed line), water-diol mixtures (red dashed line) and water-ketone-diol mixtures (full line), along with the corresponding experimental data (◆), taken from De bruyn et al.*[36] *or Chapter 5, considering the diol conformer with one intramolecular hydrogen bond.*

The predictions of COSMO-RS, depicted in Figure 6.3, are remarkable. Without the need for any experimental data other than the melting properties of the solute, the methodology here presented is able to fully predict the solubility of aspirin, ibuprofen, salicylic acid, and vanillin in water-Cyrene mixtures, while capturing the general trend satisfactorily for the remaining solutes (section A11 of the Appendix). Note that COSMO-RS does not predict any synergetic effect between the ketone and diol forms of Cyrene, with the solubility in water-diol-ketone mixtures being an intermediate value between the solubility in water-ketone mixtures (always higher) and the solubility in water-diol mixtures (always lower). As such, the solubility in water-ketone-diol mixtures is equal to that of water-diol mixtures for low Cyrene concentration and is equal to that of water-ketone mixtures for high Cyrene concentration.

The fact that COSMO-RS systematically predicts higher solubility in the binary water-ketone system than on the water-diol system is consistent with the conclusions of the previous Chapter, where the cooperative hydrotropy model suggested that the ketone form of Cyrene, rather than its diol form, played the principal role of hydrotrope. Even more interesting, according to COSMO-RS predictions the maximum in solubility of these systems occurs due to the presence of the ketone form. That is, the maximum is correctly predicted by COSMO-RS in the water-ketone system, without the need for considering the presence of the diol form of Cyrene. Evidently, there is a change in solubilization mechanism at the maximum. This can be interpreted as water behaving as a cosolvent when added to Cyrene, and is important from an application perspective, since a small amount of water can greatly increase the solubility of hydrophobic substances in Cyrene. The mechanism behind this phenomenon is rationalized in the next section.

6.3 Water-Solute Specific Interactions

The fact that the addition of small quantities of water to Cyrene increases the solubility of hydrophobic solutes is, at first glance, paradoxical. By their apolar nature, hydrophobic substances do not favourably interact with water, which is the reason behind the low solubility of the solutes here studied in water. Rationalizing this phenomenon, which possesses practical importance in terms of applying Cyrene as a solvent, is the objective of this section.

Assuming that COSMO-RS is accurately predicting the solubility curves depicted in Figure 6.3 by capturing the underlying phenomenon, the results suggest that the solubility maximum is caused by the ketone form of Cyrene rather than its diol form. Hence, the interpretation of the problem can be simplified by ignoring the presence of the diol form of Cyrene. This is also reasonable from a physical perspective, considering that, at high Cyrene concentration, the ketone is its prevailing form.

Within the framework of COSMO-RS, the software COSMOtherm calculates the most probable contacts between molecule pairs in a mixture. Since these contacts may help shed light on the role of water in increasing the solubility of hydrophobic solutes in Cyrene, they were calculated for the systems depicted in Figure 6.3 at low water concentration and are depicted in Figure 6.4.

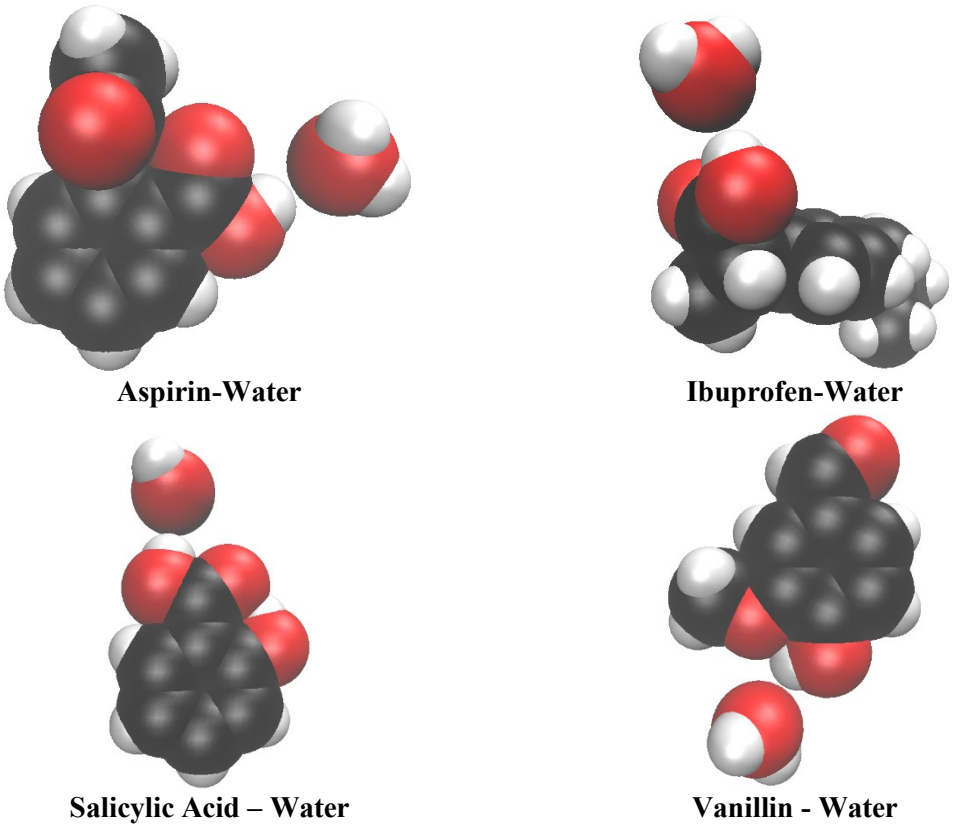

Figure 6.4. *Interaction geometry of the most probable contacts between the solute and water in water/Cyrene mixtures at low water concentration, predicted using COSMO-RS.*

Figure 6.4 reveals an interesting pattern: regardless of the solute, water always behaves as the hydrogen bond acceptor when interacting with the solute (at low water concentration). This is not surprising for the acidic solutes (aspirin, ibuprofen and salicylic acid), since the hydrogen bond between their acidic proton and the oxygen atom of water is quite strong. However, it is surprising for vanillin, whose sole positive proton is hindered by its intramolecular hydrogen bond with the neighbour methoxy group. Thus, the results depicted in Figure 6.4 suggest that water preferentially interacts with the solute by behaving as a hydrogen bond acceptor. This can be rationalized by considering the structure of the ketone form of Cyrene. As evident by its σ-surface (section A10 of the Appendix), the ketone form of Cyrene possesses three hydrogen bond acceptor centres but no hydrogen bond donor centres. Thus, Cyrene has a preference to interact with hydrogen bond donors. As such, water may be functioning as a cosolvent by establishing a favourable interaction with the

solutes, effectively doubling their hydrogen bond donning ability, thus enhancing their interaction capability with Cyrene and, consequently, increasing their solubility.

To test the hypothesis presented in the previous paragraph, the contact probability (*P*) between water molecules was calculated within the framework of COSMO-RS, using the software COSMOtherm, for the aspirin system. *P* was calculated for the entire composition range of the water/Cyrene system, considering a solute concentration of zero (to serve as reference) and increasing the concentration of the solute, until saturation. These results are reported in Figure 6.5. Note that it is advantageous to plot the probability of water-water contacts as a function of its mole fraction (as opposed to plotting it against the mole fraction of Cyrene) since this allows a fair comparison between systems that possess the same amount of water.

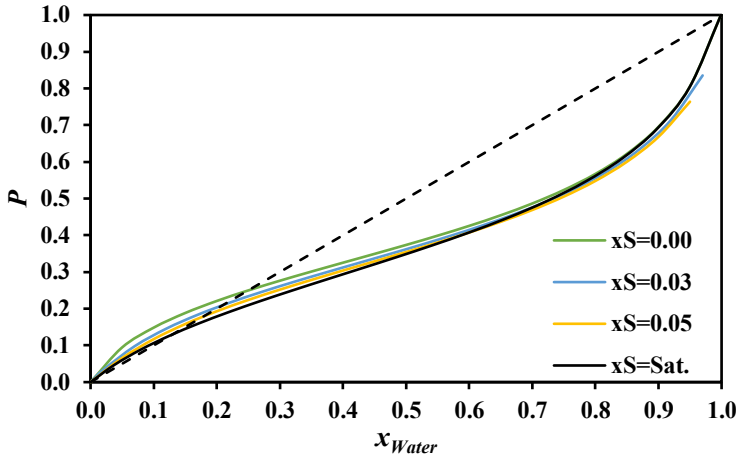

Figure 6.5. *Probability of water-water contacts in aspirin-water-Cyrene mixtures, considering only the presence of the ketone form of Cyrene, for different solute mole fractions (see inset).*

For high concentration of water (above a water mole fraction of 0.5), Figure 6.5 reveals that the presence of the solute does not alter the interaction extent between water molecules. This is consistent with the notion of hydrotropy built in the previous Chapters, where water is the effective solvent of the system and the main interactions of the solute are water-mediated aggregation of apolar moieties of the solute and the hydrotrope (Cyrene). However, this clearly changes at low water concentration, where hydrotropy ceases to occur and cosolvency sets in. At that concentration, the probability of water-water contacts changes with solute concentration. That is, water-water contacts are maximized in the absence of the solute and decrease with increasing solute concentration. This is an indicator that water is, in fact, favourably interacting with the solute, supporting the hypothesis of strong molecular pair interaction between water and the solute as the reason behind the co-solvent behaviour of water in Cyrene.

The strong solute-water interactions suggested by Figures 6.4 and 6.5 as the reason behind the cosolvency behaviour of water in Cyrene are further supported by the total hydrogen bonding energy of water and the ketone form of Cyrene, predicted by COSMO-RS and depicted in Figure 6.6.

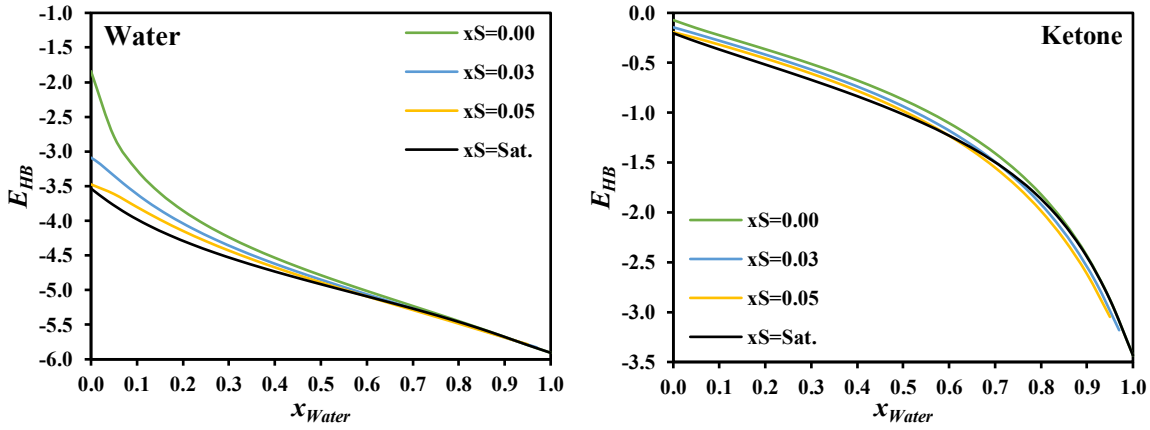

Figure 6.6. *Total hydrogen bonding interaction of water (left) and the ketone form of Cyrene (right) in aspirin-water-Cyrene mixtures, considering only the presence of the ketone form of Cyrene, for different solute mole fractions (see inset).*

Figure 6.6 shows that, at low water concentration, the presence of the solute severely impacts the total hydrogen bonding energy of water. More specifically, the increase of solute mole fraction leads to much higher (in absolute terms) hydrogen bonding energy, suggesting that water is establishing strong hydrogen bonding with the solute. Likewise Figure 6.5, this effect is no longer significant for a water mole fraction larger than approximately 0.3. In sharp contrast to water, Figure 6.6 reveals that the presence of the solute does not alter the total hydrogen bonding interaction energy of Cyrene. This suggests that Cyrene preferably establishes hydrogen bonds with water and, thus, supports the role of water as an interaction bridge between the solute and Cyrene.

Chapter 7
Conclusions & Future Work

7.1 Conclusions

In Chapter 3, the solubility of gallic acid and syringic acid was studied in aqueous solutions of glycerol ethers, a recently-proposed new class of hydrotropes, demonstrating their excellent hydrotropic ability. The use of the cooperative hydrotropy model allowed for the analysis of the feasibility of recovering solute from hydrotropic solutions by the addition of water. It was herein shown that solute recovery is not always possible. As such, the choice of hydrotrope and operating concentration for a given application should consider not only the solubility enhancement provided by the hydrotrope but also the ease of solute recovery from the system.

Chapter 4 provided experimental evidence for the cooperative theory of hydrotropy, shedding light on its mechanism and paving a way for the rational development of novel hydrotropic systems. This mechanism can be summarized in the following manner:

> Water molecules establish a strong hydrogen bond network between them. For a compound to favourably dissolve in water, it needs to reciprocate these interactions. Since a hydrogen bond between two water molecules is much stronger than the dipole-induced dipole interaction between water and an apolar moiety, the agglomeration of apolar moieties in the presence of water is a spontaneous process.
>
> A hydrotrope is a molecule that possesses a large apolar part (and, thus, can participate in water-mediated agglomeration) and a large polar part (which allows for good interactions with water, making the compound soluble). Thus, the role of a hydrotrope is to agglomerate around the solute through its apolar moieties, preventing the solute from precipitating out of solution. Note that there is no distinction between apolar moieties of hydrotrope or solute. From the perspective of water, both surfaces need to be minimized. Thus, the number of hydrotrope molecules aggregated around the solute increases as the apolar surface area of the hydrotrope increases. However, when the apolar surface area of the hydrotrope becomes larger than that of the solute, the driving force for hydrotrope-hydrotrope aggregations becomes larger than that of hydrotrope-solute aggregation, and the number of hydrotrope molecules aggregated around the solute decreases. Thus, the number of hydrotrope molecules aggregated around the solute is maximum when there is a match between the apolarity of both compounds.

In Chapter 5, the quantitative framework to consistently study the solubility of hydrophobic solutes in this solvent was introduced. Then, the cooperative hydrotropy model was applied to experimental solubility data, which led to the conclusion that the ketone form of Cyrene, and not its diol form as claimed in the literature, is the major component responsible for the solubility increase of

hydrophobic solutes in water-Cyrene mixtures. The correlations obtained for the parameters of the cooperative hydrotropy model allowed for the prediction of the solubility of phthalic acid, aspirin, gallic acid and vanillin in water-Cyrene mixtures. As such, it was demonstrated for the first time that a consistent study of solubility for a single hydrotrope, varying only the solutes, allows for the parametrization of the cooperative hydrotropy model, which can then be used to predict the solubility of any hydrophobic solute in water mixtures of that hydrotrope. In other words, the procedure reported in Chapter 5 can be perceived as a parametrization procedure for the cooperative hydrotropy model.

Finally, Chapter 6 showed that i) COSMO-RS is a useful tool to qualitatively predict the solubility of hydrophobic substances in water/Cyrene mixtures and ii) Cyrene does not always behave as a hydrotrope. In fact, depending on its concentration, Cyrene can act either as a hydrotrope or a co-solvent. In the latter case, for high concentration of Cyrene, water tends to act as a hydrogen bond acceptor for the solutes, effectively doubling their hydrogen bond donning ability, which increases their interaction ability with Cyrene, thus increasing their solubility.

7.2 Future Work

To each question that this work provided an answer for, many more have emerged. Some of the more urgent questions are raised in this section, in hopes that the search for their answers will have a deep impact in the field of hydrotropy. Perhaps, even asserting hydrotropy as an important topic in sustainable chemistry and a reliable tool to be used in separation processes.

1. Should hydrotropy be defined in terms of the water-mediated aggregation mechanism presented in Chapter 4?

Historically, hydrotropy has been defined as the increase of solubility of a hydrophobic solute in the presence of an amphiphilic molecule (the hydrotrope). This, however, leaves room for several questions. For instance, what is the difference between a co-solvent, a surfactant and a hydrotrope? These three classes of compounds increase the solubility of hydrophobic substances in water, albeit through different mechanisms. Instead of defining hydrotropy in terms of the physical response of a system (solubility enhancement), would it not be more concise and useful to define it in terms of a mechanism? Put differently, should not hydrotropy be defined as the solubility enhancement of a substance due to the water-mediated aggregation of hydrotropes around it?

Such a motivation for a different definition of hydrotropy is supported by the results presented in this work. In Chapter 4, it was shown that the necessity of water to establish strong hydrogen bonding networks forces the aggregation of apolar moieties, leading to the phenomenon of hydrotropy. Thus, when the concentration of water gets lower and lower as the concentration of both hydrotrope and

solute increase, the driving force for this aggregation is expected to decrease. In fact, in Chapter 5 Cyrene was shown to mediate the dissolution of hydrophobic solutes through hydrotropy, up until a given concentration, after which the dissolution mechanism was different (co-solvency, as explained in Chapter 6). Thus, it appears that not only the phenomenon of hydrotropy is concentration dependant, a molecule can act as both a hydrotrope and as a co-solvent.

2. Is the concept of *the perfect hydrotrope* plausible?

In Chapter 4, it was demonstrated that the number of hydrotrope molecules aggregated around the solute is maximum when the apolar surface area of the solute matches that of the hydrotrope. However, in the case of glycerol ethers, this did not translate into a solubility maximum for low concentration of hydrotrope, which was explained by considering that, even though less hydrotrope molecules (when their apolar area is larger than that of the solute) are aggregated around the solute, they are able to cover more of its apolar area due to their larger size. Is this always true or are there instances where finding the perfect apolar match is advantageous from an application-wise perspective?

The previous paragraph leads to the following question: is the process of designing novel hydrotropes as simple as indefinitely increasing the apolar (to increase driving force for aggregation) and polar (to retain amphiphilicity character and, thus, reasonable solubility in water) volumes of the molecule? In other words, is the concept of ***the perfect hydrotrope*** plausible? Since there really is no distinctive feature between apolar moieties other than their size, can we construct a molecule with the perfect apolar size and geometry (while retaining high water solubility) to interact with the apolar moieties of hydrophobic solutes? Or, is the best size/geometry of the hydrotrope dependent on the nature of the solute, allowing us to fine-tune the structure of the hydrotrope for specific applications, and thus instead of a perfect hydrotrope there are solute-dependent optimal hydrotropes?

3. What factors impact the driving force of aggregation and, hence, hydrotropy efficiency?

Hydrotropy arises from the water-mediated aggregation of hydrotrope apolar moieties with solute apolar moieties. Thus, the driving force of hydrotropy lies not only on the size of the apolar moieties but also on the strength of the hydrogen bonding network established between water molecules. Could there be a way to change this interaction strength between water and, thus, increase or decrease the magnitude of hydrotropy?

Consider, for instance, the addition of a fourth component to a hydrotropic system. If this component interacts with water stronger than the hydrogen bonding established between water, such as a salt which would establish ion-dipole intermolecular interactions, would this increase the hydrophobic

effect and, consequently, the extent of hydrotropy of the system? Another example is temperature. What is the effect of temperature on hydrotropy? Could the increase in temperature of the system decrease the energy of the hydrogen bonding of water and, thus, decrease the extent of hydrotropy? Likewise, can hydrotropy be more efficient at low temperatures?

4. Does hydrotropy play a part in biologically relevant systems?

There is a plethora of biomolecules, such as some amino acids, with characteristics similar to hydrotropes (large apolar size while retaining high solubility in water). Could there be biomolecules whose partial/sole purpose is to mediate the dissolution of highly hydrophobic solutes in water? And, can the mechanism of hydrotropy discussed in this work be a tool to find such biomolecules?

The questions above open exciting new paths for research in hydrotropy. Despite its age, the concept of hydrotropy is far from being explored! Who knows what new, exciting phenomena we will find as we try to construct answers to these questions!

References

[1] E. Lynge, A. Anttila, K. Hemminki, *Cancer Causes Control* **1997**, *8*, 406–419.

[2] O. Axelson, M. Hane, C. Hogstedt, *Scand. J. Work. Environ. Health* **1976**, *2*, 14–20.

[3] P. Arlien-Søborg, P. Bruhn, C. Gyldensted, B. Melgaard, *Acta Neurol. Scand.* **2009**, *60*, 149–156.

[4] L. Seedorff, E. Olsen, *Ann. Occup. Hyg.* **1990**, *34*, 371–378.

[5] T. C. Wilcosky, H. A. Tyroler, *J. Occup. Environ. Med.* **1983**, *25*, 879–885.

[6] M. Ikeda, *Toxicol. Lett.* **1992**, *64–65*, 191–201.

[7] F. Oosterhuis, X. Olsthoorn, P. Antunes, R. Ferreira dos Santos, P. Kaderják, J. Seják, *Eur. Environ.* **1998**, *8*, 129–136.

[8] H. Sidebottom, J. Franklin, *Pure Appl. Chem.* **1996**, *68*, 1757–1769.

[9] P. Wiederkehr, in *Stud. Environ. Sci.*, Elsevier, **1994**, pp. 11–28.

[10] I. D. Dobson, *Prog. Org. Coatings* **1996**, *27*, 55–58.

[11] P. Anastas, N. Eghbali, *Chem. Soc. Rev.* **2010**, *39*, 301–312.

[12] P. T. Anastas, J. B. Zimmerman, *Green Chem.* **2019**, *21*, 6545–6566.

[13] P. G. Jessop, *Green Chem.* **2011**, *13*, 1391.

[14] T. K. Hodgdon, E. W. Kaler, *Curr. Opin. Colloid Interface Sci.* **2007**, *12*, 121–128.

[15] L. Chen, J. Dou, Q. Ma, N. Li, R. Wu, H. Bian, D. J. Yelle, T. Vuorinen, S. Fu, X. Pan, et al., *Sci. Adv.* **2017**, *3*, e1701735.

[16] C. Cai, K. Hirth, R. Gleisner, H. Lou, X. Qiu, J. Y. Zhu, *Green Chem.* **2020**, *22*, 1605–1617.

[17] B. Soares, A. J. D. Silvestre, P. C. Rodrigues Pinto, C. S. R. Freire, J. A. P. Coutinho, *ACS Sustain. Chem. Eng.* **2019**, *7*, 12485–12493.

[18] B. Soares, D. J. P. Tavares, J. L. Amaral, A. J. D. Silvestre, C. S. R. Freire, J. A. P. Coutinho, *ACS Sustain. Chem. Eng.* **2017**, *5*, 4056–4065.

[19] Y. Song, R. P. Chandra, X. Zhang, T. Tan, J. N. Saddler, *Sustain. Energy Fuels* **2019**, *3*, 1329–1337.

[20] K. Gabov, P. Fardim, F. Gomes da Silva Júnior, *BioResources* **2013**, *8*, 3518–3531.

[21] M. Cvjetko Bubalo, S. Vidović, I. Radojčić Redovniković, S. Jokić, *J. Chem. Technol. Biotechnol.* **2015**, *90*, 1631–1639.

[22] C. Neuberg, *Biochem. Z* **1916**, *76*, 107–108.

[23] P. Bauduin, A. Renoncourt, A. Kopf, D. Touraud, W. Kunz, *Langmuir* **2005**, *21*, 6769–6775.

[24] K.-Y. Lai, Ed. , *Liquid Detergents*, CRC Press, Boca Raton, United States, **2005**.

[25] J. Y. Kim, S. Kim, M. Papp, K. Park, R. Pinal, *J. Pharm. Sci.* **2010**, *99*, 3953–3965.

[26] R. E. Coffman, D. O. Kildsig, *J. Pharm. Sci.* **1996**, *85*, 951–954.

[27] H. S. Frank, F. Franks, *J. Chem. Phys.* **1968**, *48*, 4746–4757.

[28] R. Sanghvi, D. Evans, S. H. Yalkowsky, *Int. J. Pharm.* **2007**, *336*, 35–41.

[29] Y. Cui, *Int. J. Pharm.* **2010**, *397*, 36–43.

[30] J. J. Booth, M. Omar, S. Abbott, S. Shimizu, *Phys. Chem. Chem. Phys.* **2015**, *17*, 8028–8037.

[31] J. J. Booth, S. Abbott, S. Shimizu, *J. Phys. Chem. B* **2012**, *116*, 14915–14921.

[32] W. Kunz, K. Holmberg, T. Zemb, *Curr. Opin. Colloid Interface Sci.* **2016**, *22*, 99–107.

[33] T. Buchecker, S. Krickl, R. Winkler, I. Grillo, P. Bauduin, D. Touraud, A. Pfitzner, W. Kunz, *Phys. Chem. Chem. Phys.* **2017**, *19*, 1806–1816.

[34] S. Shimizu, N. Matubayasi, *Phys. Chem. Chem. Phys.* **2016**, *18*, 25621–25628.

[35] J. Sherwood, M. De bruyn, A. Constantinou, L. Moity, C. R. McElroy, T. J. Farmer, T. Duncan, W. Raverty, A. J. Hunt, J. H. Clark, *Chem. Commun.* **2014**, *50*, 9650–9652.

[36] M. De bruyn, V. L. Budarin, A. Misefari, S. Shimizu, H. Fish, M. Cockett, A. J. Hunt, H. Hofstetter, B. M. Weckhuysen, J. H. Clark, et al., *ACS Sustain. Chem. Eng.* **2019**, *7*, 7878–7883.

[37] A. Klamt, *COSMO-RS: From Quantum Chemistry to Fluid Phase Thermodynamics and Drug Design*, Elsevier Science, **2005**.

[38] A. Klamt, V. Jonas, T. Bürger, J. C. W. Lohrenz, *J. Phys. Chem. A* **1998**, *102*, 5074–5085.

[39] A. Klamt, *J. Phys. Chem.* **1995**, *99*, 2224–2235.

[40] J. R. Elliott, C. T. Lira, *Introductory Chemical Engineering Thermodynamics*, Prentice Hall, Upper Saddle River, NJ, **1999**.

[41] J. M. Prausnitz, R. N. Lichtenthaler, E. G. de Azevedo, *Molecular Thermodynamics of Fluid-Phase Equilibria*, Prentice Hall, Upper Saddle River, NJ, **1999**.

[42] J. A. P. Coutinho, S. I. Andersen, E. H. Stenby, *Fluid Phase Equilib.* **1995**, *103*, 23–39.

[43] TURBOMOLE V7.1 2016, a development of University of Karlsruhe and Forschungszentrum Karlsruhe GmbH, 1989-2007, TURBOMOLE GmbH, since 2007; available from http://www.turbomole.com.

[44] COSMOtherm, Release 19; COSMOlogic GmbH & Co. KG, http://www.cosmologic.de.cosmotherm, Release 19; COSMOlogic GmbH & Co. KG, http://www.cosmologic.de.

[45] F. Eckert, A. Klamt, *AIChE J.* **2002**, *48*, 369–385.

[46] S. Queste, P. Bauduin, D. Touraud, W. Kunz, J.-M. Aubry, *Green Chem.* **2006**, *8*, 822–830.

[47] S. Queste, Y. Michina, A. Dewilde, R. Neueder, W. Kunz, J.-M. Aubry, *Green Chem.* **2007**, *9*, 491–499.

[48] J. I. García, H. García-Marín, J. A. Mayoral, P. Pérez, *Green Chem.* **2010**, *12*, 426–434.

[49] A. B. Leoneti, V. Aragão-Leoneti, S. V. W. B. de Oliveira, *Renew. Energy* **2012**, *45*, 138–145.

[50] M. Sutter, E. Da Silva, N. Duguet, Y. Raoul, E. Métay, M. Lemaire, *Chem. Rev.* **2015**, *115*, 8609–8651.

[51] A. Leal-Duaso, M. Caballero, A. Urriolabeitia, J. A. Mayoral, J. I. García, E. Pires, *Green Chem.* **2017**, *19*, 4176–4185.

[52] A. Leal-Duaso, P. Pérez, J. A. Mayoral, E. Pires, J. I. García, *Phys. Chem. Chem. Phys.* **2017**, *19*, 28302–28312.

[53] A. Leal-Duaso, P. Pérez, J. A. Mayoral, J. I. García, E. Pires, *ACS Sustain. Chem. Eng.* **2019**, *7*, 13004–13014.

[54] L. Moity, Y. Shi, V. Molinier, W. Dayoub, M. Lemaire, J.-M. Aubry, *J. Phys. Chem. B* **2013**, *117*, 9262–9272.

[55] R. Lebeuf, E. Illous, C. Dussenne, V. Molinier, E. Da Silva, M. Lemaire, J.-M. Aubry, *ACS*

Sustain. Chem. Eng. **2016**, *4*, 4815–4823.

[56] S. Choubey, L. R. Varughese, V. Kumar, V. Beniwal, *Pharm. Pat. Anal.* **2015**, *4*, 305–315.

[57] C. Srinivasulu, M. Ramgopal, G. Ramanjaneyulu, C. M. Anuradha, C. Suresh Kumar, *Biomed. Pharmacother.* **2018**, *108*, 547–557.

[58] B. Badhani, N. Sharma, R. Kakkar, *RSC Adv.* **2015**, *5*, 27540–27557.

[59] "ChemSpider," can be found under http://www.chemspider.com/.

[60] A. Alzagameem, B. Khaldi-Hansen, D. Büchner, M. Larkins, B. Kamm, S. Witzleben, M. Schulze, *Molecules* **2018**, *23*, 2664.

[61] J. Setschenow, *Z. Phys. Chem.* **1889**, *4*, 117–125.

[62] Chemat, Abert Vian, Ravi, Khadhraoui, Hilali, Perino, Tixier, *Molecules* **2019**, *24*, 3007.

[63] E. Perales, J. I. García, E. Pires, L. Aldea, L. Lomba, B. Giner, *Chemosphere* **2017**, *183*, 277–285.

[64] J. I. García, E. Pires, L. Aldea, L. Lomba, E. Perales, B. Giner, *Green Chem.* **2015**, *17*, 4326–4333.

[65] A. Noubigh, A. Aydi, A. Mgaidi, M. Abderrabba, *J. Mol. Liq.* **2013**, *187*, 226–229.

[66] A. Noubigh, A. Akermi, *J. Chem. Eng. Data* **2017**, *62*, 3274–3283.

[67] A. Noubigh, C. Jeribi, A. Mgaidi, M. Abderrabba, *J. Chem. Thermodyn.* **2012**, *55*, 75–78.

[68] I. Dali, A. Aydi, C. C. Alberto, Z. A. Wüst, A. Manef, *J. Mol. Liq.* **2016**, *222*, 503–519.

[69] A. F. M. Cláudio, M. C. Neves, K. Shimizu, J. N. Canongia Lopes, M. G. Freire, J. A. P. Coutinho, *Green Chem.* **2015**, *17*, 3948–3963.

[70] T. E. Sintra, K. Shimizu, S. P. M. Ventura, S. Shimizu, J. N. Canongia Lopes, J. A. P. Coutinho, *Phys. Chem. Chem. Phys.* **2018**, *20*, 2094–2103.

[71] S. Abbott, J. J. Booth, S. Shimizu, *Green Chem.* **2017**, *19*, 68–75.

[72] V. Dhapte, P. Mehta, *St. Petersbg. Polytech. Univ. J. Phys. Math.* **2015**, *1*, 424–435.

[73] R. H. McKee, *Ind. Eng. Chem.* **1946**, *38*, 382–384.

[74] V. G. Gaikar, M. M. Sharma, *Sep. Technol.* **1993**, *3*, 2–11.

[75] A. Stark, M. Sellin, B. Ondruschka, K. Massonne, *Sci. China Chem.* **2012**, *55*, 1663–1670.

[76] J. Palomar, J. S. Torrecilla, J. Lemus, V. R. Ferro, F. Rodríguez, *Phys. Chem. Chem. Phys.* **2010**, *12*, 1991.

[77] S. Kudo, N. Goto, J. Sperry, K. Norinaga, J. Hayashi, *ACS Sustain. Chem. Eng.* **2017**, *5*, 1132–1140.

[78] F. Cao, T. J. Schwartz, D. J. McClelland, S. H. Krishna, J. A. Dumesic, G. W. Huber, *Energy Environ. Sci.* **2015**, *8*, 1808–1815.

[79] F. P. Bouxin, J. H. Clark, J. Fan, V. Budarin, *Green Chem.* **2019**, *21*, 1282–1291.

[80] L. Mistry, K. Mapesa, T. W. Bousfield, J. E. Camp, *Green Chem.* **2017**, *19*, 2123–2128.

[81] M. M. Mention, A. L. Flourat, C. Peyrot, F. Allais, *Green Chem.* **2020**, *22*, 2077–2085.

[82] N. Guajardo, P. Domínguez de María, *Mol. Catal.* **2020**, *485*, 110813.

[83] L. Ferrazzano, D. Corbisiero, G. Martelli, A. Tolomelli, A. Viola, A. Ricci, W. Cabri, *ACS Sustain. Chem. Eng.* **2019**, *7*, 12867–12877.

[84] K. L. Wilson, J. Murray, C. Jamieson, A. J. B. Watson, *Org. Biomol. Chem.* **2018**, *16*, 2851–2854.

[85] T. W. Bousfield, K. P. R. Pearce, S. B. Nyamini, A. Angelis-Dimakis, J. E. Camp, *Green Chem.* **2019**, *21*, 3675–3681.

[86] J. Zhang, G. B. White, M. D. Ryan, A. J. Hunt, M. J. Katz, *ACS Sustain. Chem. Eng.* **2016**, *4*, 7186–7192.

[87] P. Ray, T. Hughes, C. Smith, M. Hibbert, K. Saito, G. P. Simon, *Polym. Chem.* **2019**, *10*, 3334–3341.

[88] H. J. Salavagione, J. Sherwood, M. De bruyn, V. L. Budarin, G. J. Ellis, J. H. Clark, P. S. Shuttleworth, *Green Chem.* **2017**, *19*, 2550–2560.

[89] M. De bruyn, C. Sener, D. D. Petrolini, D. J. McClelland, J. He, M. R. Ball, Y. Liu, L. Martins, J. A. Dumesic, G. W. Huber, et al., *Green Chem.* **2019**, *21*, 5000–5007.

[90] H.-J. Buschmann, H.-H. Füldner, W. Knoche, *Ber. Bunsengesell. Phys. Chem.* **1980**, *84*, 41–44.

[91] A. Misefari, Investigation of the Spectroscopic, Chemical and Physical Properties of Cyrene and Its Hydrate, University of York, **2017**.

[92] S. Kim, J. Chen, T. Cheng, A. Gindulyte, J. He, S. He, Q. Li, B. A. Shoemaker, P. A. Thiessen, B. Yu, et al., *Nucleic Acids Res.* **2019**, *47*, D1102–D1109.

[93] R. Collander, *Acta Chem. Scand.* **1951**, *5*, 774–780.

[94] A. E. Beezer, C. A. Gooch, W. H. Hunter, P. L. O. Volpe, *J. Pharm. Pharmacol.* **1987**, *39*, 774–779.

[95] J. Teixeira, T. Silva, S. Benfeito, A. Gaspar, E. M. Garrido, J. Garrido, F. Borges, *Eur. J. Med. Chem.* **2013**, *62*, 289–296.

[96] J. Burri, M. Graf, P. Lambelet, J. Löliger, *J. Sci. Food Agric.* **1989**, *48*, 49–56.

[97] R. S. Govardhan Singh, P. S. Negi, C. Radha, *J. Funct. Foods* **2013**, *5*, 1883–1891.

[98] J. H. P. M. Santos, M. Martins, A. J. D. Silvestre, J. A. P. Coutinho, S. P. M. Ventura, *Green Chem.* **2016**, *18*, 5569–5579.

[99] G. L. Perlovich, A. Bauer-Brandl, *J. Therm. Anal. Calorim.* **2001**, *63*, 653–661.

[100] D. J. Good, N. Rodríguez-Hornedo, *Cryst. Growth Des.* **2009**, *9*, 2252–2264.

[101] F. L. Mota, A. J. Queimada, S. P. Pinho, E. A. Macedo, *Ind. Eng. Chem. Res.* **2008**, *47*, 5182–5189.

[102] R. Sabbah, L. Perez, *Can. J. Chem.* **1999**, *77*, 1508–1513.

[103] F. Cilurzo, E. Alberti, P. Minghetti, C. G. M. Gennari, A. Casiraghi, L. Montanari, *Int. J. Pharm.* **2010**, *386*, 71–76.

[104] K. Guo, G. Sadiq, C. Seaton, R. Davey, Q. Yin, *Cryst. Growth Des.* **2010**, *10*, 268–273.

[105] A. J. Queimada, F. L. Mota, S. P. Pinho, E. A. Macedo, *J. Phys. Chem. B* **2009**, *113*, 3469–3476.

[106] M. Temprado, M. V. Roux, J. S. Chickos, *J. Therm. Anal. Calorim.* **2008**, *94*, 257–262.

Appendix

A1. List of Glycerol Ethers Studied

Table A1.1. List of glycerol ethers used in this work along with their CAS number, source and purity.

Substance	CAS Number	Source	Purity (wt%)
Glycerol	56-81-5	Fisher Chemical	>99.8
[1.0.0]	623-39-2	Synthetized[1]	>98[b)]
[2.0.0]	1874-62-0	Synthetized[1]	>99[b)]
[3.0.0]	61940-71-4	Synthetized[1]	>99[b)]
[4.0.0]	624-52-2	Synthetized[1]	>99[b)]
[5.0.0]	22636-32-4	Synthetized[1]	>99[b)]
[6.0.0]	**a)**	Synthetized[1]	>99[b)]
[1.0.1]	623-69-8	Synthetized[1]	>99[b)]
[2.0.2]	4043-59-8	Synthetized[1]	>99[b)]

a) Compound has no CAS number available. **b)** Estimated by NMR.

A2. Cooperative Hydrotropy Model (Glycerol Ethers)

In order to use the cooperative hydrotropy model to fit the experimental solubility data of gallic and syringic acids in aqueous solutions of glycerol ethers, it was necessary to convert the concentration of hydrotrope in the solute (free-solute basis) to its mole fraction in the ternary system ($x_{Hydrotrope}$), as well as the solubility of the solute to mole fraction in the ternary system (x_{Solute}). It was assumed that the density of the system is equal to that of water. Hence, Equations A2.1 and A2.2 were used:

$$x_{Hydrotrope} = \frac{\frac{(1000-S_3)\cdot w_2}{M_2}}{\frac{(1000-S_3)\cdot w_1}{M_1}+\frac{(1000-S_3)\cdot w_2}{M_2}+\frac{S_3}{M_3}} \quad \text{(A2.1)}$$

$$x_{Solute} = \frac{\frac{S_3}{M_3}}{\frac{(1000-S_3)\cdot w_1}{M_1}+\frac{(1000-S_3)\cdot w_2}{M_2}+\frac{S_3}{M_3}} \quad \text{(A2.2)}$$

where w_1 and w_2 are the mass fractions of water and hydrotrope in the solvent (free-solute basis), respectively, M_1, M_2 and M_3 are the molar masses of water, hydrotrope and solute, respectively, and S_3 is the solubility of the solute in the hydrotropy system (mol/L).

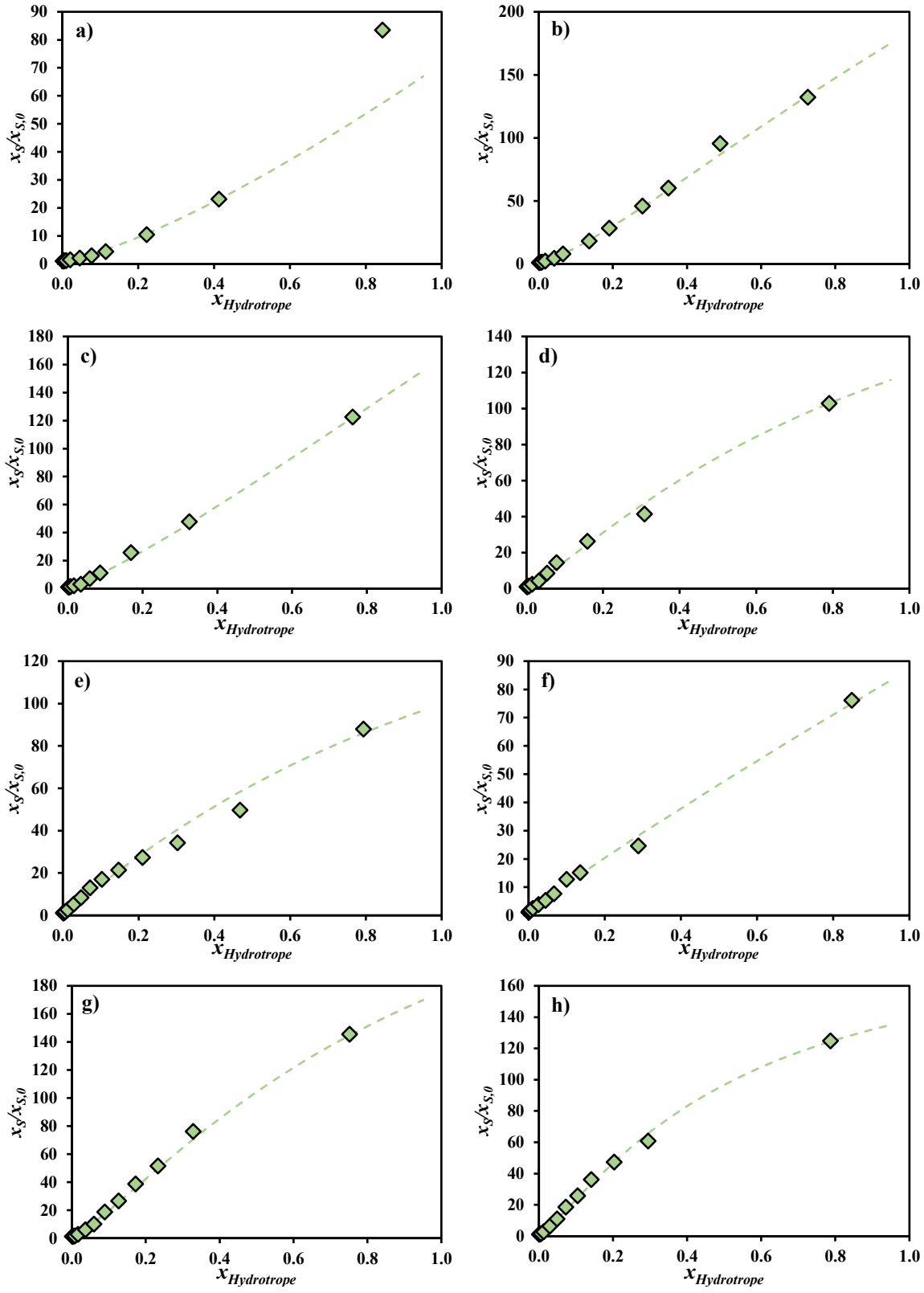

Figure A2.1. *Experimental solubility data, ◆, for gallic acid in aqueous solutions of a) [0.0.0], b) [1.0.0], c) [2.0.0], d) [3.0.0], e) [4.0.0], f) [5.0.0], g) [1.0.1] and h) [2.0.2], fitted using the cooperative hydrotropy model (- - -). The x-axys represents the mole fraction of the hydrotrope in the ternary system (as opposed to its mole fraction in the solvent free of solute).*

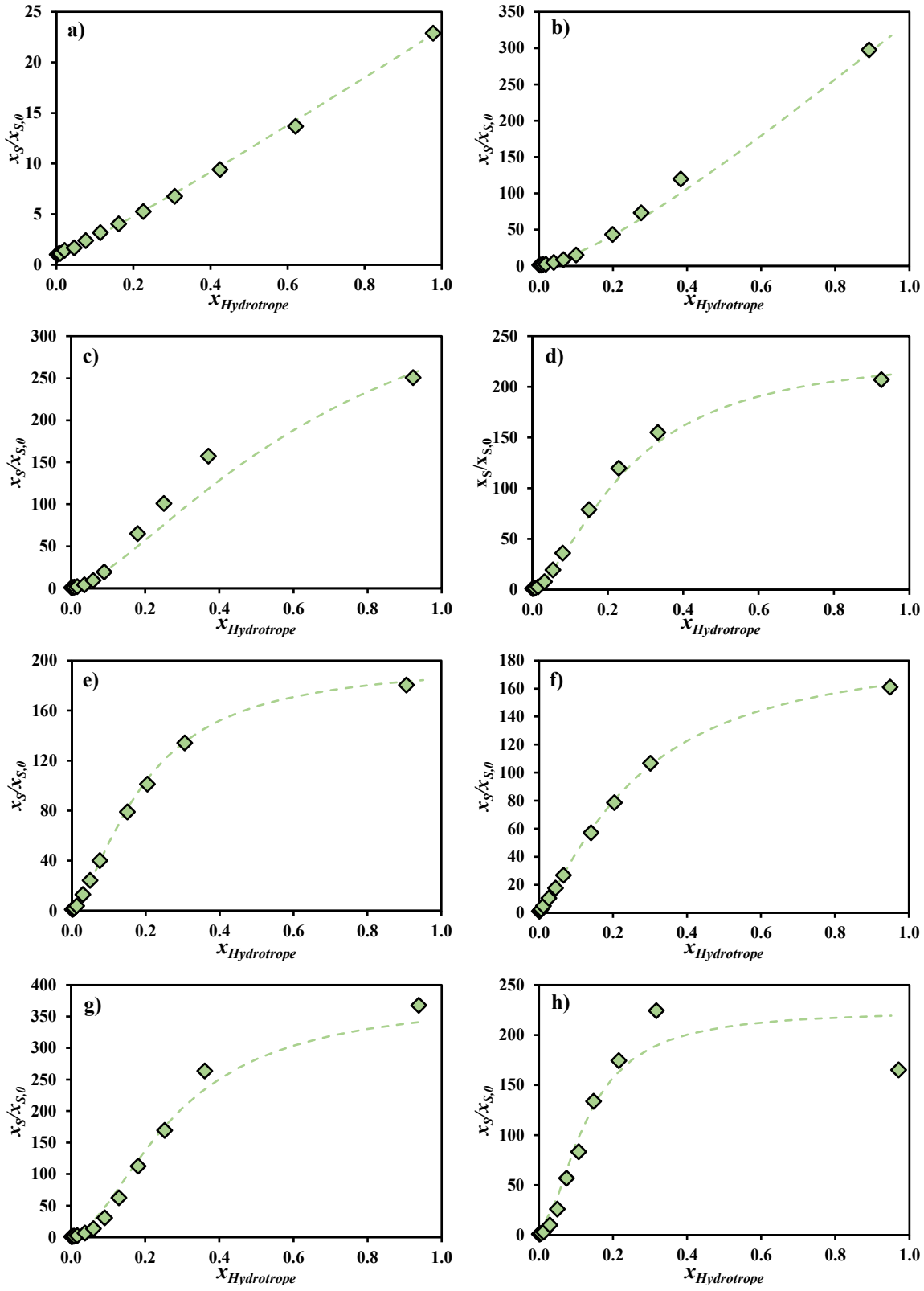

Figure A2.2. *Experimental solubility data, ◆, for syringic acid in aqueous solutions of a) [0.0.0], b) [1.0.0], c) [2.0.0], d) [3.0.0], e) [4.0.0], f) [5.0.0], g) [1.0.1] and h) [2.0.2], fitted using the cooperative hydrotropy model (- - -). The x-axys represents the mole fraction of the hydrotrope in the ternary system (as opposed to its mole fraction in the solvent free of solute).*

Table A2.1. *Parameters of the cooperative hydrotropy model for the solubility of gallic and syringic acids in glycerol ether-based hydrotrope solutions.*

	Hydrotrope	m*ax*	*m*	*b*
Gallic acid	[0.0.0]	10000[a)]	1.317	-4.949
	[1.0.0]	675	1.313	-0.988
	[2.0.0]	1606	1.208	-2.178
	[3.0.0]	236	1.200	0.013
	[4.0.0]	228	1.084	-0.259
	[5.0.0]	10000[a)]	0.932	-4.746
	[1.0.1]	347	1.252	0.014
	[2.0.2]	201	1.235	0.769
Syringic acid	[0.0.0]	562	1.126	-3.183
	[1.0.0]	2371	1.382	-1.801
	[2.0.0]	432	1.482	0.490
	[3.0.0]	236	1.628	2.260
	[4.0.0]	199	1.561	2.593
	[5.0.0]	192	1.330	1.782
	[1.0.1]	379	1.782	2.299
	[2.0.2]	225	1.789	3.729

a) unbounded optimization: increasing the value *ad infinitum* decreases the quadratic error sum.

A3. Solute Recovery (Glycerol Ethers)

The feasibility of adding water to recover dissolved solute from the hydrotropic system was preliminarily studied in this work using the solubility curves fitted with the cooperative hydrotropy model. The concept relies on calculating the mass fraction of solute that is recovered by the addition of a given volume of water. The algorithm used to calculate the recovery curves is as follow. The hydrotropic system, with total mole number n_t^0, is selected (solute-hydrotrope pair and hydrotrope mole fraction).

1. Select fraction of water to be added (n_{H_2O}/n_t^0).

2. Arbitrate the fraction of solute that precipitates (n_p/n_t^0).

3. Calculate increase of the new system (n_t/n_t^0):

$$\frac{n_t}{n_t^0} = 1 + \frac{n_{H_2O}}{n_t^0} - \frac{n_p}{n_t^0}$$

4. Calculate hypothetical composition of the new system (x_1, x_2, x_3) from the composition of the original system (x_1^0, x_2^0, x_3^0):

$$x_1 = \frac{x_1^0 + n_{H_2O}/n_t^0}{n_t/n_t^0}$$

$$x_2 = \frac{x_2^0}{n_t/n_t^0}$$

$$x_3 = \frac{x_3^0 - n_p/n_t^0}{n_t/n_t^0}$$

5. Calculate saturation mole fraction of solute (x_3') for the hypothetical mole fraction of hydrotrope obtained in step 3 (Equation 3 of the main text with the parameters of Table SX).

6. If $x_3 = x_3'$, stop iteration. If $x_3 > x_3'$, return to step 1 and arbitrate higher n_p. If $x_3 < x_3'$, return to step 1 and arbitrate lower n_p.

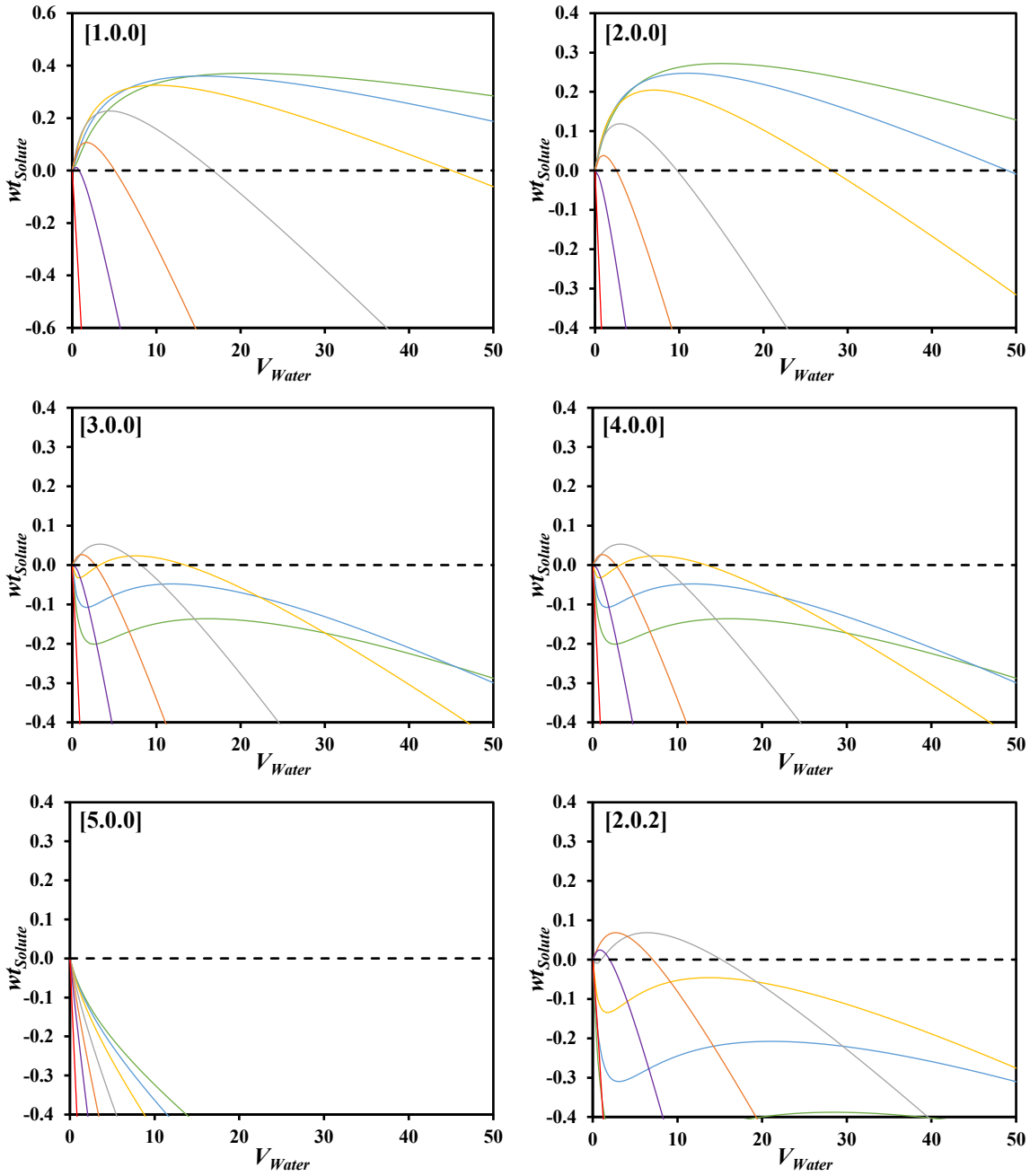

Figure A3.1. *Estimated fraction of gallic acid (wt_{Solute}) recovered from hydrotrope solution by the addition of water (V_{Water} is the volumetric reason between added water and initial system), with an initial hydrotrope mole fraction of 0.01 —, 0.05 —, 0.1 —, 0.2 —, 0.4 —, 0.6 — and 0.8 —. A negative value indicates that no precipitation happens, with the system being able to dissolve further solute.*

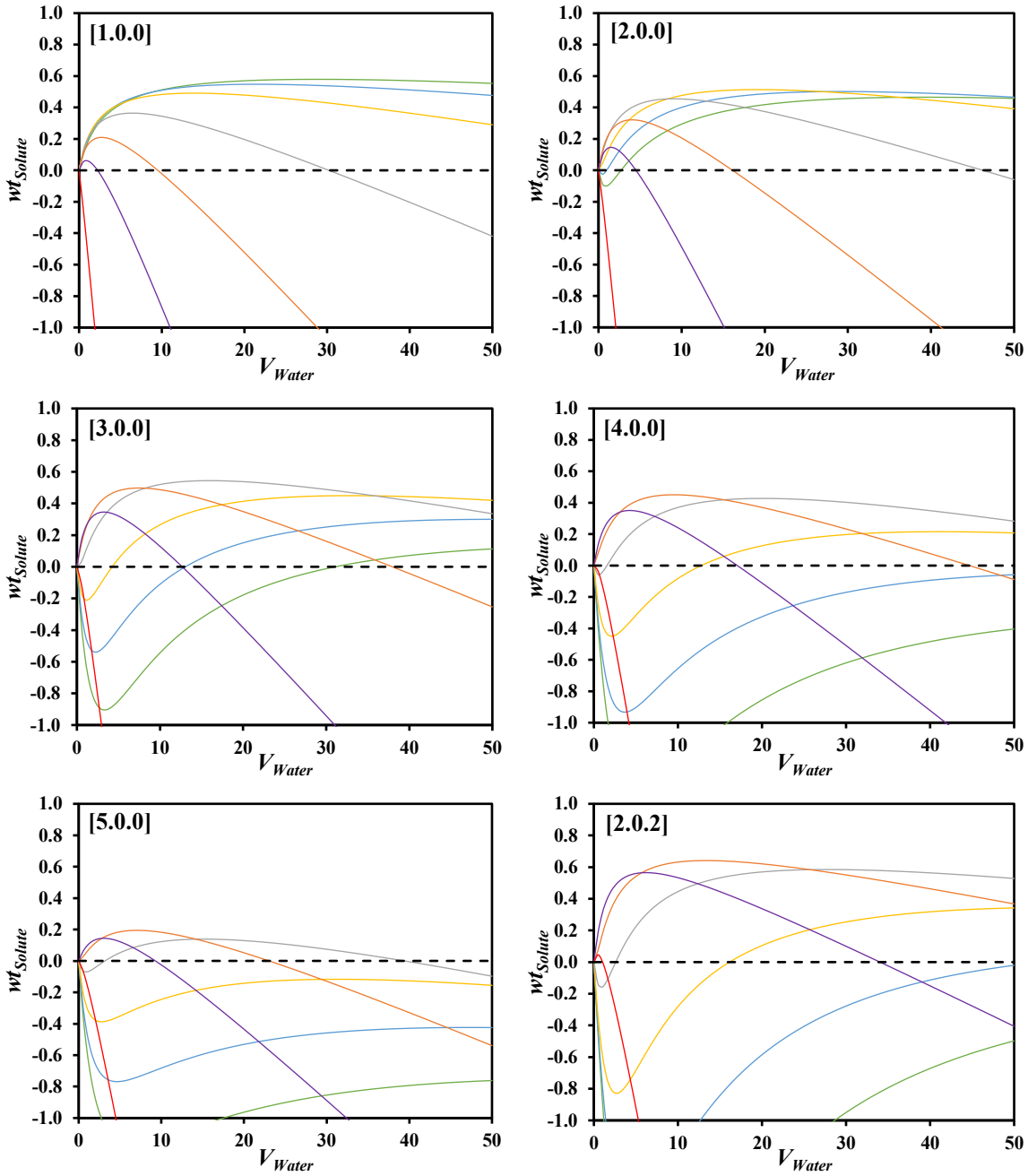

Figure A3.2. *Estimated fraction of syringic acid (wt_{Solute}) recovered from hydrotrope solution by the addition of water (V_{Water} is the volumetric reason between added water and initial system), with an initial hydrotrope mole fraction of 0.01 —, 0.05 —, 0.1 —, 0.2 —, 0.4 —, 0.6 — and 0.8 —. A negative value indicates that no precipitation happens, with the system being able to dissolve further solute.*

A4. ^{1}H-NMR Peaks

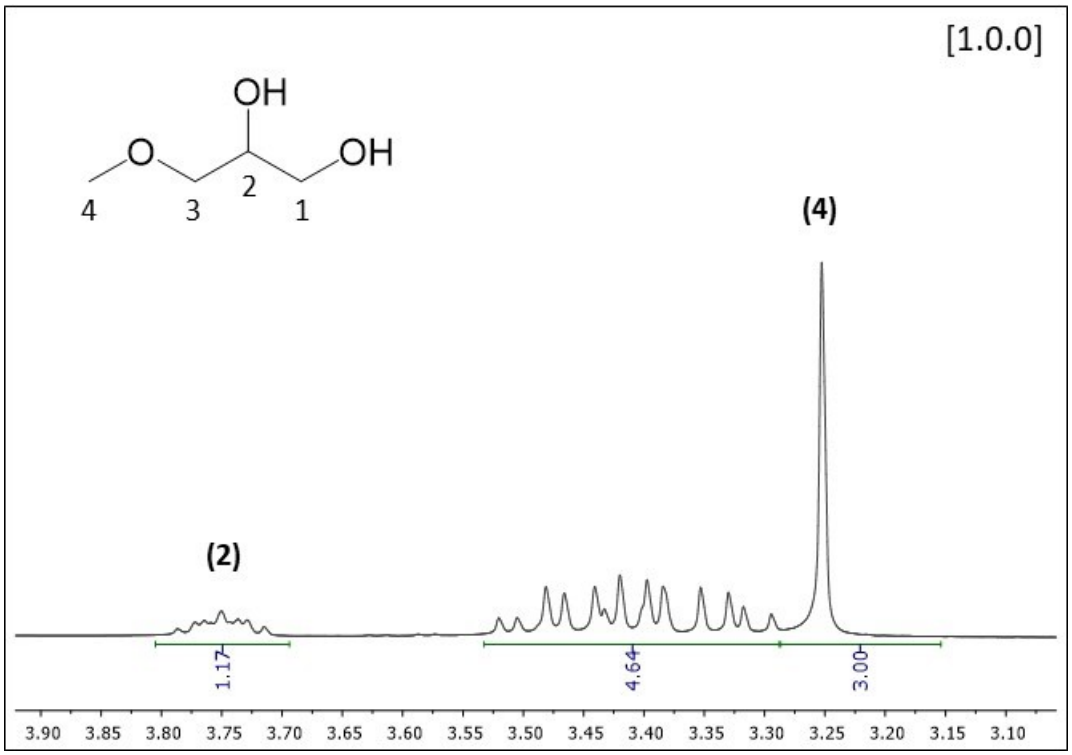

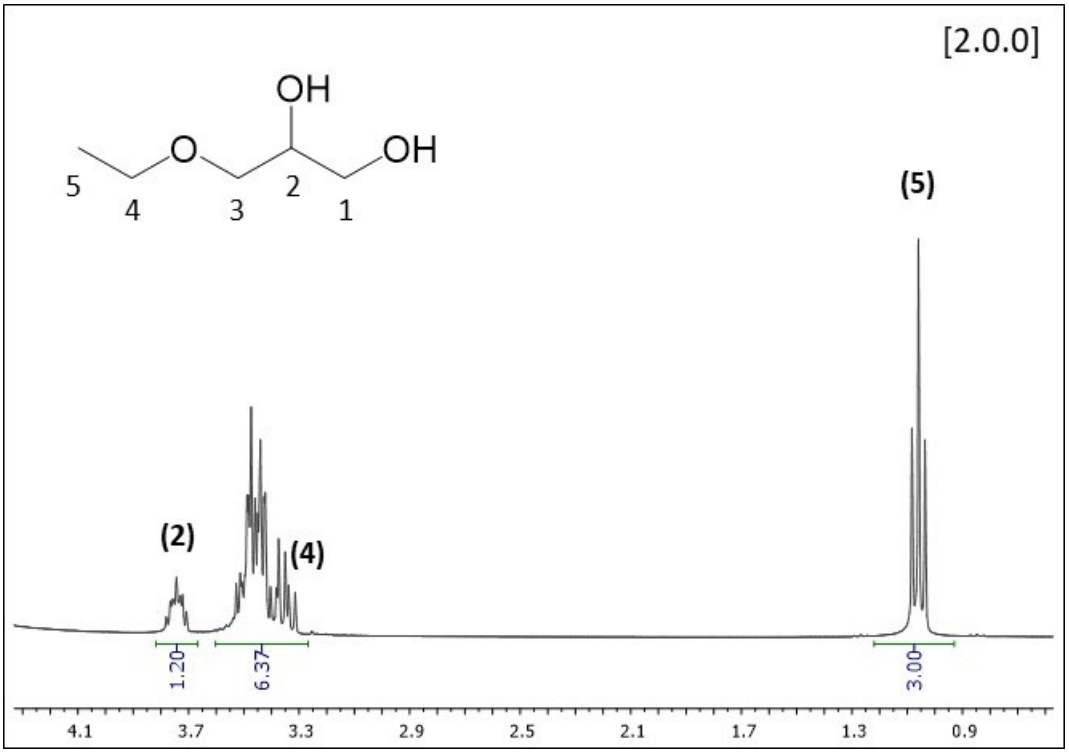

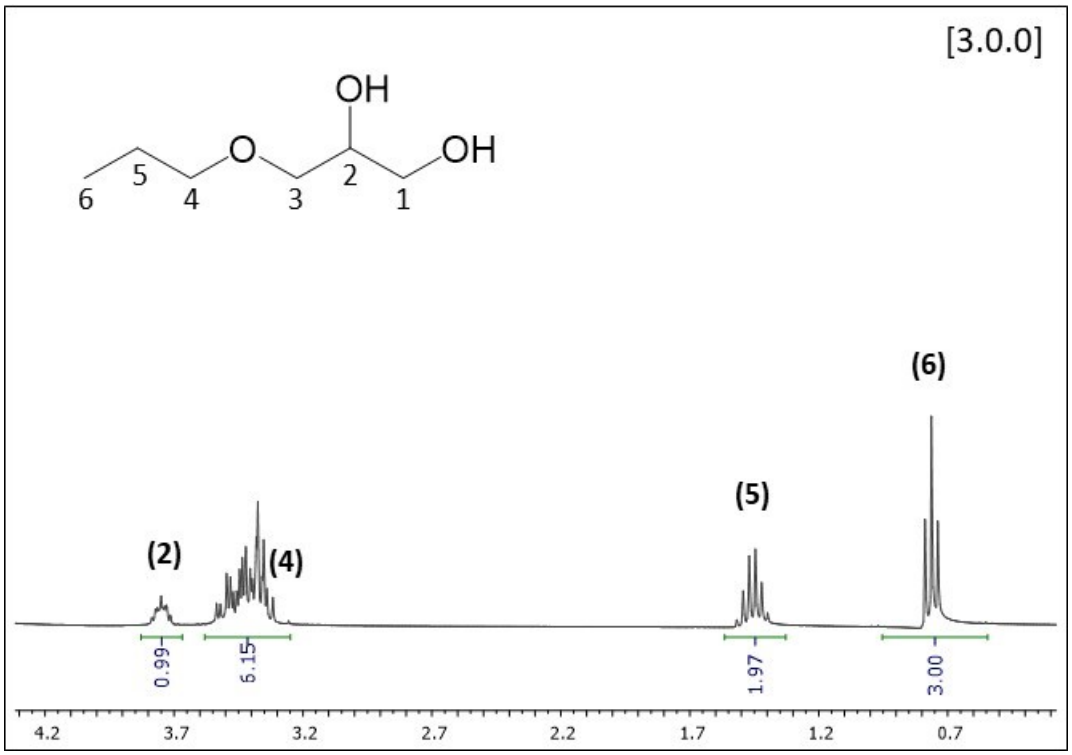
[3.0.0]
OH
O
OH
6
5
4
3
2
1
(6)
(5)
(2)
(4)
0.99
6.15
1.97
3.00
4.2
3.7
3.2
2.7
2.2
1.7
1.2
0.7

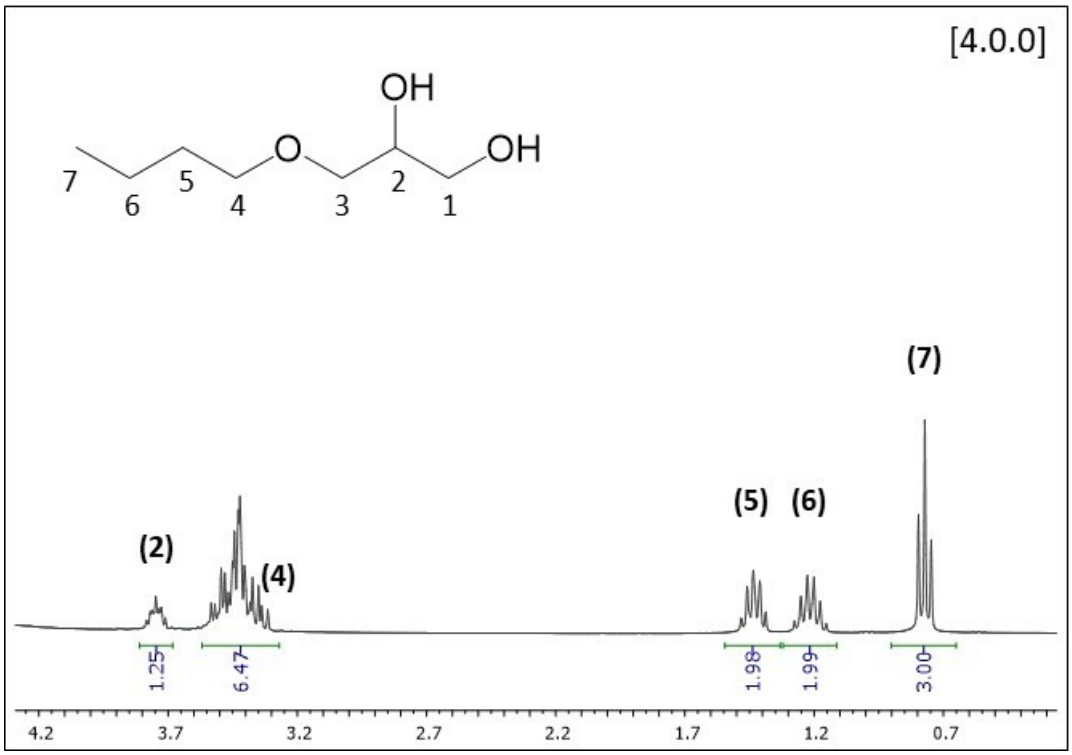
[4.0.0]
OH
O
OH
7
6
5
4
3
2
1
(7)
(5)
(6)
(2)
(4)
1.25
6.47
1.98
1.99
3.00
4.2
3.7
3.2
2.7
2.2
1.7
1.2
0.7

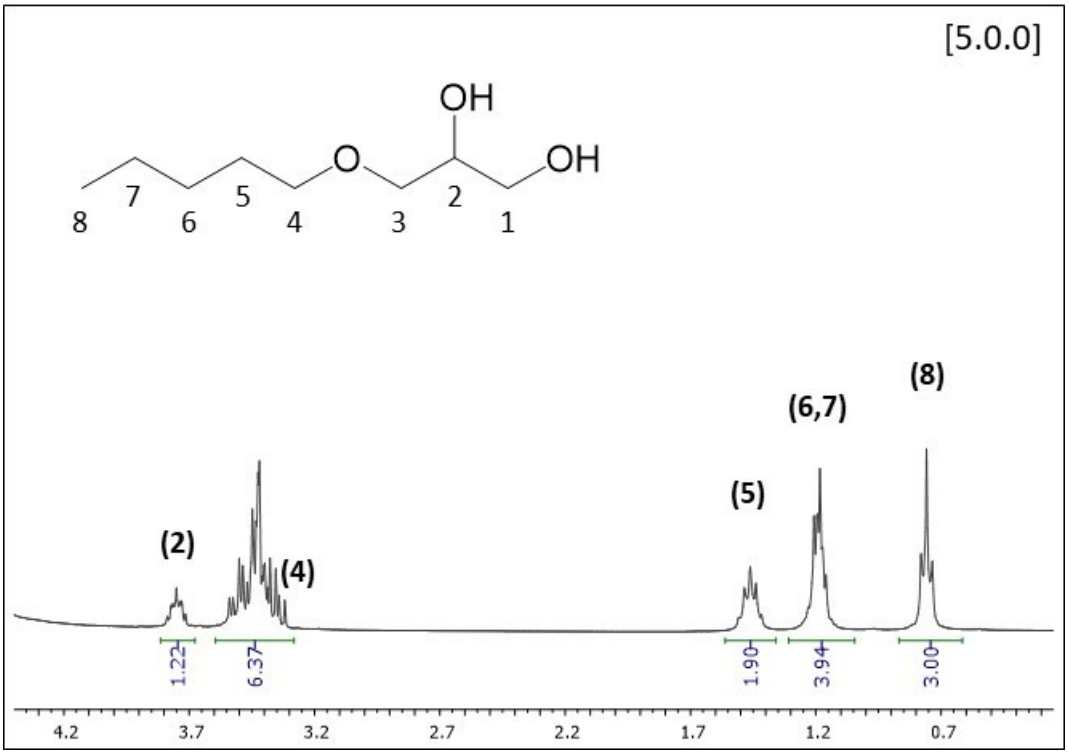

Figure A4.1. *^{1}H-NMR spectra for aqueous solutions of monoalkylglycerol ethers (0.4 mol/kg concentration) in the chemical shift window used in this work. From top to bottom, [1.0.0], [2.0.0], [3.0.0], [4.0.0] and [5.0.0], with the structure of each substance reported as inset. Signaled peaks are those used in this work, with the number matching the number sequence of the inset structure. Chemical shifts (x-axis) are reported in ppm.*

A5. Chemical Shifts

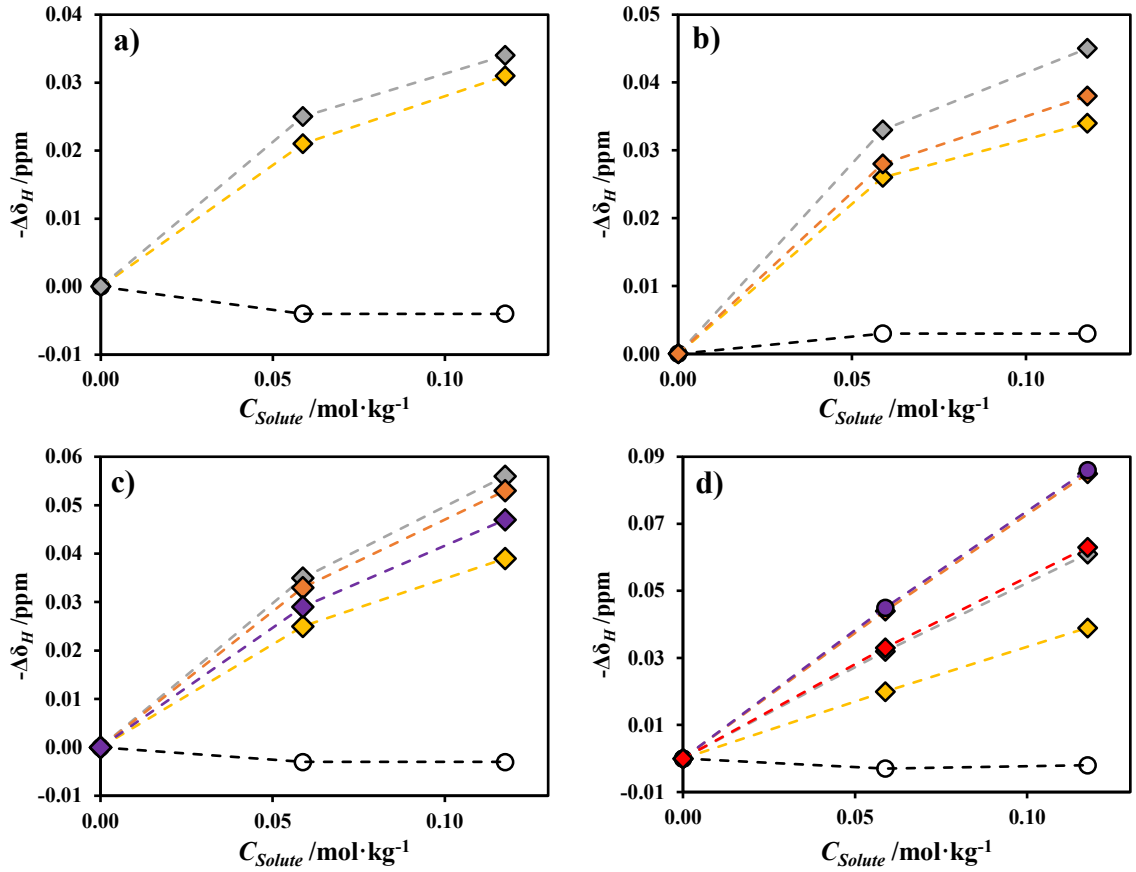

Figure A5.1. *Change in chemical shift of the protons ($-\Delta\delta_H$) associated to water and several methyl groups of a) [1.0.0], b) [2.0.0], c) [3.0.0] and d) [5.0.0] dissolved in water (0.4 mol/kg) as a function of gallic acid concentration. Similar data for [4.0.0] is reported in the main text (Figure 1). Legend: -○- water; -◇- 2nd carbon; -◇- 4th carbon; -◇- 5th carbon; -◇- 6th carbon; -◇- 7th carbon; -◇- 8th carbon. For [5.0.0] the peaks from the hydrogens of the 6th and 7th carbon are undistinguishable and are represented as -●-.*

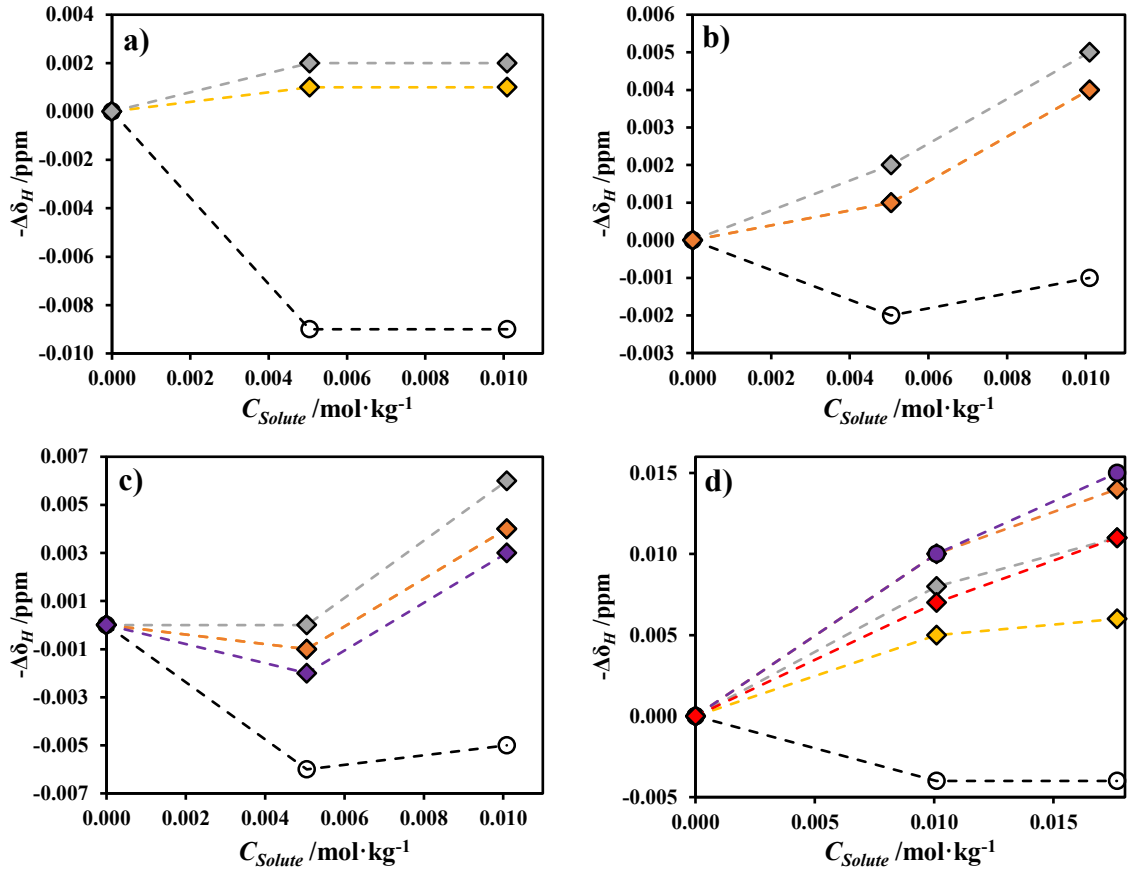

Figure A5.2. *Change in chemical shift of the protons ($-\Delta\delta_H$) associated to water and several methyl groups of a) [1.0.0], b) [2.0.0], c) [3.0.0] and d) [5.0.0] dissolved in water (0.4 mol/kg) as a function of syringic acid concentration. Similar data for [4.0.0] is reported in the main text (Figure 1). Legend: -○- water; -◇- 2nd carbon; -◇- 4th carbon; -◇- 5th carbon; -◇- 6th carbon; -◇- 7th carbon; -◇- 8th carbon. For [5.0.0] the peaks from the hydrogens of the 6th and 7th carbon are undistinguishable and are represented as -●-.*

A6. Chemical Shifts

For chloride-based ionic liquids, the cation was optimized separately from the chloride anion. The apolar factor of the ionic liquid is obtained by summing the apolar factors of the cation and of the anion.

Note that, unlike for the glycerol ether hydrotrope series, the hydrotropy extent of some chloride-based ionic liquids does not correlate well with the corresponding apolar factor (Figure A6.1). This is most likely due to the role of the chloride ion, which may stay solvated or accumulate around the solute-cation cluster for charge stabilization.

Table A6.1. *Apolar Factor of substances and ions used in the literature as hydrotropes.*

Substance/Ion	**Apolar Factor ($\cdot 10^3$)**	**Substance/Ion**	**Apolar Factor ($\cdot 10^3$)**
1-ethyl-3-methylimidazolium	0.4755	Chloride	0
1-butyl-3-methylimidazolium	0.7120	Gallic Acid	0.4981
1-hexyl-3-methylimidazolium	0.9684	Syringic Acid	0.7235
1-octyl-3-methylimidazolium	1.2264	[0.0.0]	0.3352
1-butyl-3-methylpyridinium	0.8495	[1.0.0]	0.5041
1-butyl-1-methylpiperidinium	0.7764	[2.0.0]	0.6481
1-butyl-1-methylpyrrolidinium	0.6958	[3.0.0]	0.7820
Tetrabutylammonium	1.6684	[4.0.0]	0.9117
Tetrabutylphosphonium	1.7036	[5.0.0]	1.0406
Cholinium	0.2170	[1.0.1]	0.6828
Sodium	0	[2.0.2]	0.9636

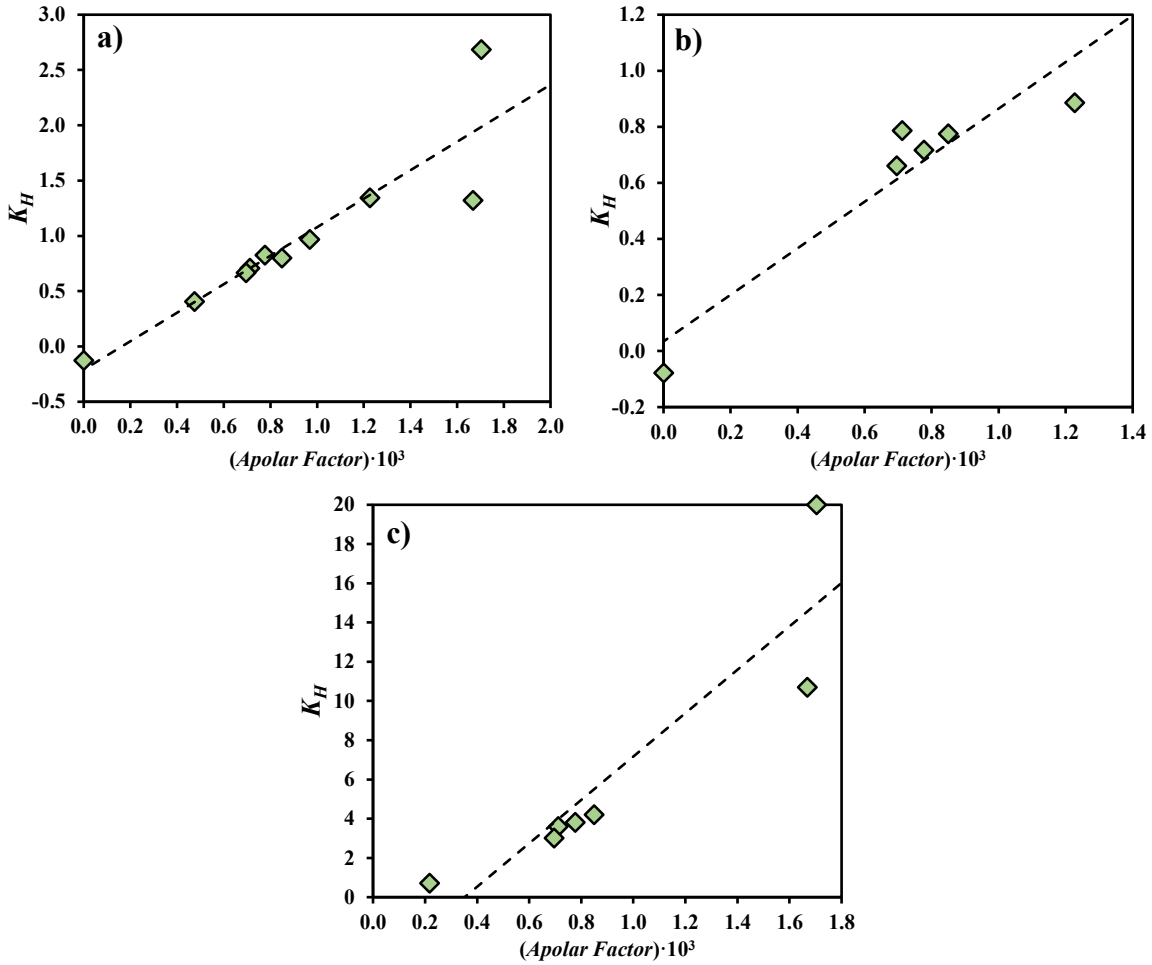

Figure A6.1. *Setschenow constants of a) vanillin,*[2] *b) gallic acid*[2] *and c) ibuprofen*[3] *for chloride-based ionic liquid hydrotropic systems as a function of the apolar factor of the ionic liquid. The dashed lines ate the straight lines fitted to the data using the least squares method.*

A7. Cyrene Acidity

De bruyn et al.[4] reported the pH of water-Cyrene mixtures in a narrow composition range, from pure water to around 30 wt% of Cyrene. This data, complemented with data measured in this work for the full composition range of the water-Cyrene system, is depicted in Figure A7.1. Since a pH of 2.5 corresponds to a hydronium ion concentration of around 3 mM, the concentration of dissociated diol is much smaller than the concentration of protonated diol in the system. The pH was measured using a Mettler Toledo U402-M3- S7/200 micro electrode. The instrument was previously calibrated with a standard solution in the pH range of 4.0, 7.0 and 9.0. The readings were performed in triplicate at a temperature of (300.2 ± 0.5) K.

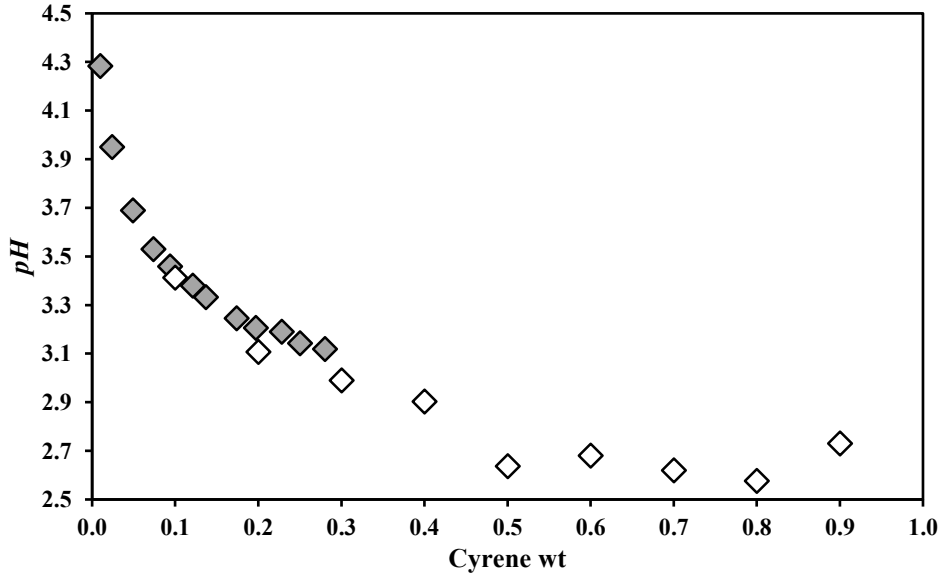

Figure A7.1. *Acidity of water-Cyrene mixtures in terms of the pH of the mixture as a function of the mass fraction of pure Cyrene added to water (◆ De bruyn et al.[4]; ◇ This work).*

To test if acidifying a water-Cyrene mixture changes its chemical equilibrium (which would be problematic when studying the solubility of acidic solutes), the ultraviolet absorbance spectrum of water-Cyrene mixtures, in the concentration range from 0 to 15 wt% of Cyrene, was measured in this work. All spectra were acquired using 1 mm quartz cells in a SHIMADZU UV-1700, Pharma-Spec spectrometer, in the wavelength range 220-350 nm, with 1 nm step intervals.

The UV spectra data is reported in Figure A7.2 (left) and reveals the existence of a double peak around a wavelength (λ) of 260 nm. The absorbance of this peak, namely at a wavelength of 261 nm, is proportional to the concentration of Cyrene, as shown if Figure A7.2 (right). Figure A7.3 depicts the same Spectra with the additional spectrum of a 10 wt% water-Cyrene mixture buffered at a pH value of one, using HCl.

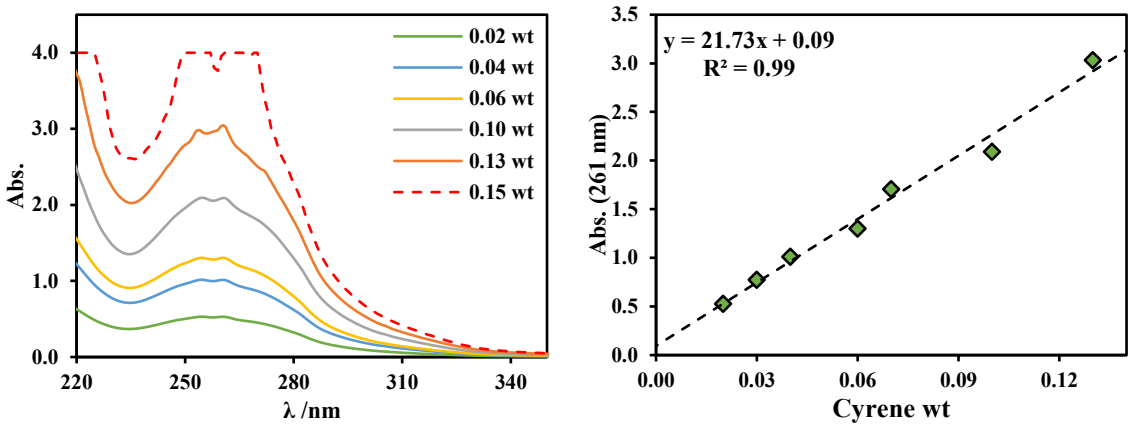

Figure A7.2. *UV spectra of water-Cyrene mixtures in the Cyrene concentration range 0-15 wt% (left) and absorvance of water-Cyrene mixtures at a wavelength (λ) of 261 nm as a function of Cyrene concentration (right). The dashed line (right) is the line fitted to the data using the least squares method (coefficient of determination is 0.99).*

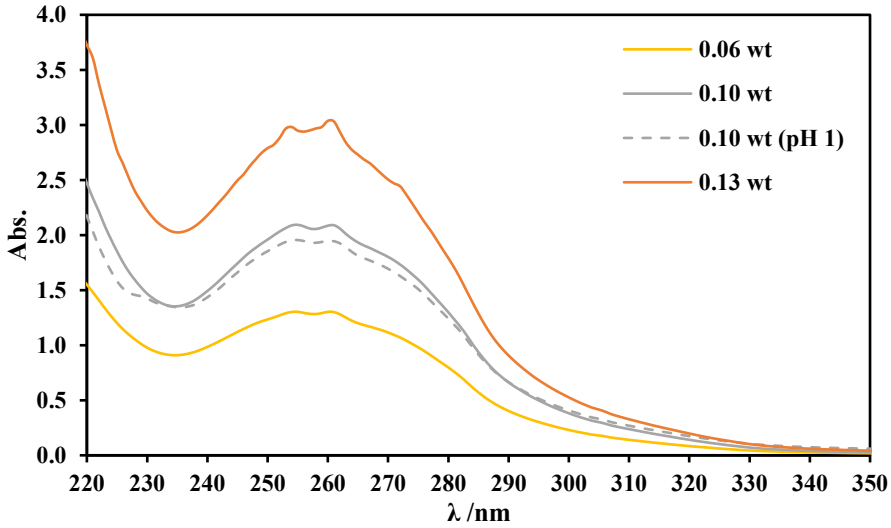

Figure A7.3. *UV spectra of water-Cyrene mixtures in the Cyrene concentration range 6-13 wt% along with the UV spectrum of a water-Cyrene mixture buffered at a pH of 1 with HCl, showing the negligible influence of pH in the chemical equilibrium of Cyrene in water.*

A8. Water-Cyrene System Composition

De bruyn et al.[5] reported the molar concentration of water (C_w) and of the ketone (C_{C_1}) and diol (C_{C_2}) forms of Cyrene for the entire composition range of the water-Cyrene system. From this data, the mole fractions of the individual components are calculated using:

$$x_i = \frac{C_i}{C_w + C_{C_1} + C_{C_2}} \tag{A8.1}$$

where x_i is the mole fraction of component i (w, C_1 or C_2) and C_i its molar concentration.

The mole percentage of each form of Cyrene ($Mole_i$ %) is defined as:

$$Mole_i\ \% = \frac{x_i}{x_{C_1} + x_{C_2}} \tag{A8.2}$$

The total mole fraction of Cyrene ($x_{Total\ Cyrene}$) is defined as:

$$x_{Total\ Cyrene} = x_{C_1} + x_{C_2} \tag{A8.3}$$

Similar to Equation S1, mass fractions of the individual components are calculated using:

$$w_i = \frac{C_i \cdot M_i}{C_w \cdot M_w + C_{C_1} \cdot M_{C_1} + C_{C_2} \cdot M_{C_2}} \tag{A8.4}$$

where w_i is the mole fraction of component i, M_i its molar mass, and M_w, M_{C_1} and M_{C_2} are the molar masses of water, and the ketone and the diol forms of Cyrene, respectively. To avoid ambiguity, the original mass fraction of Cyrene (w_{OC}) is defined as:

$$w_{OC} = \frac{m_{Cyrene}}{m_{Cyrene} + m_w} \tag{A8.5}$$

where m_{Cyrene} and m_w are the masses of **pure** Cyrene and pure water used to prepare a given water-Cyrene mixture.

Due to the difficulty of assigning an equilibrium constant to the water-Cyrene system, the mass fraction of the individual components in the final system (after equilibrium is achieved) was fitted against the original mass fraction of Cyrene. The resulting fitting is depicted in Figure A8.1 and the expressions are:

$$w_{C_1} = 1.6228 \cdot w_{OC}^6 - 9.6663 \cdot w_{OC}^5 + 16.4868 \cdot w_{OC}^4 - 9.6440 \cdot w_{OC}^3 + 2.3399 \cdot w_{OC}^2 - 0.1432 \cdot w_{OC} + 0.0017 \tag{A8.6}$$

$$w_{C_2} = -1.6668 \cdot w_{OC}^6 + 10.4154 \cdot w_{OC}^5 - 18.0321 \cdot w_{OC}^4 + 10.5373 \cdot w_{OC}^3 - 2.5396 \cdot w_{OC}^2 + 1.2902 \cdot w_{OC} - 0.0019 \tag{A8.7}$$

where w_{OC} is an abbreviation of $w_{Original\ Cyrene}$.

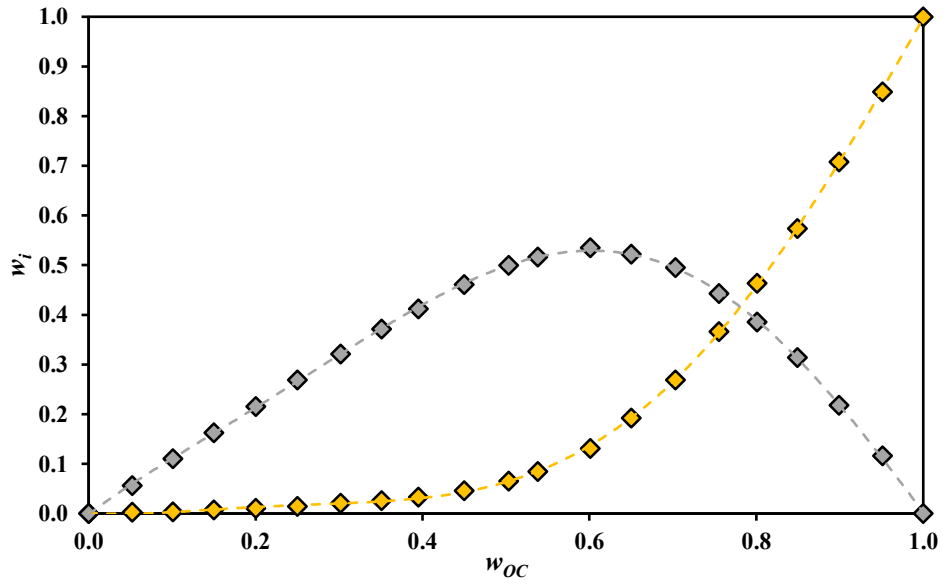

Figure A8.1. *Composition of water-Cyrene mixtures: mass fraction of ketone form (◆) and diol form (◆) of Cyrene as a function of its original mass fraction calculated from the data reported by De bruyn et al.*[5] *and fitted with sixth degree polynomials (- - - for the ketone form and - - - for the diol form).*

The density of water-Cyrene mixtures (ρ), depicted in Figure A8.2, was calculated from the data reported by De bruyn et al.[5] using the following expression:

$$\rho\left(\frac{g}{mL}\right) = \frac{C_w \cdot M_w + C_{C_1} \cdot M_{C_1} + C_{C_2} \cdot M_{C_2}}{1000} \tag{A8.8}$$

This data was then fitted using a third-degree polynomial:

$$\rho\left(\frac{g}{mL}\right) = -0.50550 \cdot w_{OC}^3 + 0.45749 \cdot w_{OC}^2 + 0.29735 \cdot w_{OC} + 0.99797 \tag{A8.9}$$

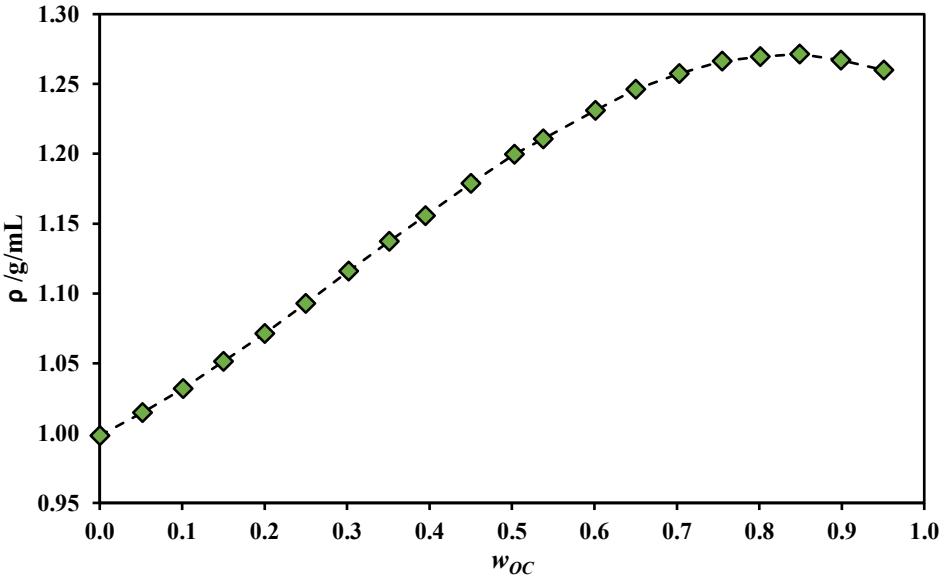

Figure A8.2. *Density of water-Cyrene mixtures as a function of the original mass fraction of Cyrene. The dashed line is a visual aid.*

A9. Solubility in Water-Cyrene Mixtures

As explained in the main text, the presence of the solute, due to its low concentration, does not affect the equilibrium established between both forms of Cyrene. This is true also for acidic solutes. In the following calculations it is assumed that, due to the low concentration of the solute, the density of the final mixture is equal to that of the solvent. For any given hydrotropic mixture, using 1 L as the basis for calculations, the total mass (m_t) is given by:

$$m_t = 1000 \cdot \rho \tag{A9.1}$$

Note that ρ is calculated using Equation S9. The mass of each component (m_i) is calculated as follow:

$$m_S = S_S \cdot M_S \tag{A9.2}$$

$$m_w = (m_t - m_S) \cdot \left(1 - w_{C_1} - w_{C_2}\right) \tag{A9.3}$$

$$m_{C_1} = (m_t - m_s - m_w) \cdot \left(\frac{w_{C_1}}{w_{C_1}+w_{C_2}}\right) \tag{A9.4}$$

$$m_{C_2} = (m_t - m_s - m_w) \cdot \left(\frac{w_{C_2}}{w_{C_1}+w_{C_2}}\right) \tag{A9.5}$$

where m_i is the mass of component i (w for water, C_1 for the ketone form of Cyrene, C_2 for the diol form of Cyrene and S for the solute). Finally, the mole fraction of each component (x_i) is calculated using the following expression:

$$x_i = \frac{\frac{m_i}{M_i}}{\frac{m_w}{M_w}+\frac{m_{C_1}}{M_{C_1}}+\frac{m_{C_2}}{M_{C_2}}+\frac{m_S}{M_S}} \tag{A9.6}$$

where M_i is the molar mass of component i.

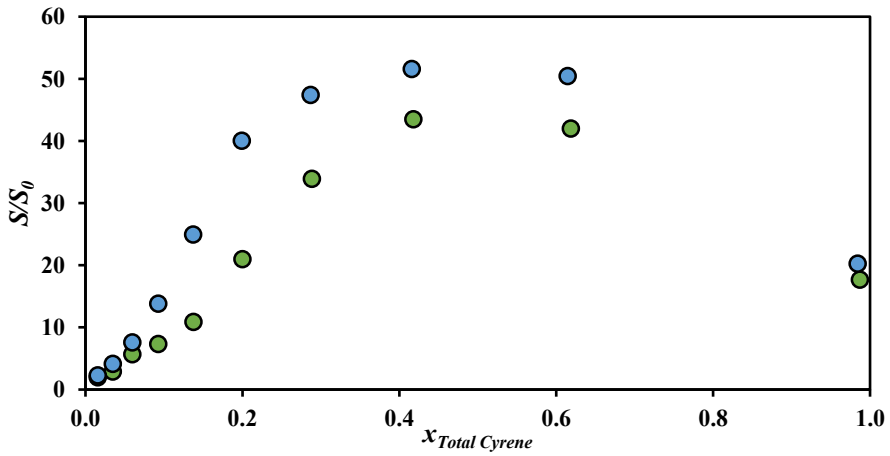

Figure A9.1. *Solubility of syringic acid in water-Cyrene mixtures at 20 ºC* (●) *and at 30 ºC* (●) herein experimentally measured.

A10. Solutes Structure and σ-Surface

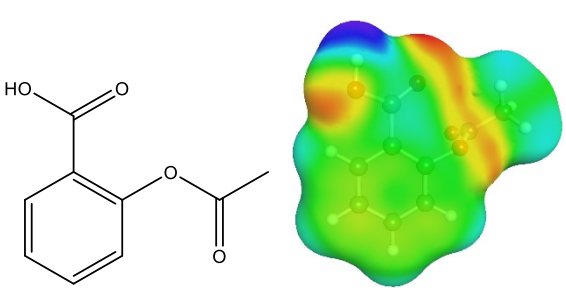

Aspirin

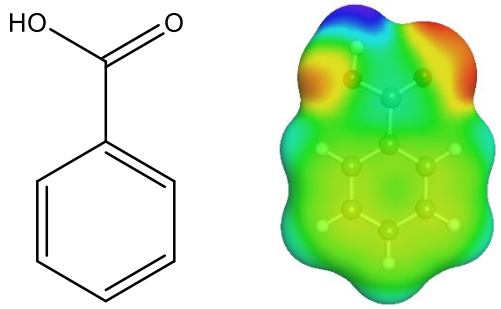

Benzoic Acid

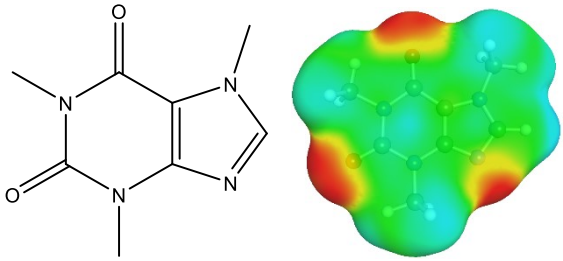

Caffeine

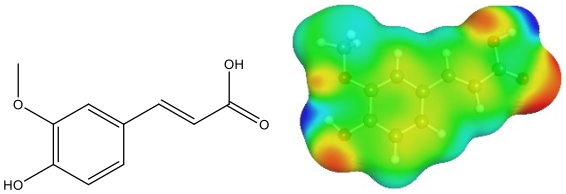

Ferulic Acid

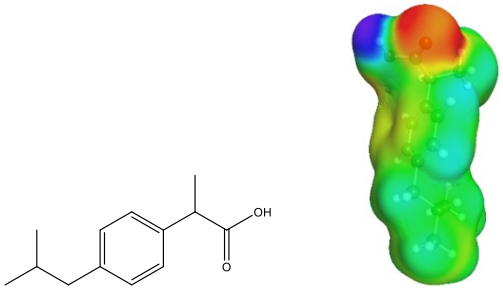

Ibuprofen

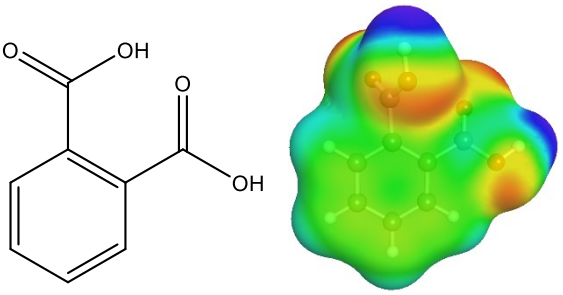

Phthalic Acid

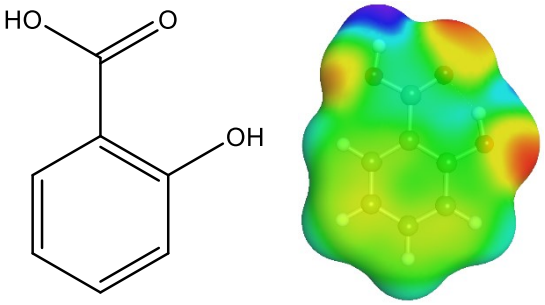

Salicylic Acid

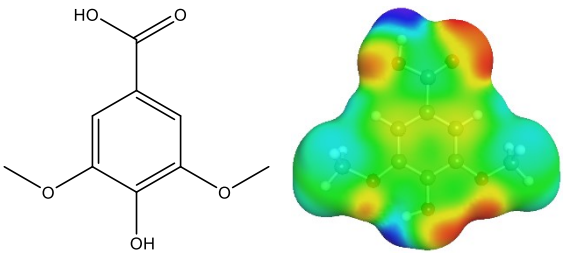

Syringic Acid

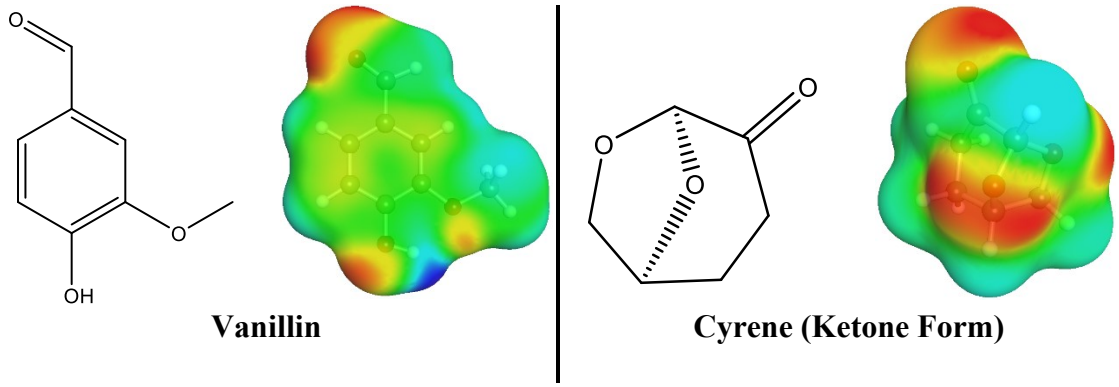

Figure A10.1. *Chemical structures and σ-surface of the solutes studied in Chapter 6 and of the ketone form of Cyrene.*

A11. COSMO-RS Solubility Prediction

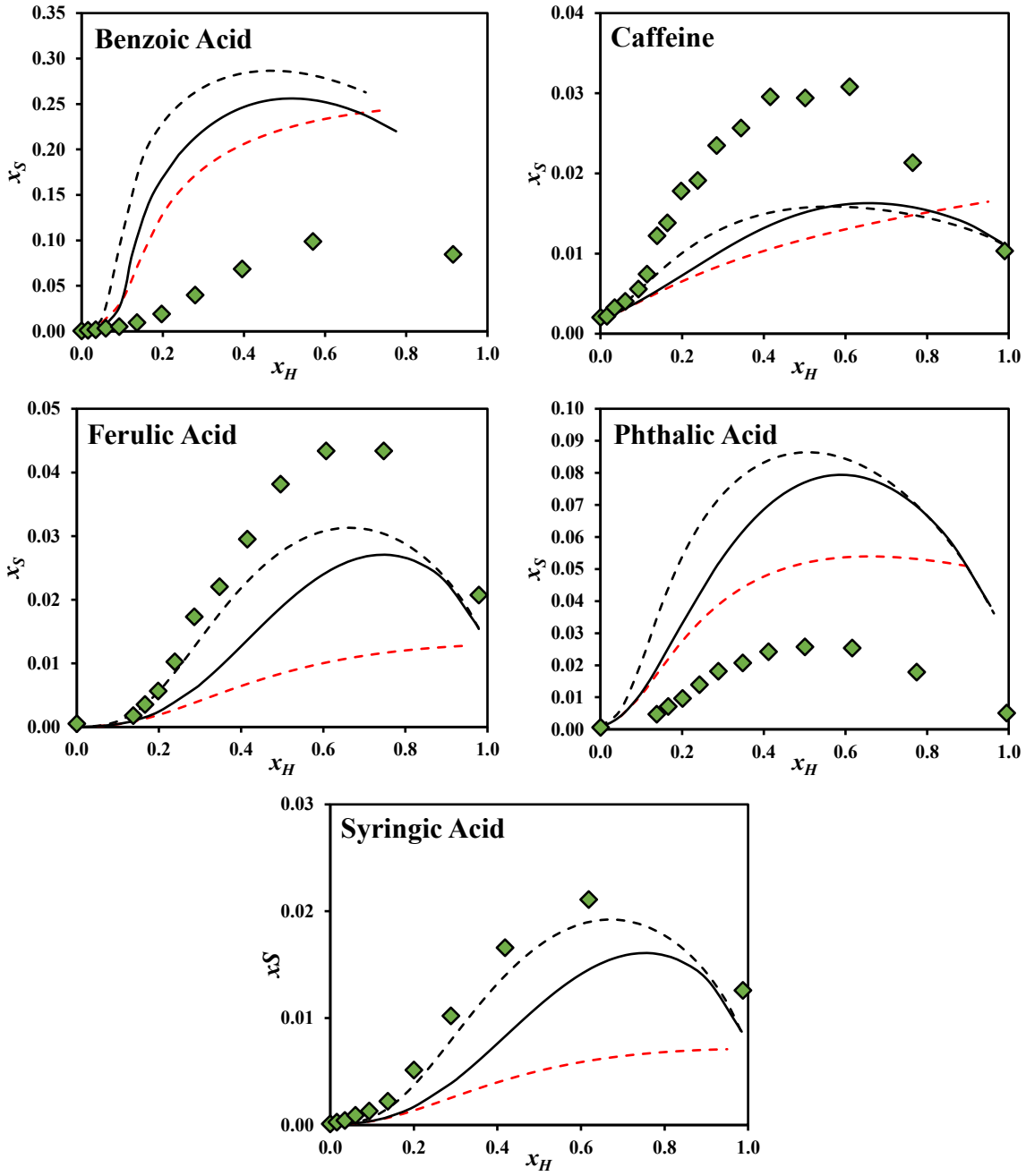

Figure A11.1. *Predicted solubility of hydrophobic solutes in water-ketone mixtures (black dashed line), water-diol mixtures (red dashed line) and water-ketone-diol mixtures (full line), along with the corresponding experimental data (◆), taken from De bruyn et al.*[5] *or Chapter 5, considering the diol conformer with one intramolecular hydrogen bond.*

A12. Other Diol Conformers

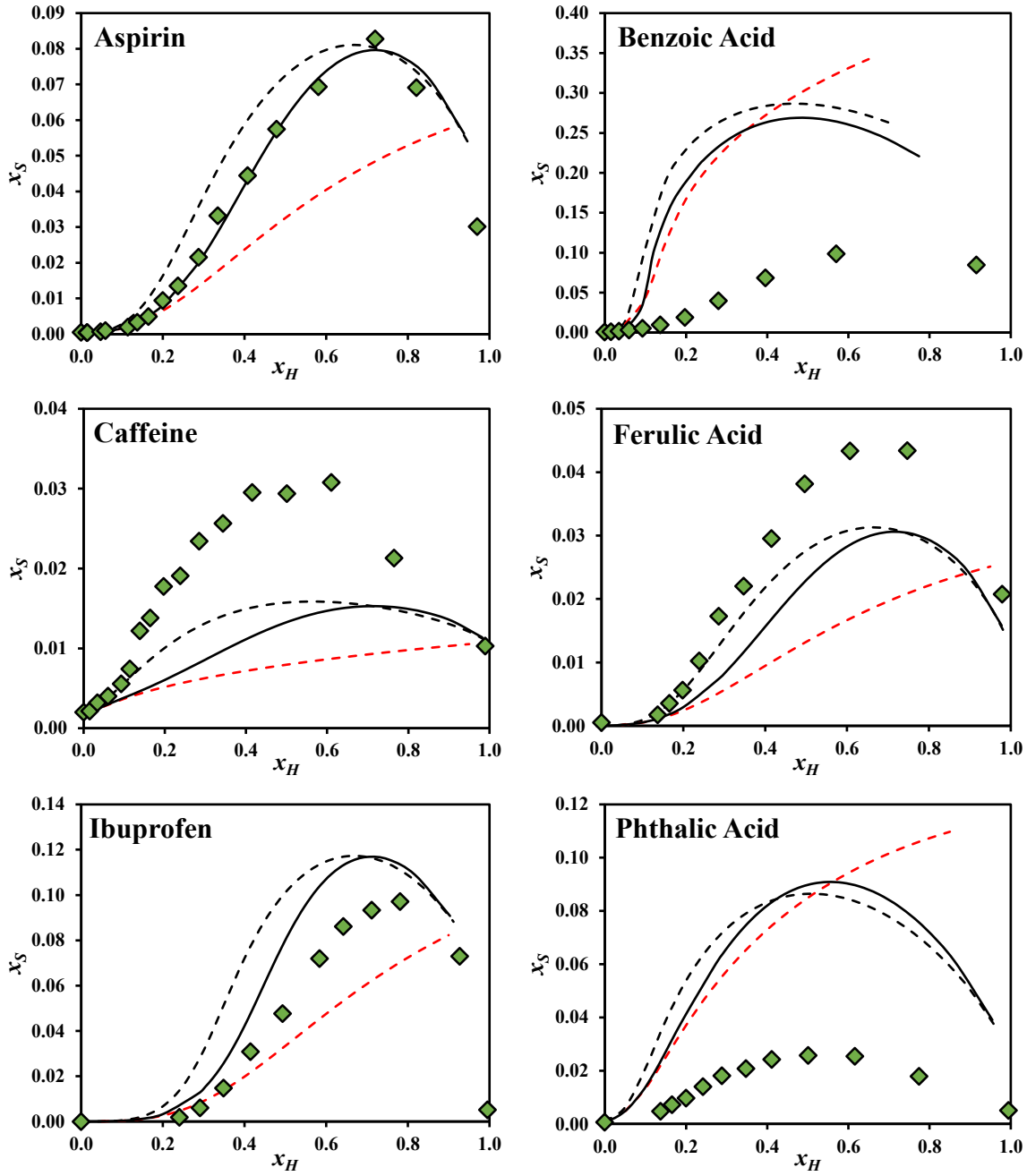

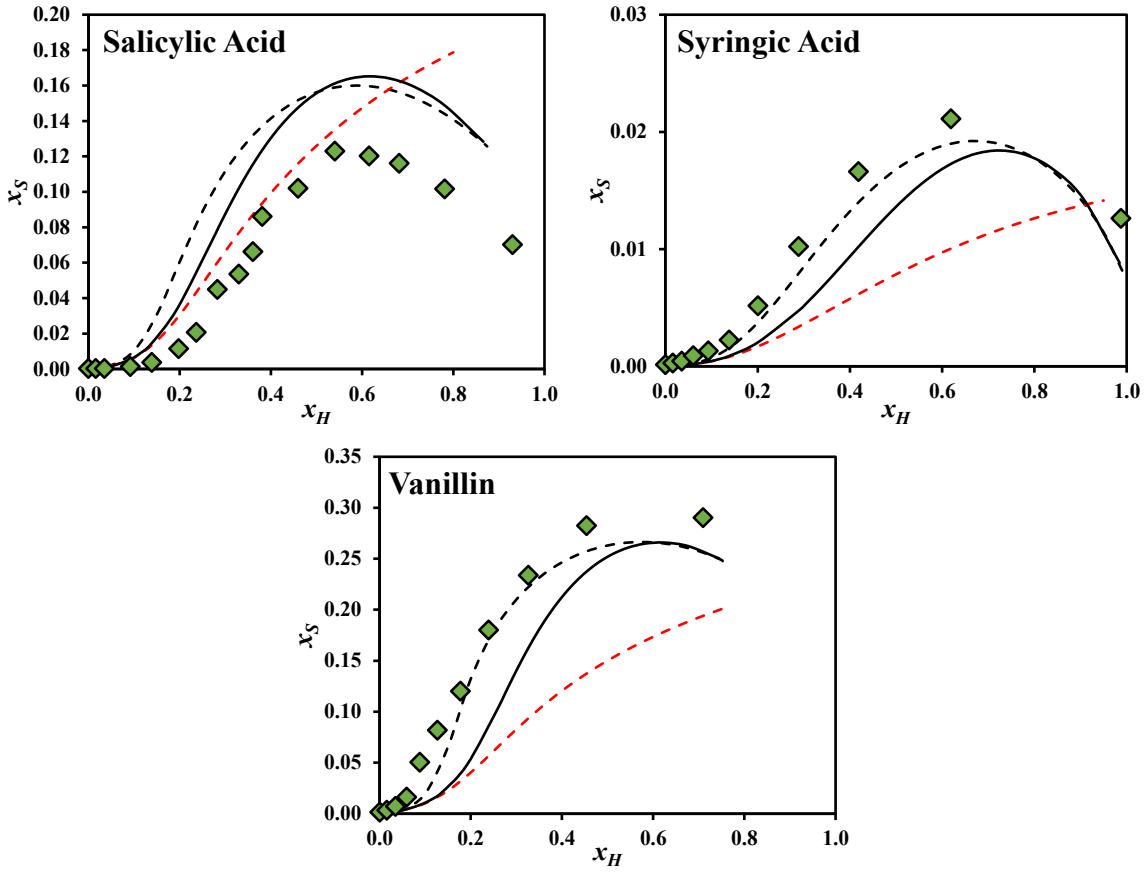

Figure A12.1. *Predicted solubility of hydrophobic solutes in water-ketone mixtures (black dashed line), water-diol mixtures (red dashed line) and water-ketone-diol mixtures (full line), along with the corresponding experimental data (◆), taken from De bruyn et al.*[5] *or Chapter 5, considering the diol conformer with no intramolecular hydrogen bonding.*

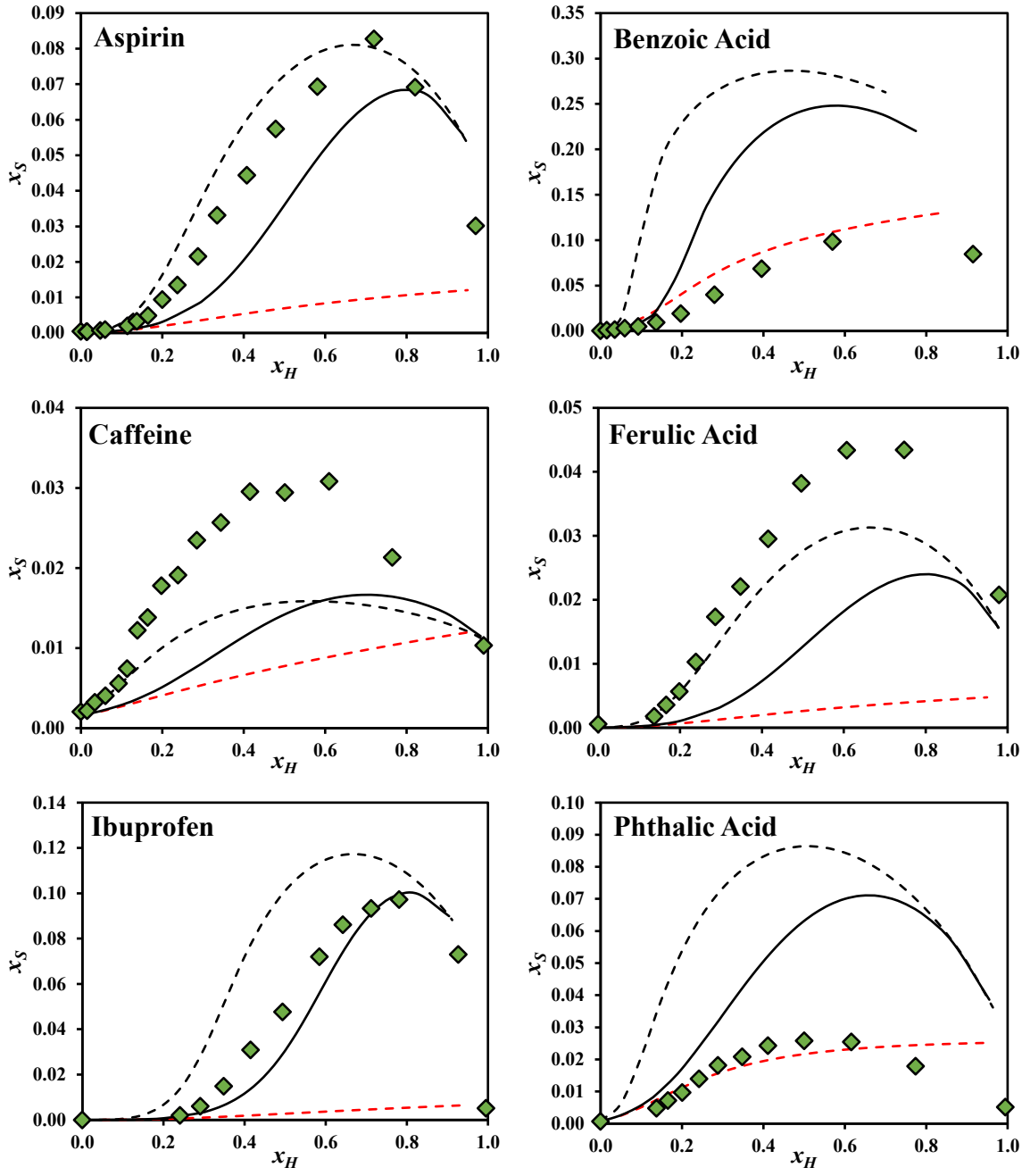
Aspirin
Benzoic Acid
Caffeine
Ferulic Acid
Ibuprofen
Phthalic Acid
x_S
x_H

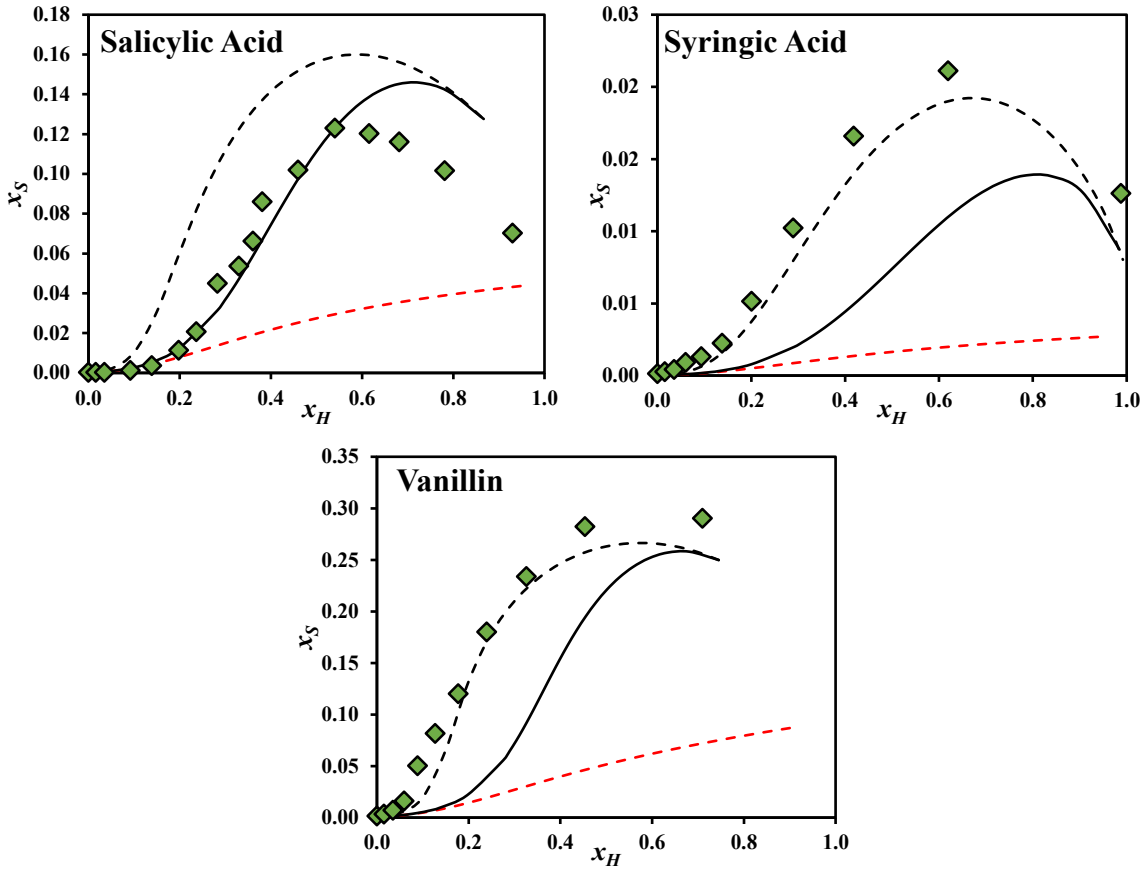

Figure A12.2. *Predicted solubility of hydrophobic solutes in water-ketone mixtures (black dashed line), water-diol mixtures (red dashed line) and water-ketone-diol mixtures (full line), along with the corresponding experimental data (◆), taken from De bruyn et al.*[5] *or Chapter 5, considering the diol conformer with two intramolecular hydrogen bonds.*

A13. References

[1] B. P. Soares, D. O. Abranches, T. E. Sintra, A. Leal-Duaso, J. I. García, E. Pires, S. Shimizu, S. P. Pinho, J. A. P. Coutinho, *ACS Sustain. Chem. Eng.* **2020**, *8*, 5742–5749.

[2] A. F. M. Cláudio, M. C. Neves, K. Shimizu, J. N. Canongia Lopes, M. G. Freire, J. A. P. Coutinho, *Green Chem.* **2015**, *17*, 3948–3963.

[3] T. E. Sintra, K. Shimizu, S. P. M. Ventura, S. Shimizu, J. N. Canongia Lopes, J. A. P. Coutinho, *Phys. Chem. Chem. Phys.* **2018**, *20*, 2094–2103.

[4] M. De bruyn, C. Sener, D. D. Petrolini, D. J. McClelland, J. He, M. R. Ball, Y. Liu, L. Martins, J. A. Dumesic, G. W. Huber, et al., *Green Chem.* **2019**, *21*, 5000–5007.

[5] M. De bruyn, V. L. Budarin, A. Misefari, S. Shimizu, H. Fish, M. Cockett, A. J. Hunt, H. Hofstetter, B. M. Weckhuysen, J. H. Clark, et al., *ACS Sustain. Chem. Eng.* **2019**, *7*, 7878–7883.